Formation of Thick Coatings of Intermetallic Compound Al_3Ti and its Composites by Powder Metallurgical Techniques

粉末冶金法による金属間化合物Al_3Tiとその複合材料の厚膜形成

2000

TOSHIO MATSUBARA

Department of Manufacturing Science

Osaka University

Acknowledgements

The author wishes to express his sincere gratitude to Professor K.F.Kobayashi, Osaka University for his supervision and encouragement throughout this study. He also wishes to thank Professor K.Nishimoto and Professor Y.Miyamoto, Osaka University, for providing valuable suggestions. He is also grateful to Dr.A.Hirose and Dr.K.Uenishi for their useful advice in accomplishing this work.

The author is indebted to all the members of Prof. Kobayashi's research group, especially Messrs. H.Kimura, S.Morino, S.Fujiwara, T.Shibutani and T.Wakita for their general guidance and support in this stuy.

The author thanks to Messrs. M.Morita, R.Kawave, A.Sugiyama and K.Ohmitsu, Osaka University, for all of the experimental assistance.

The author is deeply grateful to my parents and my grandmother for their support and devotion.

Contents

Chapter 1 General introduction 1
1.1 Background 1
1.2 Application of powder metallurgical techniques in surface modification and purpose of this thesis 3
Reference 5

Chapter 2 Formation of thick coatings of Al_3Ti on TiAl and Cu substrates by combustion synthesis 7
2.1 Introduction 7
2.2 Experimental 8
2.2.1 Materials 8
2.2.2 Combustion synthesis and bonding 8
2.2.3 Microstructural observation 8
2.2.4 Evaluation of coatings 9
2.3 Results and discussion 10
2.3.1 Combustion synthesis of Al_3Ti 10
2.3.2 Formation of thick coatings of Al_3Ti on TiAl substrate 12
2.3.3 Formation of thick coatings of Al_3Ti on Cu substrate 17
2.3.4 Properties of Al_3Ti coatings 24
2.4 Conclusions 26
References 26

Chapter 3 Application of mechanically alloyed powders to form homogeneous coatings of Al_3Ti 28
3.1 Introduction 28
3.2 Experimental 28
3.3 Results and discussion 29
3.3.1 Effect of initial Ti size on microstructure of Al_3Ti 29
3.3.2 Fine mixing of Al and Ti powders by MA 32
3.3.3 Formation of homogeneous Al_3Ti coatings and their properties 35
3.4 Conclusions 41
References 41

Chapter 4 Formation of homogeneous and dense coatings of Al_3Ti on Ti substrates by reactive-pulsed electric current sintering 42
4.1 Introduction 42
4.2 Experimental 42
4.3 Results and discussion 44
4.3.1 Formation of Al_3Ti phase 44
4.3.2 Formation of Al_3Ti coatings 50

4.3.3 Properties of Al_3Ti coatings 53
4.4 Conclusions 55
References 55

Chapter 5 Formation of thick coatings of ceramic particles dispersed Al_3Ti on Ti substrate by reactive-pulsed electric current sintering 57
5.1 Introduction 57
5.2 Experimental 57
5.3 Results and discussion 58
5.3.1 MA and the subsequent heat treatment 58
5.3.2 Densification and phase formation of IMC coatings 60
5.3.3 Reactions with Ti substrate 64
5.3.4 Properties of IMC coatings 67
5.4 Conclusions 72
References 73

Chapter 6 Summary 74

List of related publications 76

Chapter 1 General introduction

1.1 Background

Recent industrial progress demands materials to be equipped with high performance under severe conditions such as wear, corrosion, and oxidation at elevated temperatures, resulting in development of new materials like intermetallic compounds, advanced ceramics, and their composites. Such resistant properties against wear, corrosion, and oxidation can be provided at surface of materials by various coating methods. The coating process is called surface modification as well [1]. The surface modification can be hybridized such as conventional carburizing and nitriding for steel. Wear-resistant coatings need to be relatively thick, so they are generally formed by the liquid phase processes with high energy dense sources such as laser or plasma. On the other hand, since oxidation-resistant ones should be dense, they are formed by diffusion or physical vapor deposition (PVD) processes despite of their low coating rate. To avoid the coating from delamination and cracking, it is required to be well bonded with the substrate. Although the coating of ceramics such as Al_2O_3, TiB_2 or AlN can improve wear, corrosion or oxidation properties, there are many problems in coating on metal substrates, for example (1) thermal stress due to the thermal expansion mismatch between ceramics and metals, (2) poor reactivity of ceramics to metals, and (3) low bonding strength of ceramic/metal joints [2]. While, intermetallc compounds have better similarities to metals in thermal expansion, reactivity and diffusivity than ceramics. Therefore, they are more promising as reliable coating materials on metallic substrates [3].

In the last some decades, a great deal of fundamental and developmental research on intermetallic compounds has been made for aerospace, automotive and other land-based applications [4]. These intermetallics include aluminides of titanium, nickel or iron, and silicides of transition metals. Among them, titanium aluminides are promising materials in high temperature applications because of their low density, high specific strength at high temperatures, and good oxidation resistance. In the Al-Ti system, three intermetallic phases, Al_3Ti, TiAl (γ) and Ti_3Al (α_2) are stable at room temperature [5]. They can be applied not only as bulk forms, but also as coating ones. There are many researches concerning the formation of surface modified coatings of titanium aluminides as shown in **Table 1.1**. These coatings were mainly applied for the improvement of wear or oxidation properties. It can be also found that many coatings consist of the Al_3Ti phase.

The Al_3Ti is attractive as a high temperature structural material because of its low density (3.4Mg/m^3), high strength, high hardness, high melting temperature (>1623K) and excellent oxidation resistance [22-24]. Although the Al_3Ti has not been applied to practical use as a bulk material due to the low ductility at room temperature, it is expected to exhibit excellent wear and oxidation properties as a coating. The thermal

Table 1.1 *Various surface modified coatings of Ti-Al intermetallic compounds.*

Coating material	Substrate	Process	Thickness, μm	Evaluated properties	Ref.
Ti(Al)	Ti	laser alloying	~1000	oxidation	[6]
Ti_3Al/TiAl	Ti	laser alloying	~1000	wear	[7]
Ti_3Al/TiAl	Al	plasma spraying	~1000	wear	[8]
Ti_3Al/TiAl	TiAl	plasma spraying	~500	wear	[9]
TiAl	Carbon	vacuum arc deposition	~1	-	[10]
TiAl/Al_3Ti	Ti	laser alloying	~1000	oxidation, wear	[11]
Al_3Ti	Al	laser cladding	~500	wear	[12]
Al_3Ti	Ti	hot dipping	~400	-	[13]
Al_3Ti	Ti	pack cementation	~50	oxidation	[14]
Al_3Ti	Ti_3Al	pack cementation	~50	oxidation	[15]
Al_3Ti	TiAl	pack cementation	~50	oxidation	[16]
Al_3Ti	Ti	vapor deposition	~30	-	[17]
Al_3Ti	TiAl	sulfidation	~20	oxidation	[18]
Al_3Ti	TiAl	ion plating	~20	wear	[19]
Al_3Ti	Ti	ion plating	~5	oxidation	[20]
Al_3Ti	Al	ion implanting	~0.5	-	[21]

spraying, laser cladding and laser alloying have been developed as rapidly processes for the formation of thick coatings of titanium aluminides. However, since the Al_3Ti is formed by peritectic reaction from the liquid phase and has negligibly small solubility in the phase diagram, it is not always advantageous to apply the liquid phase process to obtain the monolithic Al_3Ti.

1.2 Application of powder metallurgical techniques in surface modification and purpose of this thesis

The net shaping capability of powder metallurgy (P/M) is attractive especially for brittle materials such as intermetallic compounds, since machining or deformation steps can be eliminated [25]. Additionally, many of them have a high melt viscosity that inhibits casting. Moreover, the grain size control is difficult and segregation is problem. Thus, P/M techniques are suited for process of intermetallic compounds.

Combustion synthesis, also called as self-propagating high temperature synthesis (SHS) is known to be one of the P/M techniques obtaining refractory compounds such as intermetallics, ceramics or their composites [26]. Synthesis from a mixed powder of constituent elemental powders can take place well below their melting temperatures, using the significant negative heat from the formation of the system. Since the combustion synthesis is heat-generating and self-sustaining, this process offers advantages with respect to process economic and simplicity, and over 500 compounds have been reportedly synthesized [27, 28]. Additionally, the starting materials need only to be heated to the ignition temperature, which is hundreds degree lower than the melting temperature of the products. These unique advantages of the combustion synthesis are applied not only to materials synthesis, but also to heat sources for welding and chemical oven [29-31].

An early application of the combustion synthesis was the thermite reduction of metal oxide powders with aluminum powder. The heat generated by the exothermic reaction enables welding railroad tracks and also heat treatment of metals. Uenishi *et al.* successfully applied the combustion synthesis to the bonding of intermetallic compound TiAl [32]. The bonding of intermetallic compounds is usually exposed to high temperatures, which induces material's degradation due to the structural change or grain coarsening [33]. By applying the combustion synthesis of a mixed powder of elemental Al and Ti used as filler metals, a relatively simple bonding process, *i.e.* hot pressing at low temperatures and heat treating without any load at higher temperatures was achieved. The bondings of Fe_3Al, NiAl and Ni-based superalloy were also obtained by applying the combustion synthesis [34-38].

Similarly, the combustion synthesis can be applied to a novel surface modification process. When a mixed powder of elemental Al and Ti with a composition of stoichiometric Al_3Ti pre-placed on the substrate is heated to the ignition temperature for the combustion synthesis, Al and Ti in the mixed powder react and form a coating of

Al_3Ti, resulting in simultaneous bonding with the substrate by the heat of formation of Al_3Ti. The advantages of this process are the capability for obtaining the coating with high bonding strength at a low temperature for a short time, and for easy controlling the thickness or microstructure of the coating by changing the thickness or composition of starting powders. For example, hybrid coatings of such as intermetallic matrix composites (IMC) or functionally gradient materials (FGM) can be formed.

However, it is well known that combustion synthesized materials are likely to include voids and unreacted elements. To eliminate these inhomogeneity, *i.e.* to form homogeneously reacted and dense coating, mechanical alloying (MA) and pulsed electric current sintering (PECS) are considered to be effective. MA is a high energy ball milling operation involving repeated welding, fracturing and rewelding of powder particles [39]. By using the MA process and subsequent heat treatment, several powders of intermetallic compounds and their composites were produced [40, 41]. Furthermore, when the fine mixed MA powders are consolidated, the microstructure reveals homogeneous and fine crystalline, leading to enhanced physical and mechanical properties. On the other hand, PECS, sometimes called as plasma activated sintering (PAS) or spark plasma sintering (SPS) has been reported to densify powders at a lower temperature, and for a shorter time than other conventional sintering processes by charging a pulsed electric current directly through the raw powders [42-45]. There are many researches concerning the consolidation of intermetallic compounds [46-50] and ceramics [51, 52] by PECS, and some of them reported the enhanced densification of materials at lower temperatures, and for shorter times than by conventional hot-pressing. These rapid sintering is considered to be effective to retain the fine microstructure of powders introduced by MA.

In this thesis, thick coatings of the Al_3Ti and its composites are formed on metallic substrates by applying the P/M techniques of the combustion synthesis, MA and PECS.

In Chapter 2, thick coatings of the Al_3Ti on the TiAl or Cu substrates were formed by the combustion synthesis. The combustion synthesis of the Al_3Ti from elemental Al and Ti powders was investigated. The microstructural changes in the coating and bonding interface during the combustion synthesis were also discussed. The surface properties of obtained coatings were evaluated by the micro hardness measurement and wear test.

In Chapter 3, to form a homogeneous Al_3Ti coating, fine mixed powders of elemental Al and Ti were prepared by MA. The microstructural evolution during MA and the combustion synthesis were investigated. Based on the calculated relation from a spherical model incorporating diffusion and reaction kinetics between Al and Ti, a homogeneous Al_3Ti layer was formed on the Cu substrate by using the MA powders. The reaction between the coating and the substrate, and the wear properties of obtained coatings were also investigated.

In Chapter 4, a dense and homogeneous coating of the Al_3Ti was formed on the Ti substrate by reactive PECS of the MA powders. The densification behavior of the synthesized coating, and the reaction kinetics between the coating and the Ti substrate

were investigated. The surface properties of obtained coatings were also evaluated by wear and oxidation test.

In Chapter 5, to further enhance the wear resistance, the ceramics particle (TiB_2 or Al_2O_3) dispersed Al_3Ti composite, *i.e.* IMC coatings were formed on the Ti substrate by reactive PECS of the MA powders. Effects of ceramic particles on the densification behavior of the IMC coatings, reaction kinetics between the coatings and the Ti substrate, and on the surface properties were investigated.

In Chapter 6, the summary of this thesis was shown.

References

[1] K.Uenishi and K.F.Kobayashi, *Intermetallics*, **4**(1996), s95.

[2] Y.Nakao, K.Nishimoto and K.Saida, *Trans. JWS.*, **20**(1989), 66.

[3] P.C.Patnaik, *Mater. Manuf. Proc.*, 4(1989), 133.

[4] M.Yamaguchi, H.Inui and K.Ito, *Acta Mater.*, **48**(2000), 307.

[5] C.McCullough, J.J.Valencia, C.G.Levi and R.Mehrabian, *Acta Metall.*, **37**(1989), 1321.

[6] J.D.Majumdar, A.Weisheit, B.L.Mordike and I.Manna, *Mater. Sci. Eng. A*, **266**(1999), 123.

[7] J.H.Abboud and D.R.F.West, *Mater. Sci. Tech.*, **7**(1991), 827.

[8] K.Uenishi, M.Murase and K.F.Kobayashi, *Z. Metallkd.*, **90**(1999), 289.

[9] K.Honda, A.Hirose and K.F.Kobayashi, *Mater. Sci. Eng. A*, **222**(1997), 212.

[10] S.Y.Chun, A.Chayahara and Y.Horino, *Mater. Trans., JIM*, **41**(2000), 44.

[11] A.Hirose, T.Ueda and K.F.Kobayashi, *Mater. Sci. Eng. A*, **160**(1993), 143.

[12] K.Uenishi, A.Sugimoto and K.F.Kobayashi, *Z. Metallkd.*, **83**(1992), 241.

[13] A.A.Abdel-Hamid, *Z. Metallkd.*, **82**(1991), 921.

[14] J.Subrahmanyam and J.Annapurna, *Oxid. Met.*, **26**(1986), 275.

[15] J.Subrahmanyam, *J. Mater. Sci.*, **23**(1988), 1906.

[16] H.Mabuchi, T.Asai and Y.Nakayama, *Scripta Met.*, **23**(1989), 685.

[17] N.R.Short and J.Mackowiak, *J. Less-Common Met.*, **45**(1976), 301.

[18] T.Narita, T.Izumi, M.Yatagai and T.Yoshioka, *Intermetallics*, **8**(2000), 371.

[19] D.G.Teer and F.B.Salem, *Thin Solid Films*, **45**(1977), 583.

[20] Y.Nakao, K.Shinozaki, H.Ishii and A.Kida, *Preprints of the National Meeting of JWS*, **66**(1992), 330.

[21] F.H.Sanchez, F.Namavar, J.I.Budnick, A.Fasihuddin, C.H.Koch and H.C.Hayden, *Mater. Sci. Eng.*, **90**(1987), 149.

[22] Y.Umakoshi, M.Yamaguchi, T.Sakagami and T.Yamane, *J. Mater. Sci.*, **24**(1989), 1599.

[23] M.Yamaguchi, Y.Umakoshi and T.Yamane, *Phil. Mag. A*, **55**(1987), 301.

[24] M.Yamaguchi, Y.Shirai and Y.Umakoshi, *Dispersion Strengthened Aluminum*

Alloys, TMS(1988), 721.
[25] R.M.German and R.G.Iacocca, *MRS Symp. Proc.*, **350**(1994), 13.
[26] A.G.Merzhanov and I.P.Borovinskaya, *Dolk. Chem.*, **204**(1972), 429.
[27] H.C.Yi and J.J.Moore, *J. Mater. Sci.*, **25**(1990), 1159.
[28] J.Subrahmanyam and M.Vijayakumar, *J.Mater. Sci.*, **27**(1992), 6249.
[29] J.J.Moore and H.J.Feng, *Prog. Mater. Sci.*, **39**(1995), 243.
[30] J.J.Moore and H.J.Feng, *Prog. Mater. Sci.*, **39**(1995), 275.
[31] J.S.Lin, Y.Miyamoto, K.Tanaka, M.Yamamoto and R.Tanaka, *J. Mater. Sci.*, **33**(1998), 869.
[32] K.Uenishi, H.Sumi and K.F.Kobayashi, *Z.Metallke.*, **86**(1995), 64.
[33] Y.Nakao, K.Shinozaki and M.Hamada, *ISIJ Int.*, **31**(1991), 1260.
[34] J.K.Wright, R.N.Wright and G.A.Moore, *Scripta Metall. Mater.*, **28**(1993), 501.
[35] R.D.Torres and T.R.Strohaecher, *Scripta Metall. Mater.*, **30**(1994), 463.
[36] T.T.Orling and R.W.Messler, Jr., *Welding Res. Suppl.*, **42**(1996), s93.
[37] R.W.Messler, Jr., M.A.Zurbuchen and T.T.Orling, *Welding J.*, **74**(1995), 37.
[38] J.A.Hawk, A.V.Petty, C.P.Dogan and J.C.Rawers, *MRS Symp. Proc.*, 3**14**(1993), 183
[39] J.S.Benjamin, *Metall. Trans.*, **1**(1970), 2943.
[40] F.H.Froes, C.Suryanarayana, K.Russell and C.G.Li, *Mater. Sci. Eng. A*, **192/193**(1995), 612.
[41] C.C.Koch, *Mater. Sci. Eng. A*, **244**(1998), 39.
[42] M.Tokita, *J. Soc. Powder Tech. Jpn.*, **30**(1993), 790.
[43] J.R.Groza and A.Zavaliangos, *Mater. Sci. Eng. A*, **287**(2000), 171.
[44] M.Omori, *Mater. Sci. Eng. A*, **287**(2000), 183.
[45] D.C.Newman, *Mater. Sci. Eng. A*, **287**(2000), 198.
[46] T.Y.Um, Y.H.Park, H.Hashimoto, S.Sumi, T.Abe and R.Watanabe, *J. Jpn. Soc. Powder Powder Metall.*, **44**(1997), 530.
[47] K.Kobayashi, A.Matsumoto, K.Ozaki, A.Sugiyama and T.Nishio, *J. Jpn. Inst. Metals*, **63**(1999), 1161.
[48] H.Kimura and S.Kobayashi, *J. Jpn. Inst. Metals*, **58**(1994), 201.
[49] M.A.Venkataswamy, J.A.Schneider, J.R.Groza, A.K.Mukherjee, K.Yamazaki and K.Shoda, *Mater. Sci. Eng. A*, **207**(1996), 153.
[50] J.R.Groza, *Scripta Metall.*, **30**(1994), 47.
[51] S.H.Risbud, J.R.Groza and M.J.Kim, *Phil. Mag. B*, **69**(1994), 525.
[52] R.S.Mishra and A.K.Mukherjee, *Mater. Sci. Eng. A*, **287**(2000), 178.

Chapter 2 Formation of thick coatings of Al_3Ti on TiAl and Cu substrates by combustion synthesis

2.1 Introduction

Titanium aluminides are promising intermetallic compounds for high temperature applications because of their high specific strength at high temperatures. Among them, γ-based TiAl alloys have attracted the attentions owing to its good combination of high strength and moderate room temperature ductility [1]. However, for practical application of these alloys, the surface properties such as wear or oxidation resistance have to be improved [2].

Pure copper is often used as an electrical conductor because of its high electrical conductivity, however, it is not equipped with sufficient strength and wear resistance. The elimination of these problems would lead to many engineering applications.

If a coating layer of Al_3Ti is formed on the TiAl and Cu substrates, it is expected that their surface properties will be improved. For the formation of an Al_3Ti coating on the TiAl substrate, the strong bonding between the substrate and the coating should be achieved. There are many reports showing difficulties for the bonding of similar γ-based TiAl alloys. Welding cracks are easily introduced by the fusion welding [3, 4], and processing at high temperatures is inevitable for the solid state bonding [5, 6]. There are no reports concerning the bonding of Al_3Ti with TiAl. It is not expected to be easy by conventional bonding processes since the Al_3Ti has a lower ductility than γ-based TiAl alloys.

On the other hand, Galantucci [7] and Hirose [8] have applied laser alloying techniques to form hard surface coatings on the Cu base material. In the case of a substrate with low strength like Cu or Al, the coating easily breaks away because of the high deformability of the substrate. Hence, the thickness as well as surface properties is required for the coating. Although many surface modification techniques have been reported, they are not always applicable for the formation of thick coatings. According to their reports, the high reflectivity of Cu to a CO_2 laser poses a problem that the input heat can not be transferred to the base material effectively. Consequently, it is hard to prepare a thick coating by laser processes.

In this chapter, an Al_3Ti was formed by the combustion synthesis from a mixed powder of elemental Al and Ti with a composition of stoichiometric Al_3Ti and simultaneously bonded with TiAl and Cu substrates. By applying the combustion synthesis to the dissimilar bonding, it is expected that bonding can be achieved on easier conditions, *i.e.* at low bonding temperatures or for shorter holding times.

2.2 Experimental

2.2.1 Materials

TiAl substrate used in this research was fabricated by Ar-arc melting. The nominal composition of the substrate is shown in **Table 2.1**. The microstructure of the substrate showed a lamellar structure, comprised of γ and α_2, with an average colony size of 200μm. Cu substrate with 99.99% purity and a thickness of 3mm was also used.

Ti and Al powders with 99.9% purity and average particle sizes of 10μm and 20μm, respectively, were mixed in the stoichiometric composition of Al_3Ti (Al-25at.%Ti), or Al-20at.%Ti. These powders were die-pressed to the relative density of 88% under 300MPa for 60s. The diameter and thickness of the powder compact were fixed to 10.6mm and 2mm, respectively. In order to enhance the densification of the compact, some cold pressed compacts were hot pressed at 773K for 1.8ks under 100MPa to the relative density of 98%. The reactivity of powder compact was examined by means of differential scanning calorimetry (DSC: Perkin-Elmer DSC 7) at the heating rate of 0.33K/s under Ar flow atmosphere.

Table 2.1 Nominal composition of TiAl substrate.

	Chemical composition, mol.%				
	Ti	Al	Mo	C	O
TiAl	Bal.	45.5	1.96	0.0004	0.0013

2.2.2 Combustion synthesis and bonding

Combustion synthesis and simultaneous bonding were performed by hot pressing under a vacuum of 5.0×10^{-2}Pa. The surface of the substrates was ground with 0.3μm alumina powders to obtain a flat and clean surface prior to bonding. The powder compact was put in the alumina die placed on the substrate as shown in **Fig. 2.1**. Then, the sample was heated at the heating rate of 0.33K/s by a high frequency induction heating equipment and held at the bonding temperatures. The bonding pressure was applied from the beginning of heating to the end of cooling.

2.2.3 Microstructural observation

The specimens for microstructural observations were cut in the perpendicular direction to the bonding interface and mechanically polished using emery papers and 0.3μm Al_2O_3 powders. After polishing, the samples were observed using optical microscopy and scanning electron microscopy (SEM: HITACHI X-650T). To identify the phases formed in the samples during the combustion synthesis and simultaneous bonding, electron dispersive X-ray (EDX) and X-ray diffraction analyses using Co-Kα and Cu-Kα radiations were performed.

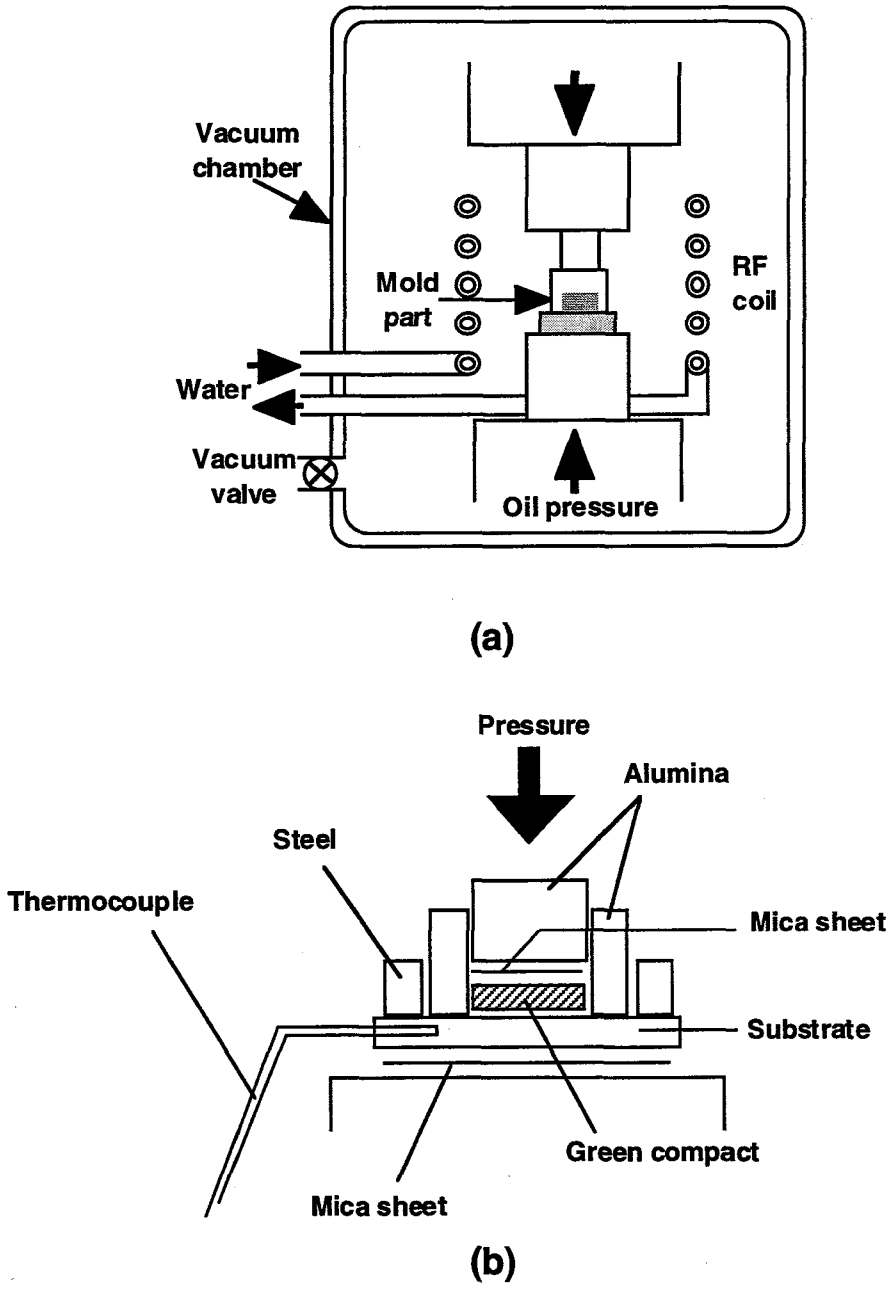

Fig. 2.1 Schematic illustration of hot-press apparatus. (a) General view, and (b) mold part.

2.2.4 Evaluation of coatings

The hardness of the obtained sample was measured by Vickers hardness test using a load of 1.96N for 15s.

The wear properties of the obtained coatings were examined by Ogoshi abrasion test [9]. The surface of the test sample was polished with 0.3μm alumina powders. A heat treated SUJ2 steel (HV 650) ring was used as an opponent abraser. Abrasion distance (L), load (P) and speed were fixed to 100m, 10N and 4.36m/s, respectively. The specific wear (W_s) was calculated by measuring the volume of the abraded indentation (W)

according to eq. (2.1).

$$W_s = \frac{1.5W}{PL} \tag{2.1}$$

2.3 Results and discussion

2.3.1 Combustion synthesis of Al_3Ti

Figure 2.2 shows a DSC trace obtained when a mixed powder of elemental Al and Ti with a composition of stoichiometric Al_3Ti (Al-25at.%Ti) was continuously heated to 1003K at a heating rate of 0.33K/s. The DSC curve showed two exothermal peaks staring from about 900K and from about 930K.

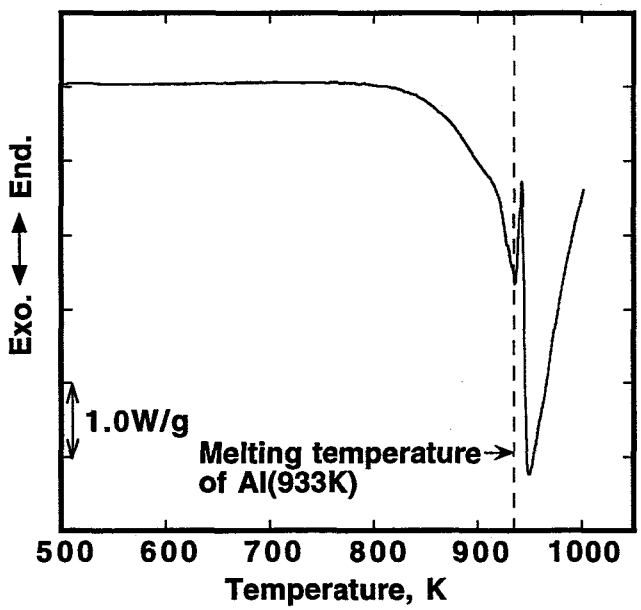

Fig. 2.2 DSC trace of a mixed powder of elemental Al and Ti with a composition of stoichiometric Al_3Ti.

Figure 2.3 shows the X-ray diffraction patterns of the mixed powders continuously heated to various temperatures. Diffraction peaks of pure Al and Ti observed in the as-mixed powders never changed by heating to 900K, which is lower than the onset temperature of the first exothermal reaction. However, these peaks completely disappeared and Al_3Ti peaks appeared after heating to a temperature above the exothermal peak. These results indicate that elemental Al and Ti spontaneously reacted and formed Al_3Ti during the exothemal peak.

As described by Uenishi *et al.* about the combustion synthesis of TiAl [10], this spontaneous reaction is related to the interdiffusion of both elements and is ignited by the melting of Al. Namely, the diffusion velocity of Al in Ti or Ti in Al in the solid state

is in the order of several nanometers per second [11], which is much smaller than the particle size of powders and is insufficient for complete reaction. However, after melting of Al, the diffusion velocity of Ti into Al increases up to the order of ten microns per second [12]. In the first exothermal peak which occurs at a lower temperature than the melting of Al, Al and Ti partially reacted in the solid state. Immediately after melting of Al, molten Al and solid Ti drastically reacted and released the spontaneous exothermal heat.

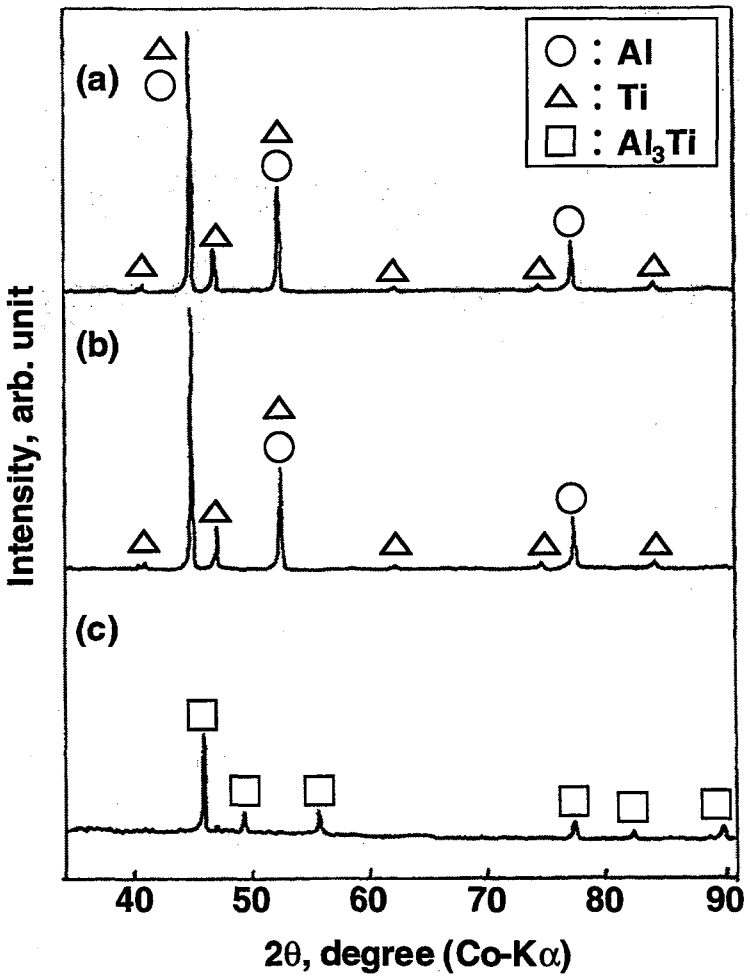

Fig. 2.3 X-ray diffraction patterns of (a) as-mixed powders, (b) continuously heated to 900K (immediately below the ignition temperature) and (c) to 973K (above the ignition temperature).

The maximum combustion temperature achieved under adiabatic conditions can be estimated by thermodynamical calculations [13]. Assuming that the combustion synthesis of Al_3Ti is ignited completely under adiabatic conditions at an initial ignition temperature (T_{i0}), the enthalpy is self-generated by exothermic reaction and utilized in raising the temperature of the products. The maximum temperature (adiabatic temperature: T_{ad}) thus attained, can be calculated from the heat balance condition, according to eq. (2.2), when T_{ad} is equal to or less than the melting temperature of the product (T_m).

$$-\Delta H_{T_{io}} = \int_{T_{io}}^{T_{ad}} C_p(T)dT + \nu L, \quad T_{ad} \le T_m \tag{2.2}$$

where ΔH_{Tio} is the enthalpy of reaction at T_{i0}. $C_p(T)$, ν and L is the combined heat capacity, fusion ratio and latent heat of the synthesized products, respectively. As T_{i0} and T_m are 933 and 1623K, respectively for Al_3Ti, substitution in eq. (2.2) of ΔH_{933}=46.86kJ/mol, $C_p(T)$=21.43+6.171x10^{-3}T J/Kmol and L=32.14kJ/mol [14] gives T_{ad}=1623K and ν=0.83. Namely, the synthesized Al_3Ti is predicted to be partially melted by self-heating. **Figure 2.4** shows the experimentally measured temperature profile of the mixed powder compact with a composition of Al-25at.%Ti continuously heated by hot pressing. The temperature increased sharply at the melting point of Al, and reached the maximum temperature in a short time. This maximum temperature equals to the melting temperature of Al_3Ti and is consistent with the calculated value. After the combustion synthesis, the temperature decreased to the furnace temperature rapidly. The process time was only 30s.

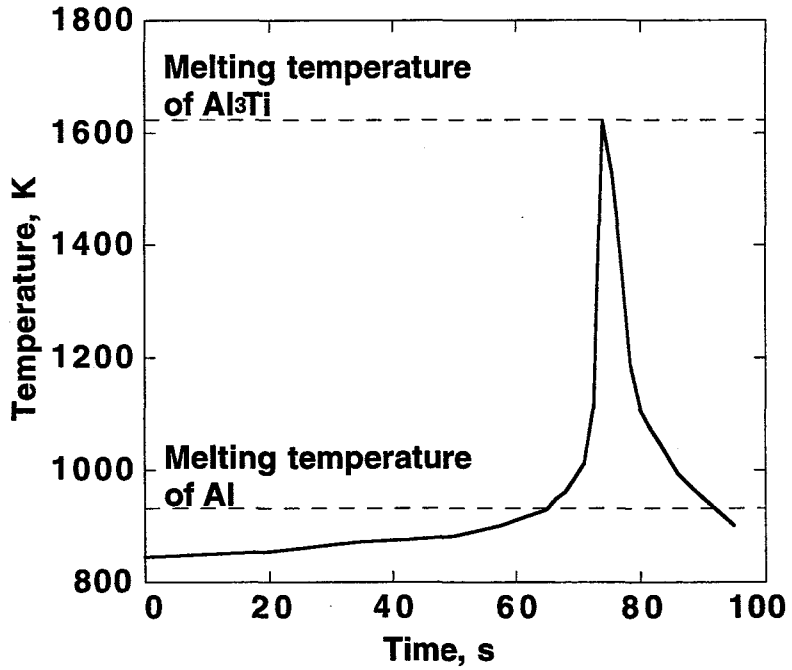

Fig. 2.4 Measured temperature profile of the mixed powder compact with a composition of Al-25at.%Ti continuously heated by hot pressing.

2.3.2 Formation of thick coatings of Al_3Ti on TiAl substrate

Combustion synthesis of Al_3Ti was carried out on a TiAl substrate to form a surface modified coating. **Figure 2.5** shows the microstructures of the sample obtained by hot pressing at 1023K for 300s under 10MPa. The powder compact was confirmed to be bonded well with the TiAl substrate. The thickness of the alloyed coating was about 1.5mm, exhibiting a smooth surface. As shown in **Fig. 2.5(b)**, the microstructure of the

layer was almost homogeneous although small volume fraction of voids (dark contrast) and unreacted Ti (bright contrast) were observed.

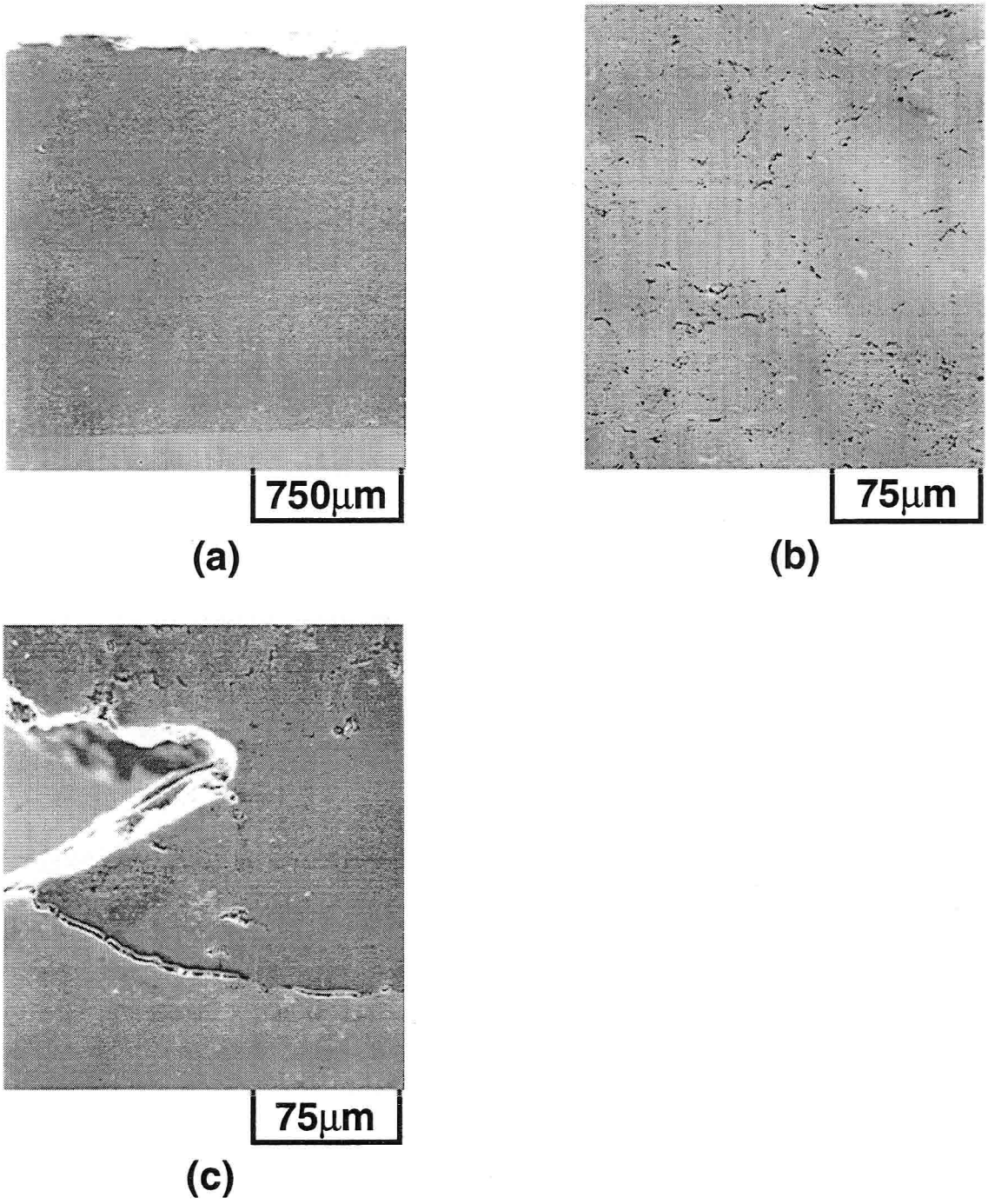

Fig. 2.5 *Al_3Ti coating formed on the TiAl substrate by hot pressing at 1023K for 300s under 10MPa. (a) General view, (b) microstructure of the combustion synthesized Al_3Ti layer and (c) the reaction layer formed on the bonding interface between the Al_3Ti coating and the TiAl substrate.*

Figure 2.6 shows the X-ray diffraction patterns of the Al_3Ti coating and the reaction layer formed on the bonding interface between the Al_3Ti coating and the TiAl substrate. From these figures, the Al and Ti were completely reacted and formed Al_3Ti after hot pressing. Compared with the particle size of Ti, the diffusivity of Al into Ti was not sufficiently large, which may cause Ti partially unreacted. However, as shown in **Fig. 2.6(c)**, any diffraction peaks of Ti are not present in the diffraction pattern, showing that the volume fraction of unreacted Ti is not significant.

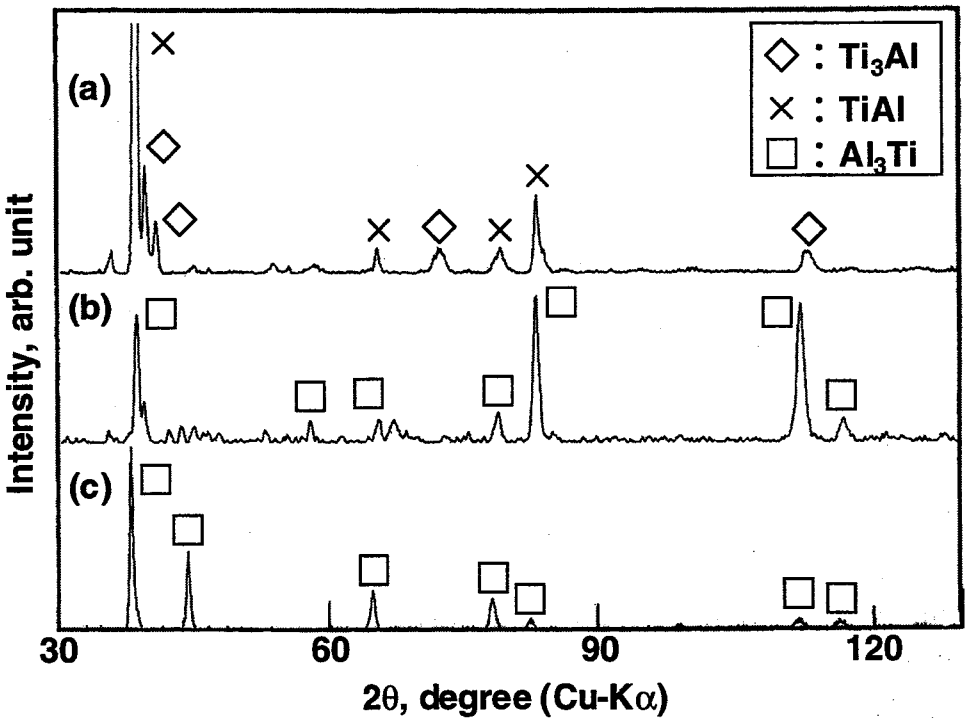

Fig. 2.6 X-ray diffraction patterns of (a) TiAl substrate, (b) reaction layer and (c) Al_3Ti coating.

The pores observed in the synthesized Al_3Ti coating were mainly introduced during the combustion synthesis, because the volume fraction of pores hardly changed by heating below the ignition temperature and because it increased drastically by heating above the ignition temperature. The combustion synthesized materials have been reported to be very porous [13]. When no pressure was applied for densification, for example, the relative density of NiTi was only 50~60% [15]. Rice distinguished these voids into two types, namely extrinsic and intrinsic voids [16]. Extrinsic voids are caused due to the expansion of voids or out gassing in the green compact. The formation of intrinsic voids is caused from the molar volume change or Kirkendall effect during the conversion reaction of the constituent elemental powders to the products. During the reaction to form Al_3Ti from elemental Al and Ti, the molar volume change can be estimated from their crystal structure to be 7%. Thus this process needs external pressure application for the densification. Also, initial powder compact with fewer voids

should be used for decreasing the formation of external voids.

Figure 2.7 shows the effect of bonding pressure on the relative density of the Al_3Ti coatings. The application of pressure decreased the voids. With increasing the pressure up to 20MPa, the density of the coating increased almost up to the theoretical density. By using a dense powder compact as a starting material, the voids decreased so drastically that the density reached the theoretical density when a pressure of 10MPa was applied. However, the voids hardly decreased by changing the bonding time. According to Lerf *et al.*, even after consolidation of Al_3Ti powder at 1273K, there were traces of void and evidence of poorly bonded powder particles [17], therefore the present temperature (973K) is not high enough to achieve full densification. In the present combustion synthesis process, there is a chance to decrease the voids at lower temperatures. Since the starting material contains pure Al, a sufficient pressure application during melting of Al is considered to decrease the voids. Once they are formed, the present pressure and temperature are not enough for densification of the powders even by the prolonged bonding time. In conclusion, the bonding pressure is effective to decrease voids just on the time when Al melts and the reaction occurs.

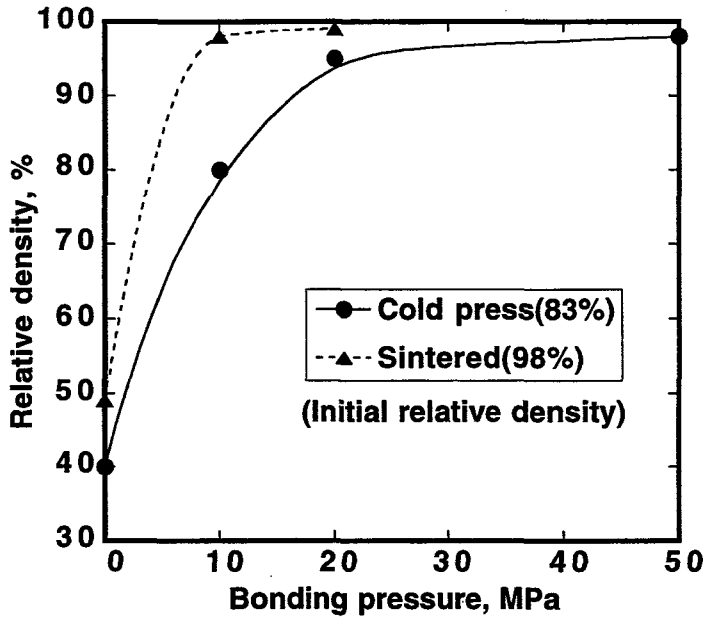

Fig. 2.7 Effect of bonding pressure and initial density of powder compacts on relative density for the combustion synthesized Al_3Ti coating. Bonding temperature time are 1023K and 300s, respectively.

As shown in **Fig. 2.5(c)**, the reaction layer was formed mainly in the TiAl substrate along the bonding interface. From the X-ray diffraction analysis shown in **Fig. 2.6(b)**, the synthesized phase in the reaction layer was identified to be Al_3Ti. Uenishi *et al.* have previously reported about the reaction between pure Al and TiAl that the reaction occurs drastically at the melting of Al resulting in formation of the Al_3Ti reaction layer [18]. Similarly, in the present case, the reaction layer was formed by the diffusion of Al from

the mixed powder into the TiAl substrate at the melting temperature of Al. Thus, the bonding was achieved simultaneously at the same temperature on which the coating was combustion synthesized. Voids were hardly observed in the reaction layer, since there are no initial voids in the TiAl substrate and the molar volume change is smaller for the formation of Al_3Ti from Al and TiAl (1.5%) than that from Al and Ti (7%).

Figure 2.8(a) shows the effect of bonding pressure on the width of the reaction layer formed for the bonding time of 300s. With increasing the bonding pressure, the width of reaction layer became slightly smaller probably due to the enhanced wettability of Al to Al_3Ti. However, as shown in **Fig. 2.8(b)**, the width hardly changed even by increasing the bonding time. Loo *et al.* reported that the diffusivity between Al_3Ti and TiAl is extremely small [19]. Once intermetallic compound is formed by the combustion synthesis, the growth of the reaction layer can be considered to be small. In other words, the bonding between Al_3Ti and TiAl should be dominate by the combustion synthesis reaction at the melting temperature of Al

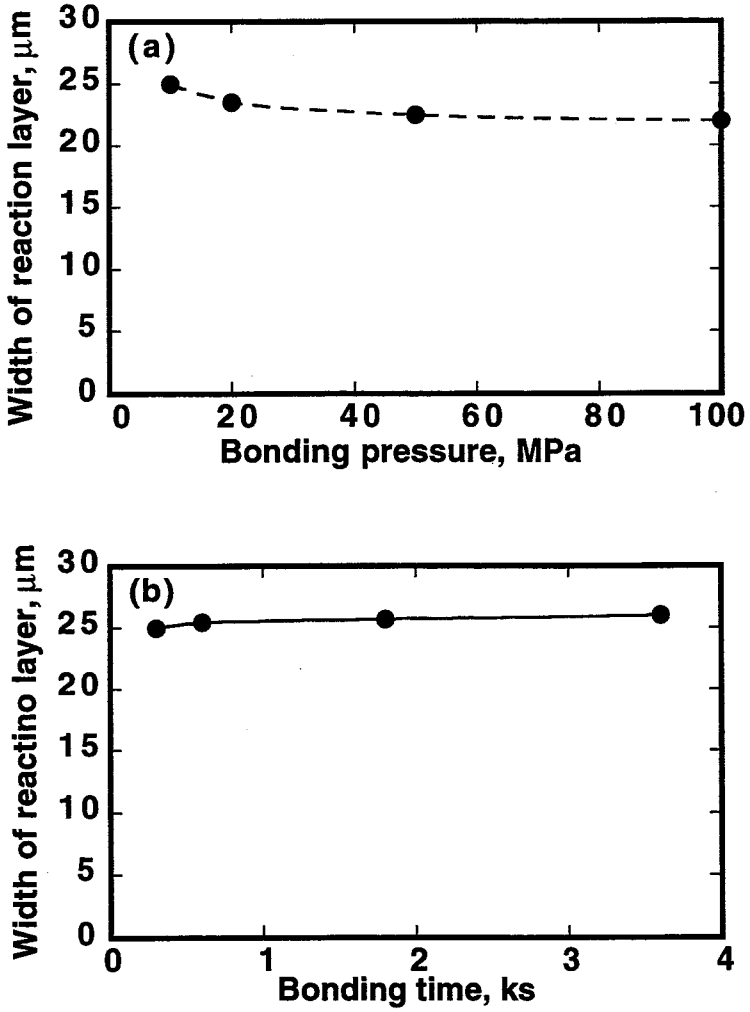

Fig. 2.8 Changes in the width of the reaction layer with increasing (a) bonding pressure (bonding time:300s) and (b) bonding time (bonding pressure:10MPa).

2.3.3 Formation of thick coatings of Al_3Ti on Cu substrate

Figure 2.9 shows microstructures of the Al_3Ti coating on the Cu substrate obtained by hot pressing at 973K for 300s under 20MPa. The thickness of the alloyed layer was about 500μm. Unlike the formation of Al_3Ti coating on the TiAl substrate, there are some distinction in the microstructure between the outer and inner coatings. As shown in **Fig. 2.9(b)**, the microstructure of the outer coating exhibited such a homogeneity that some volume fraction of voids (dark contrast) and unreacted Ti (bright contrast) were

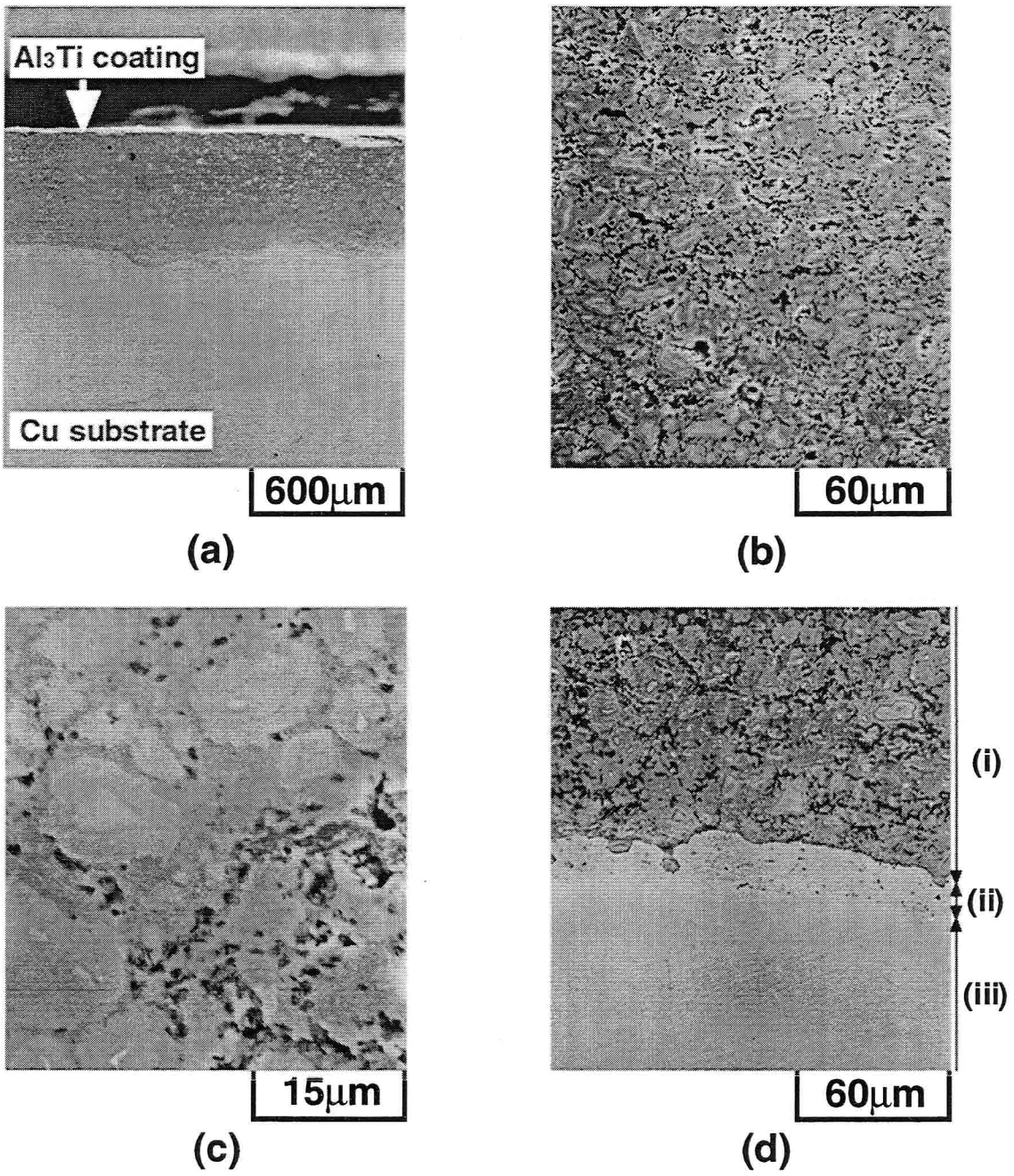

Fig. 2.9 Al_3Ti coating formed on the Cu substrate by hot pressing at 973K for 300s under 20MPa. (a) General view, microstructures of (b) the outer coating, (c) inner coating and (d) reaction layers formed on the bonding interface.

observed. **Figure 2.9(c)** shows the microstructure of the inner coating, revealing that the unreacted Ti was surrounded by dual phases which were confirmed by X-ray diffraction patterns and EDX analysis that the inner phase surrounding unreacted Ti was Al_5CuTi_2 [20] and the outer one was Al_3Ti.

Although the coating exhibited some inhomogeneity, it was confirmed to be bonded well with the Cu substrate by the formation of three reaction layers on the bonding interface as shown in **Fig. 2.9(d)**. **Figure 2.10** shows X-ray diffraction patterns of the reaction layers on the bonding interface. From this results and EDX analysis, the reaction layers from the coating were identified as Al_5CuTi_2 with some Al_3Ti and Ti inclusions (250μm), $Ti(Cu,Al)_2$ (30μm) and fcc Cu(Al) solid solution (80μm). This fcc Cu peaks shifted to lower angle, since the atom radius of Al is larger than that of Cu and the lattice parameter of fcc Cu(Al) solid solution became larger than that of pure Cu. Compared with the formation of the Al_3Ti coating on the TiAl substrate, the width of the reaction layers, especially Al_5CuTi_2 was much larger. This result can not be explained by the same mechanism as the case of TiAl substrate. Therefore, the Cu seems to affect the formation mechanism of the reaction layers and also the combustion synthesis of the coating.

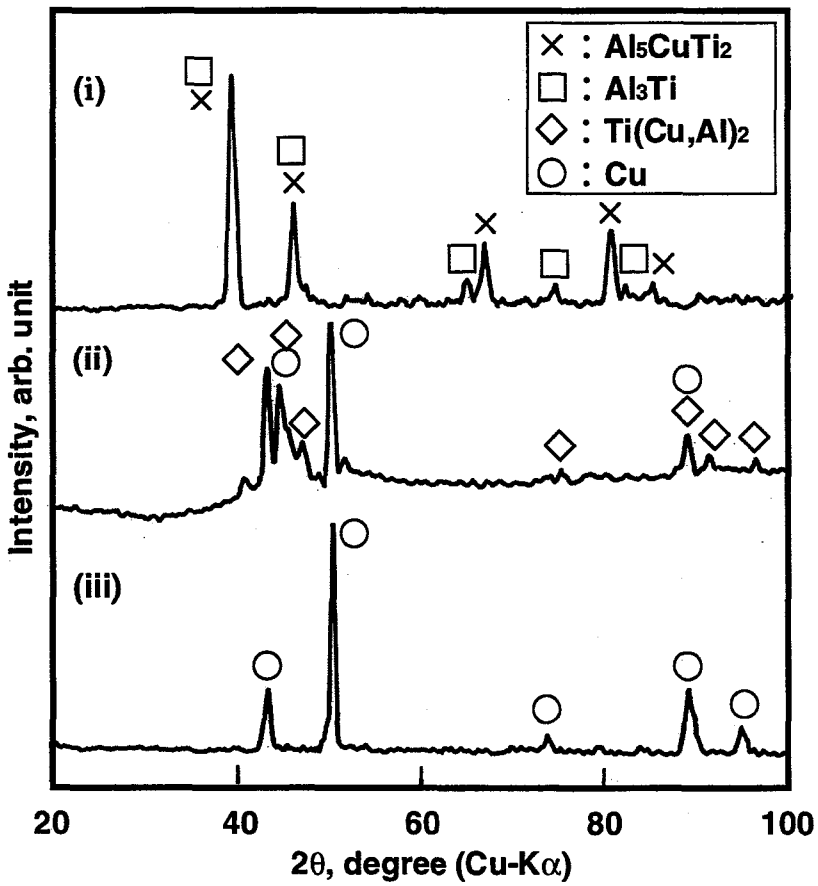

Fig. 2.10 X-ray diffraction patterns of the reaction layers shown in Fig. 2.9(d).

In order to clarify the reaction mechanism between the Cu substrate and the Al_3Ti coating, the sample was heated to 783K where the measured temperature rapidly increased during the continuous heating and then rapidly quenched to room temperature. **Figure 2.11** shows the cross section of the sample. The coating could be divided into three regions. **Figure 2.12** shows the microstructures at the bonding interface and

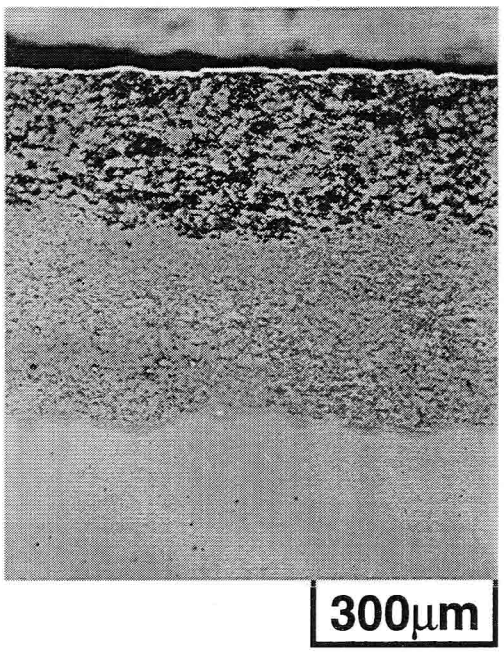

Fig. 2.11 *A cross section of the sample which was heated to 783K and rapidly quenched to room temperature.*

EDX analysis. Two reaction layers consisted of Al and Cu were formed due to interdiffusion. Enjo *et al.* reported that reaction layers of Al_2Cu (θ) and Al_4Cu_9 (γ_2) were observed on both sides of Al and Cu of the bonding interface, respectively, when diffusion bonding of Cu to Al was carried out [21]. In this case, since Ti was not detected in the reaction layers, it can be considered that the same reaction layers as θ and γ_2 were formed in the early stage of bonding. **Figure 2.13** shows the microstructure of the coating adjacent to the bonding interface and EDX analysis. Although the temperature is below the ignition temperature for the combustion synthesis of Al-Ti, Al_3Ti and dendritic compound consisted of Al and Cu were formed. **Figure 2.14** shows the X-ray diffraction pattern of the coating around this area. This dendritic phase was identified as Al_2Cu, which was formed on the bonding interface and once melted even by heating to 783K. **Figure 2.15** shows the Al-Cu binary phase diagram [22]. It was reported that rapid heating of the mixed powder of Al and Cu induces the combustion synthesis of γ_2 [23]. As the eutectic reaction between Al and θ took place at 821K, the combustion synthesis reaction occurred between Al and Cu, and the exothermic heat raised the temperature over the eutectic temperature (821K) adjacent to the bonding interface. This melting can be confirmed by the existence of solidification structured

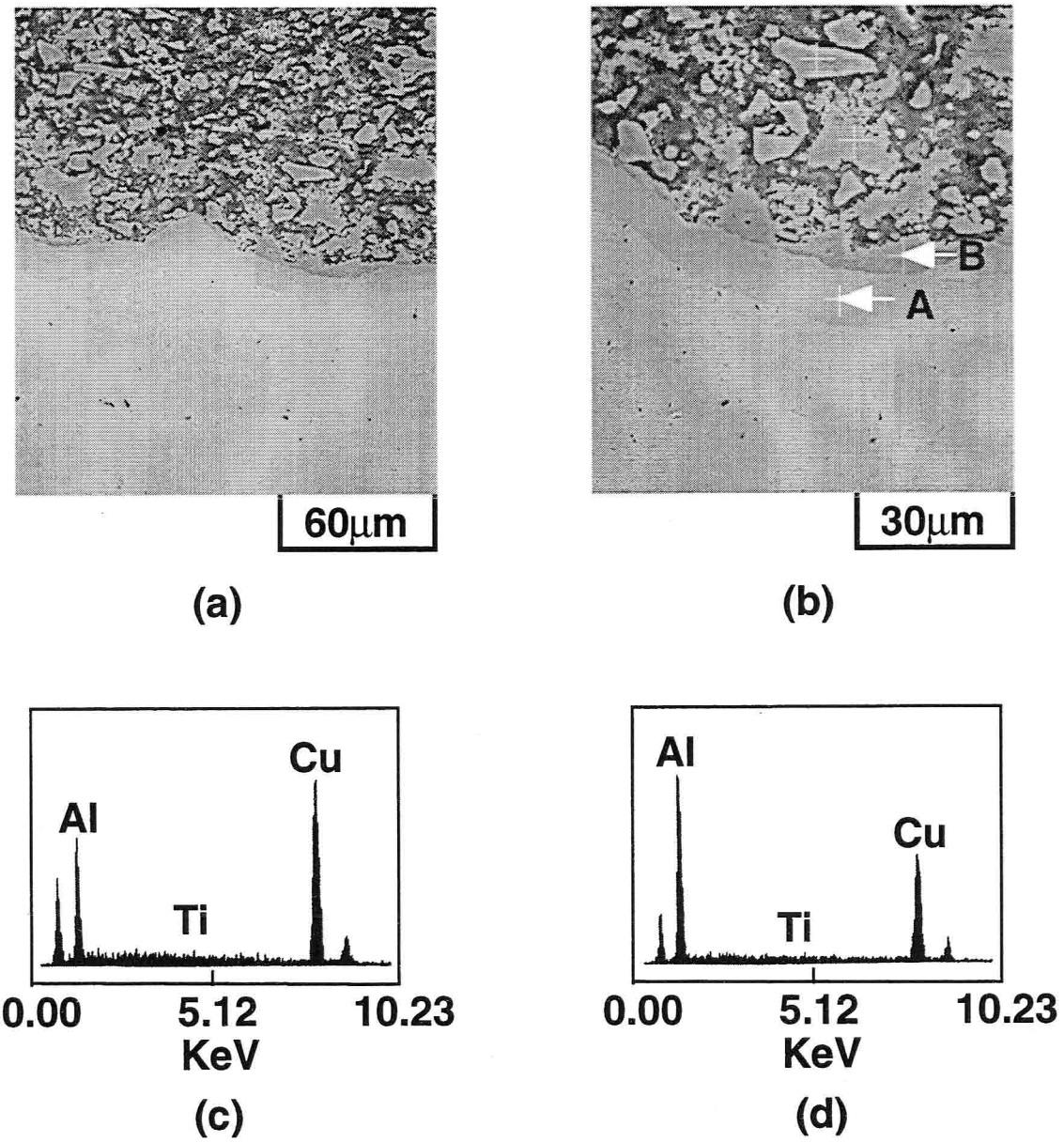

Fig. 2.12 (a) Microstructures at the bonding interface of the sample shown in **Fig. 2.11**, *(b) higher magnification of (a), (c) EDX analysis of A in (b), and (d) B in (b).*

dendrite Al_2Cu as seen in **Fig. 2.13**. Subsequently the melted Al-Cu ignited the combustion synthesis with Ti resulting in the formation of Al_3Ti or Al_5CuTi_2 [24] as shown in **Fig. 2.9(c)** and this reaction is propagated toward the coating. However, the outer coating consisted of unreacted Al and Ti as shown in **Fig. 2.16**. In conclusion, since the temperature adjacent to the bonding interface was raised due to the formation of γ_2 phase, Al and Cu formed a eutectic liquid phase, which ignited the combustion synthesis in the coating. Probably due to the absence of sufficient heat, however, the combustion synthesis reaction was not sustained and stopped on the halfway. Unreacted Al and Ti near the outer coating reacted and formed Al_3Ti by subsequently heating over the ignition temperature as shown in **Fig. 2.9(b)**.

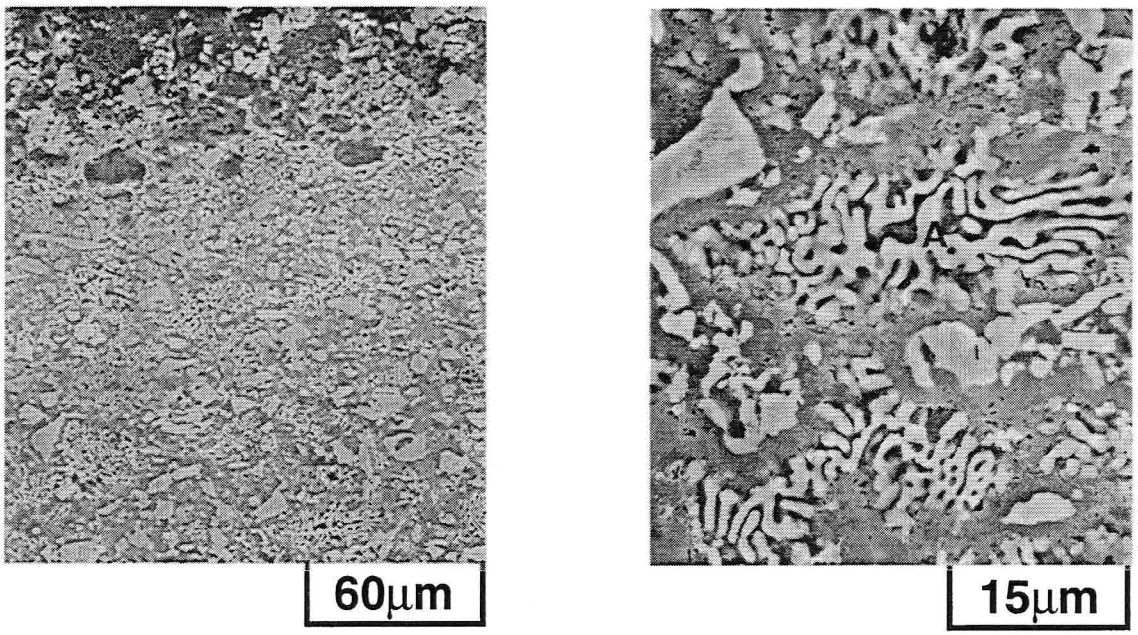

Fig. 2.13 *(a) Microstructure of the coating adjacent to bonding interface of the sample shown in* ***Fig. 2.11****, (b) higher magnification of (a), and (c) EDX analysis of A in (b).*

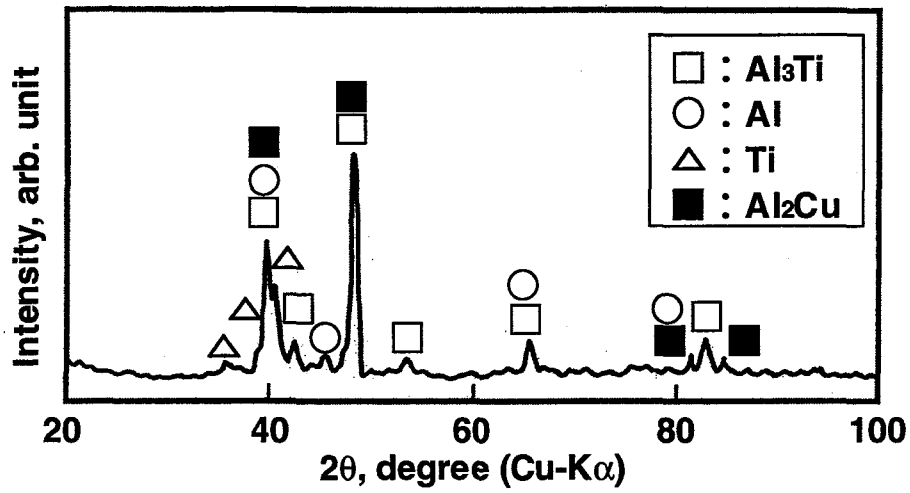

Fig. 2.14 *X-ray diffraction pattern of the coating shown in* ***Fig. 2.13.***

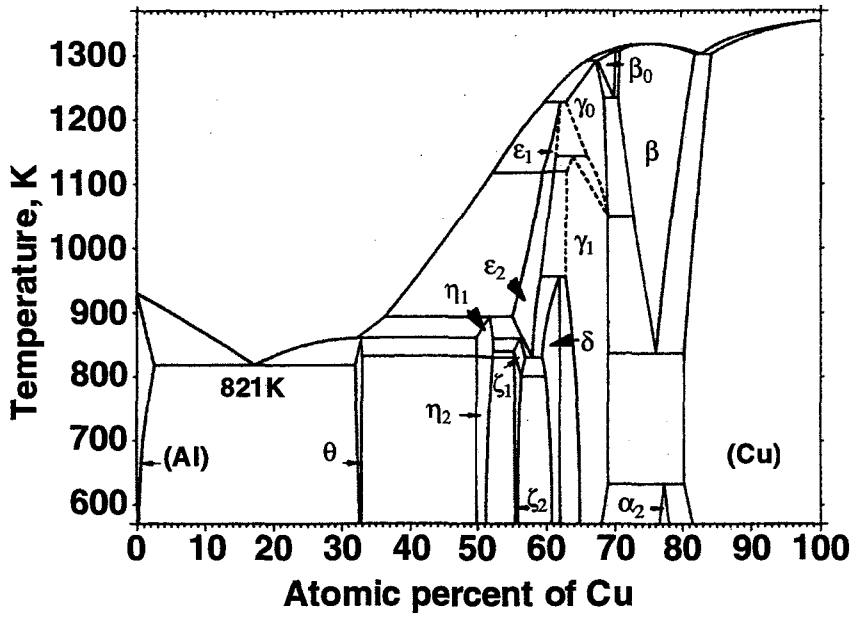

Fig. 2.15 *Binary phase diagram of Al-Cu system* [22].

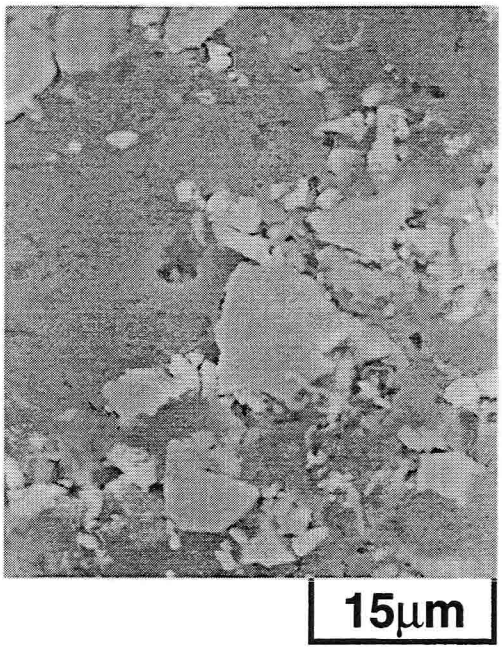

Fig. 2.16 Microstructure of the outer coating shown in ***Fig. 2.11****.*

Figure 2.17 shows the change in unreacted residual Ti ratio as a function of holding time. The residual Ti ratio shows almost no change against the holding time. As the almost homogeneous Al_3Ti coating could be formed on the TiAl substrate that way described in the previous section, it can be found that Al amount which was expected to react with Ti and to form Al_3Ti was decreased in the coating when formed on the Cu substrate. This decrease in Al is considered due to the reaction between Al and Cu, and

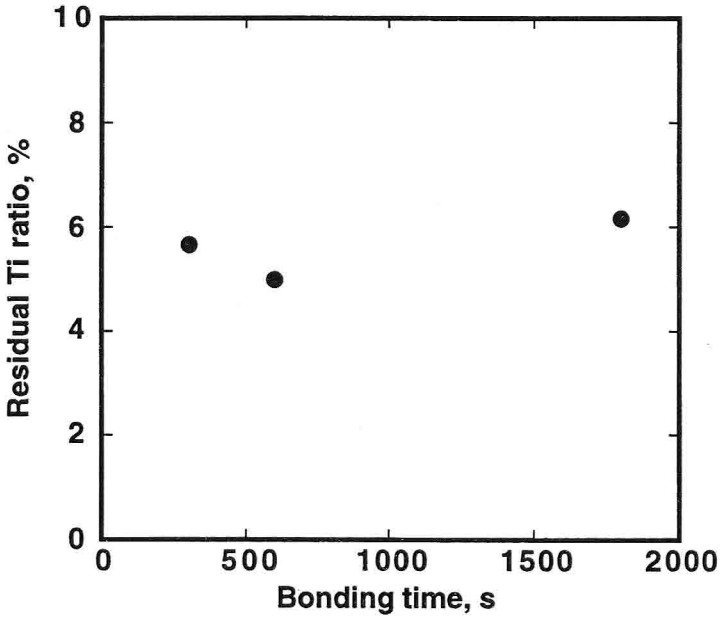

Fig. 2.17 Effect of bonding time on unreacted residual Ti ratio of the coating formed on the Cu substrate at 973K under 20MPa.

the outflow of Al, or eutectic liquid phase. So change of the composition to Al-rich and pressure control are considered to be effective to form a homogeneous Al_3Ti coating. **Figure 2.18** shows the microstructure of the Al_3Ti coating formed on the Cu substrate using the Al-20at.%Ti powders at 973K for 300s. The applied pressure was 20MPa to 773K, and 10MPa from 773K to 973K which way decreased in order to prevent out-flowing of the liquid phase. The microstructure of the coating was almost homogeneous.

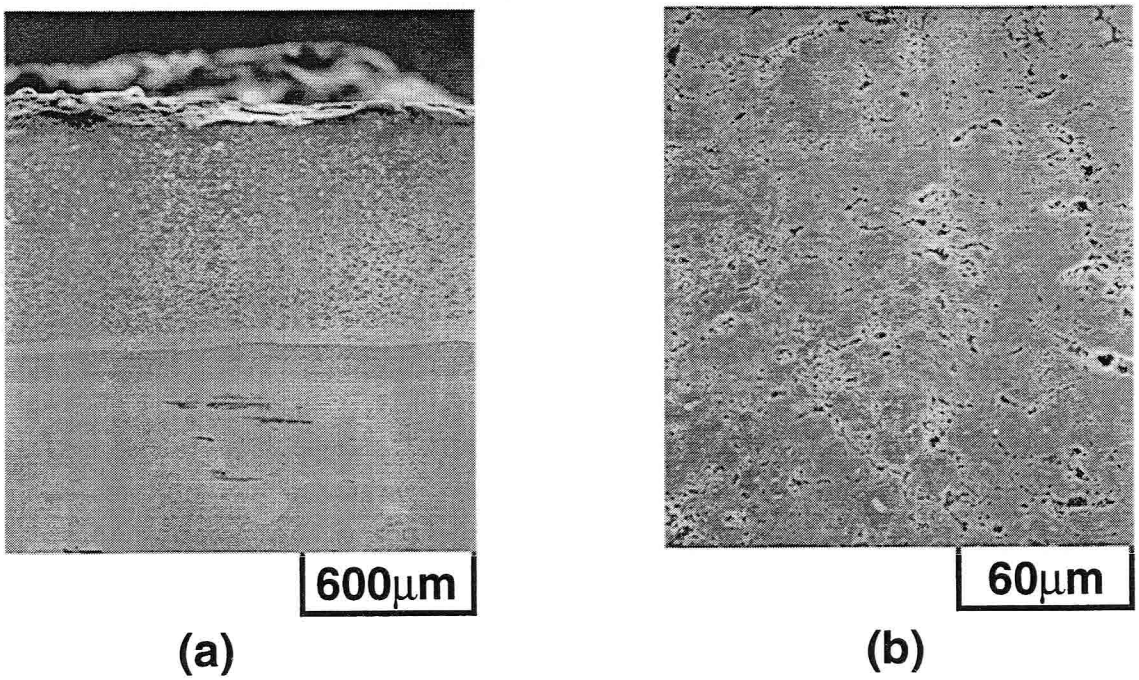

Fig. 2.18 *Al_3Ti coating formed on the Cu substrate using the Al-20at.%Ti powders at 973K for 300s. (a) General view and (b) microstructure of the coating.*

2.3.4 Properties of Al_3Ti coatings

Figure 2.19 shows the Vickers hardness profiles of the Al_3Ti coating on the TiAl and Cu substrates as a function of distance from the bonding interface. The hardness of the coating was HV630, which is almost the same as that obtained for casting. The coating formed on the Cu substrate exhibited gradual increase in hardness toward the bonding interface, indicating no brittle Al-Ti-Cu compounds formation.

Figure 2.20 shows the wear coefficients of the Al_3Ti coating and the TiAl, Cu substrate. In the present abrasion condition, the wear mechanism can be considered to be an adhesion wearing due to the heat of friction between the test material and the abrasing material. In this mechanism, wear properties are affected by hardness and melting temperature. Since the Al_3Ti has the higher melting temperature and hardness, the coating of Al_3Ti should have the better wear coefficient than that of TiAl, Cu substrate. The wear coefficient of the Al_3Ti coating was nearly the same as that of the Al_3Ti ingot material.

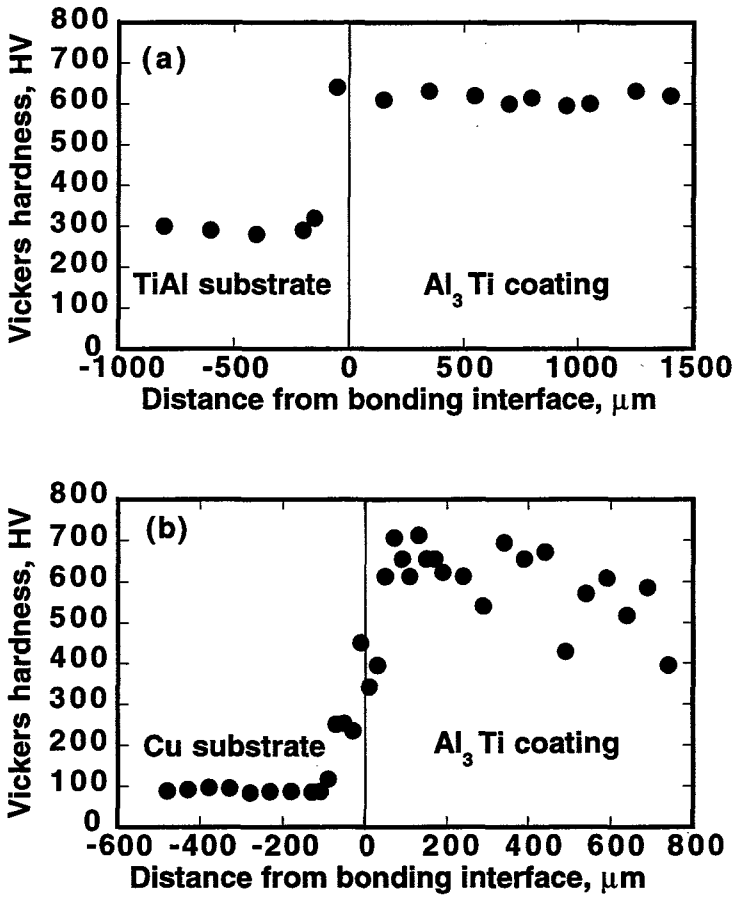

Fig. 2.19 Vickers hardness diprofiles of the Al_3Ti coating on the (a) TiAl and (b) Cu substrates.

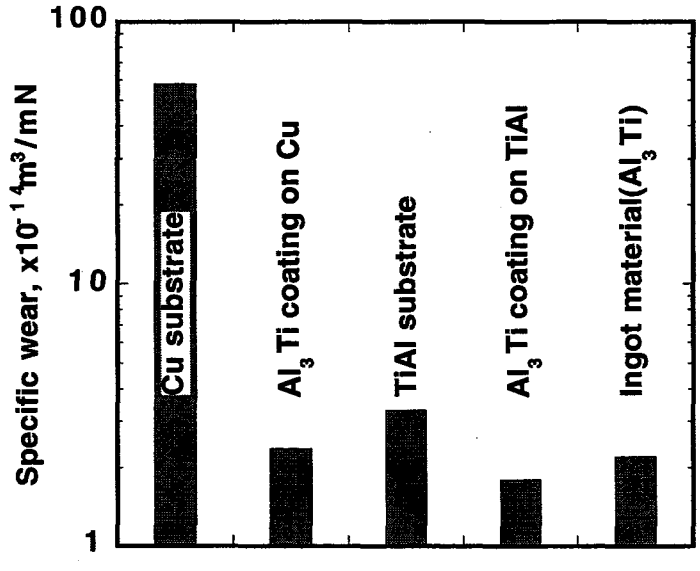

Fig. 2.20 Specific wears of the TiAl, Cu substrates, Al_3Ti coating and ingot Al_3Ti.

2.4 Conclusions

The Al_3Ti was fabricated using a mixed powder of elemental Al and Ti by the combustion synthesis. Simultaneously, the Al_3Ti was bonded with the TiAl and Cu substrate. The main results obtained in this chapter can be summarized as follows.

(1) Al and Ti in the mixed powder spontaneously reacted and formed the Al_3Ti near the melting temperature of Al.

(2) During the combustion synthesis of Al_3Ti, mainly the Al in the mixed powder reacted with the TiAl or Cu substrates and formed reaction layers of Al_3Ti, or Al-Ti-Cu compounds, which could achieve the bonding of both materials.

(3) The voids which were tend to be introduced in the combustion synthesized Al_3Ti could be decreased by increasing the bonding pressure. The use of green compacts with a less volume fraction of voids was also effective to decrease voids of the Al_3Ti.

(4) For the formation of the Al_3Ti coating on the Cu substrate, the composition of a green compact was favored to be rich in Al content against the stoichiometric Al_3Ti to form a homogeneous coating because Al was exhausted in the reaction with the Cu substrate and the liquid phase out-flows.

(5) The obtained Al_3Ti coating showed almost the same hardness and wear properties as the cast Al_3Ti.

References

[1] T.Kawabata, T.Kanai and O.Izumi, *Acta Metall.*, **33**(1985), 1355.

[2] Y.Umakoshi, M.Yamaguchi, T.Sakagami and T.Yamane, *J. Mater. Sci.*, **24**(1989), 1599.

[3] A.Hirose, Y.Arita and K.F.Kobayashi, *J. Mater. Sci.*, **30**(1995), 970.

[4] A.Hirose, Y.Arita and K.F.Kobayashi, *J. Soc. Mater. Sci. Jpn.*, **44**(1995), 1145.

[5] Y.Nakao, K.Shinozaki and M.Hamada, *ISIJ Int.*, **31**(1991), 1260.

[6] G.Cam, H.Clemens, R.Gerling and M.Kocak, *Intermetallics*, **7**(1999), 1025.

[7] L.M.Gulantucci, G.Ruta and S.Magnanelli, *High Power Laser*, Pargamon, Oxford, (1989), 78.

[8] A.Hirose and K.F.Kobayashi, *Mater. Sci. Eng. A*, **174**(1994), 199.

[9] J.Ogoshi, T.Sada and M.Mizuno, *J. Jpn. Machine Soc.*, **21**(1955), 555.

[10] K.Uenishi, H.Sumi and K.F.Kobayashi, *Z. Metallkd.*, **86**(1995), 64.

[11] J.Pouliquen, S.Offret and J.de.Fouquet, *C. R. Acad. Sci. C*, **274**(1972), 1760.

[12] J.Mackowiak and L.L.Shreir, *J. Less-Common Metals*, **15**(1968), 341.

[13] J.Subrahmanyam and M.Vijayakumar, *J. Mater. Sci.*, **27**(1992), 6249.

[14] W.W.Liang, *CALPHAD*, **7**(1983), 13.

[15] M.Otaguchi, Y.Kaieda, N.Oguro, S. Shite and T.Oie, *J. Jpn. Inst. Metals*, **54**(1990), 214.

[16] R.W.Rice and W.J.McDonough, *J. Amer. Ceram. Soc.*, **68**(1985), 122.
[17] R.Lerf and D.Morris, *Mater. Sci. Eng. A*, **128**(1990), 119.
[18] K.Uenishi, H.Sumi and K.F.Kobayashi, *Z.Metallkd.*, **86**(1995), 270.
[19] F.J.J.van Loo and G.D.Rieck, *Acta Metall.*, **21**(1973), 73.
[20] M.B.Winnicka and R.A.Varin, *Scripta Metall.*, **23**(1989), 1199.
[21] T.Enjo, K.Ikeuchi and N.Akikawa, *J. Jpn. Welding Soc.*, **48**(1979), 32.
[22] J.L.Murray, *Int. Met. Rev.*, **30**(1985), 211.
[23] H.Mitani and M.Yokota, *J. Jpn. Inst. Metals*, **34**(1970), 902.
[24] P.Virdis and U.Zwicker, *Z. Metallkd.*, **62**(1971), 46.

Chapter 3 Application of mechanically alloyed powders to form homogeneous coatings of Al_3Ti

3.1 Introduction

In Chapter 2, thick coatings of the Al_3Ti were formed on the TiAl and Cu substrates by the combustion synthesis and exhibited almost the same wear properties as the cast Al_3Ti. However, the Al and Ti did not react completely and the microstructure of the coating remained some inhomogeneity probably due to the out-flowing of the liquid phases and the shorter diffusivity of each element than the particle size of starting powders. For the formation of homogeneous coatings, (1) to fabricate at a lower temperature to prevent the out-flowing of the liquid phases and the reaction between the coating and substrate, and (2) application of fine mixed particles to reduce the diffusion distance are considered to be effective.

Mechanical alloying (MA) is a process to obtain homogeneously alloyed powders from elemental ones, and a high energy ball milling operation involving repeated welding, fracturing and rewelding of powder particles. During the initial stages of milling, lamellar structures or fine dispersions of elemental powders are produced. Since further milling leads to refinement in the lamellar space or particle size and to increase the interfacial region between elemental powders, the reactivity between elements is further improved. Furthermore, since there are little contamination such as an oxide layer at the lamellar interface, the ignition temperature for the MA powders becomes lower [1, 2].

The application of the MA powders is considered to be effective to form homogeneous coatings of the Al_3Ti due to (1) a lower ignition temperature and (2) fine mixed elemental powders.

In this chapter, the effect of initial particle size in the reactant powders on the microstructure of the products formed by the combustion synthesis was investigated. By discussing the compound formation mechanism and diffusion kinetics during the combustion synthesis, the initial particle size required for complete reaction was estimated. By applying the MA process to obtain fine mixed powders, a homogeneous Al_3Ti layer was formed and its wear properties were evaluated.

3.2 Experimental

Al (99.9%, <20μm) and Ti (99.9%, <44μm or <10μm) powders were mixed in a composition of Al-25at.%Ti. MA was performed by vibrating ball mill (Nisshin Giken, SUPER MISUNI NEV-MA8) with a frequency of 13.1Hz. The mixed powders were put into a cylindrical stainless vial (SUS304, $9.0 \times 10^{-5} m^3$) with stainless balls (SUS304, ϕ:11mm) under Ar gas atmosphere. The weight ratio of balls to powders was fixed to 17.

To avoid the adhesion of powders to balls and vial, ethanol with 1wt.% of the mixed powders was added as a process control agent. The obtained MA powders were cold pressed under 567MPa to a cylindrical powder compact (ϕ:10.6mm, 1.6mm thickness) with a relative density of 87.5%. The powder compact was hot pressed at 773K for 3.6ks under 100MPa to the relative density of 95%.

Combustion synthesis and bonding, microstructural observation and evaluation of coatings were performed as described in Chapter 2.

3.3 Results and Discussion

3.3.1 Effect of initial Ti particle size on microstructure of Al_3Ti

Figure 3.1 shows DSC traces of the green compacts including Ti powders with particle sizes of 10μm and 44μm. When smaller Ti particles were used, an exothermal peak started from about 600K, and become sharp at about 930K which is close to the melting point of Al. In this case, the combustion synthesis is interpreted to be the reaction between solid Ti and molten Al. On the contrary, there was no exothermic reaction both for the first and the second run when larger Ti particles were used. **Figure 3.2** shows the microstructures of green compacts heated to1003K in DSC measurement. Although almost all of Al and Ti reacted and formed Al_3Ti (A in **Fig. 3.2(a)**) by the combustion synthesis when using 10μm Ti particles, Al_3Ti was only formed at the Al/Ti interface (B in **Fig. 3.2(b)**) and Ti particles remained without any reaction with Al when

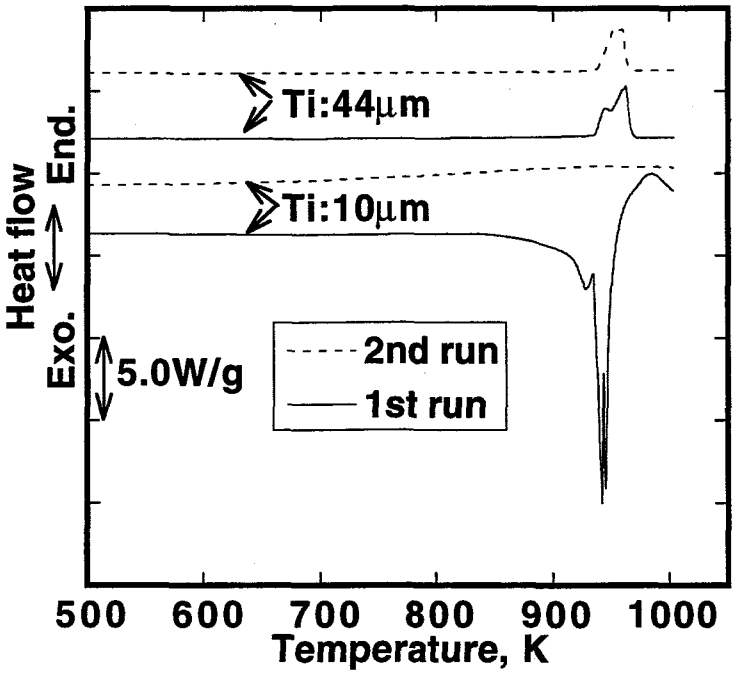

Fig. 3.1 DSC traces of the green compacts including Ti powders with particle sizes of 10μm and 44μm.

using 40μm Ti particles (C in **Fig. 3.2(b)**). Since the interface area decreased for larger Ti particles, the reactivity became low so that unreacted Ti and Al elements seemed to remain.

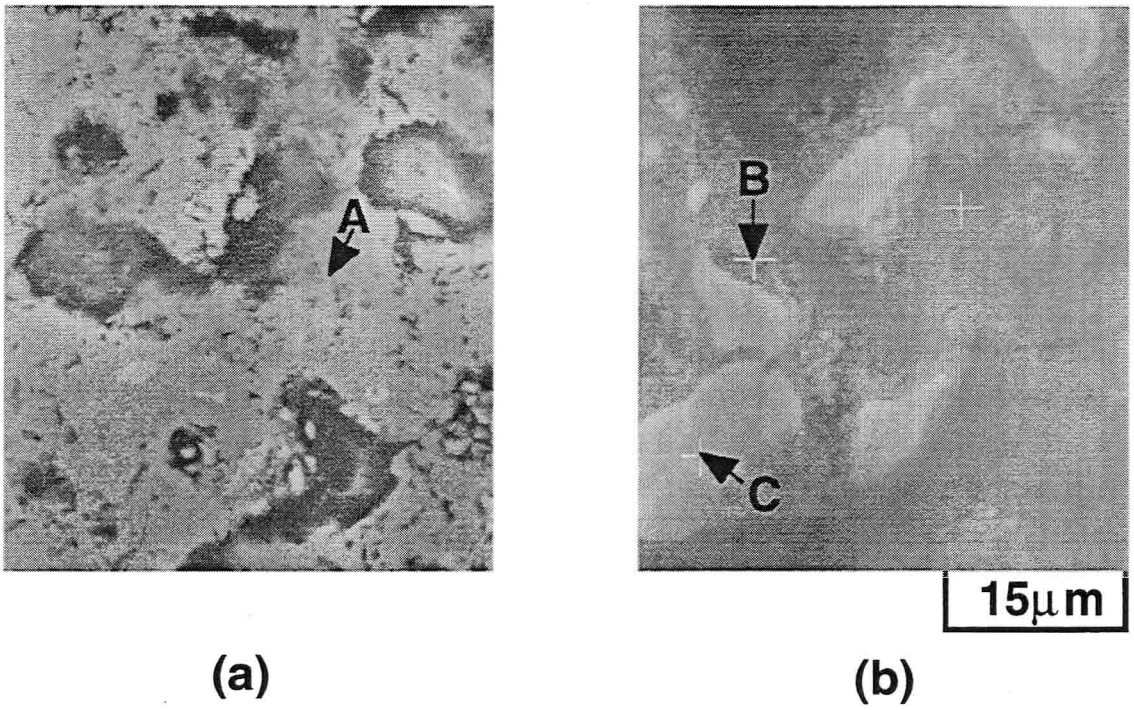

Fig. 3.2 Microstructures of the green compacts including Ti powders with particle sizes of (a) 10μm and (b) 44μm heated to 1003K in DSC measurement.

For the optimization of the Ti particle size to obtain homogeneous a Al_3Ti coating after the combustion synthesis, a spherical shell model [3, 4] shown in **Fig. 3.3** was applied to the reaction between Al and Ti. Based on the microstructural observation, the mixed powders are consisted of Ti particles with a initial diameter of r_o and which is surrounded by Al particles, and Ti particle size decreases to r_i as the reaction develops.

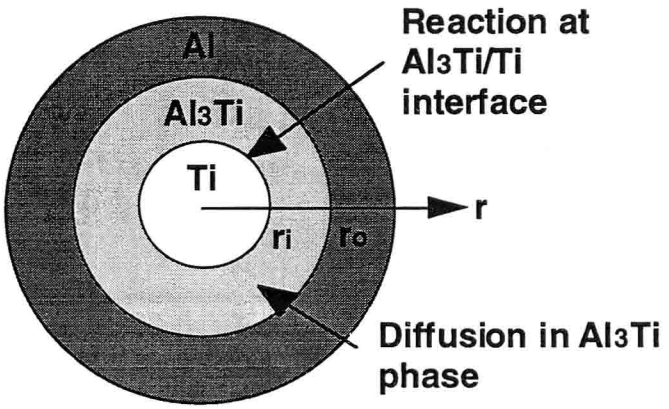

Fig. 3.3 Schematic illustration of a spherical shell model for the formation of Al_3Ti.

It is assumed that any other compounds such as TiAl but Al_3Ti are formed [5-7] through the following two processes. One is the diffusion of Al in Al_3Ti to the Al_3Ti/Ti interface, and another is the reaction between Al and Ti at the Al_3Ti/Ti interface.

The diffusion velocity (v_d, mol/s) can be represented by eq. (3.1).

$$v_d = 4\pi r^2 \frac{D_{Al}}{\gamma_{Al}}\left(\frac{\partial a_{Al}}{\partial r}\right) \tag{3.1}$$

where D_{Al}, γ_{Al} and a_{Al} are the diffusion coefficient of Al in Al_3Ti, the activity coefficient and the activity of Al in Al_3Ti, respectively. By the integration of this equation by r on the condition that v_d is constant between r_i and r_o, eq. (3.2) can be obtained.

$$v_d = 4\pi \frac{D_{Al}}{\gamma_{Al}} \cdot \frac{r_o r_i}{r_o - r_i}(1 - a_{Al}) \tag{3.2}$$

The reaction velocity (v_d, mol/s) can be represented by eq. (3.3).

$$v_c = \frac{4}{3}\pi r_i^2 (k_c \cdot a_{Al} - k_b) \tag{3.3}$$

$$Al + \frac{1}{3}Ti \underset{k_b}{\overset{k_c}{\rightleftharpoons}} \frac{1}{3}Al_3Ti \tag{3.4}$$

where k_c and k_b is rate constants toward the direction as shown in eq. (3.4). By taking the conservation law of mass at the Al_3Ti/Ti interface into consideration, the overall reaction velocity, v can be represented by eq. (3.5).

$$v = \frac{4\pi r_o^2}{\dfrac{\gamma_{Al} \cdot r_o (r_o - r_i)}{r_i \cdot D_{Al}} + \dfrac{3r_o^2}{r_i^2 \cdot k_c}} \tag{3.5}$$

Since this velocity was equal to that of the decrease of Ti volume, the Ti particle size to form the homogeneous Al_3Ti can be obtained by integration with r_i from r_o to zero. In the present calculation, D_{Al}=3.82x10^{2}exp(-2.93x10^5/RT) m^2/s [8], k_c=5.55x10^{3}exp (-1.25x10^5/RT) mol/(m^{2}s) [3], and γ_{Al}=1 were used. **Figure 3.4** shows the estimated Ti particle size required for complete formation of Al_3Ti at various temperature and was about 1μm at 973K for 180s. Since Ti is easily oxidized and the production of such fine powders is difficult, application of the MA process is considered to be effective to obtain the mixed powder including fine Ti particles.

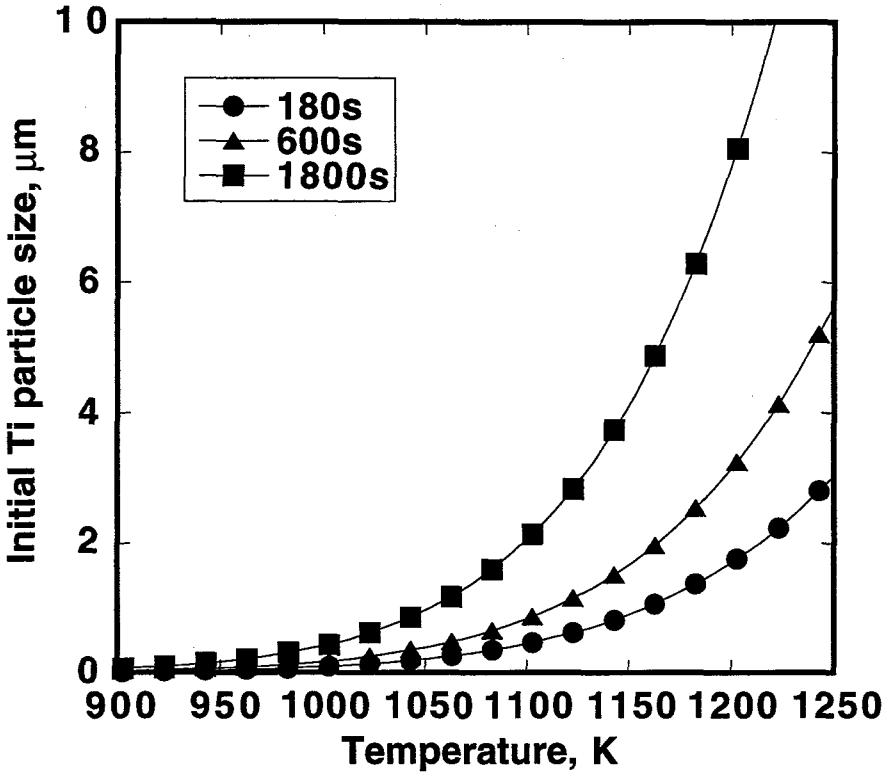

Fig. 3.4 Calculated initial Ti particle sizes required for homogenization under the corresponding heat treatment conditions.

3.3.2 Fine mixing of Al and Ti powders by MA

Figure 3.5 shows the microstructures of the MA powders. It is found that the bright contrasted Ti with particle size of 10μm dispersed in the Al matrix after 18ks MA. It can be also observed that the Ti particles embeded in the Al matrix became fine to less than about 1μm in size by repetitive fracturing and kneading after 36ks MA. After 72ks MA, it became almost impossible to distinguish Al and Ti particles. **Figure 3.6** shows the X-ray diffraction patterns of the MA powders. Although each Al and Ti particle was distinguishable within 36ks MA, the diffraction patterns became broader with increasing the MA time. Finally, only broadened Al peaks were observed after 72ks MA. As Al peaks shifted to higher angle, it is considered that the super saturated solid solution of Al(Ti) was formed [9-12]. However, any compound phase formation was not detected by the X-ray diffraction analysis.

Figure 3.7 shows the DSC traces of the MA powders. Compared with the combustion synthesis of elemental Al-Ti powders, the exothermal peak was broad and shifted to lower temperatures. Because these reactions of the MA powders occurred below the Al melting point, it was interpreted to be the solid state reaction. **Figure 3.8** shows the X-ray diffraction patterns of the MA powders after continuous heating to 1003K. Regardless of the MA time, the Al_3Ti phase was formed after the heat treatment. A high

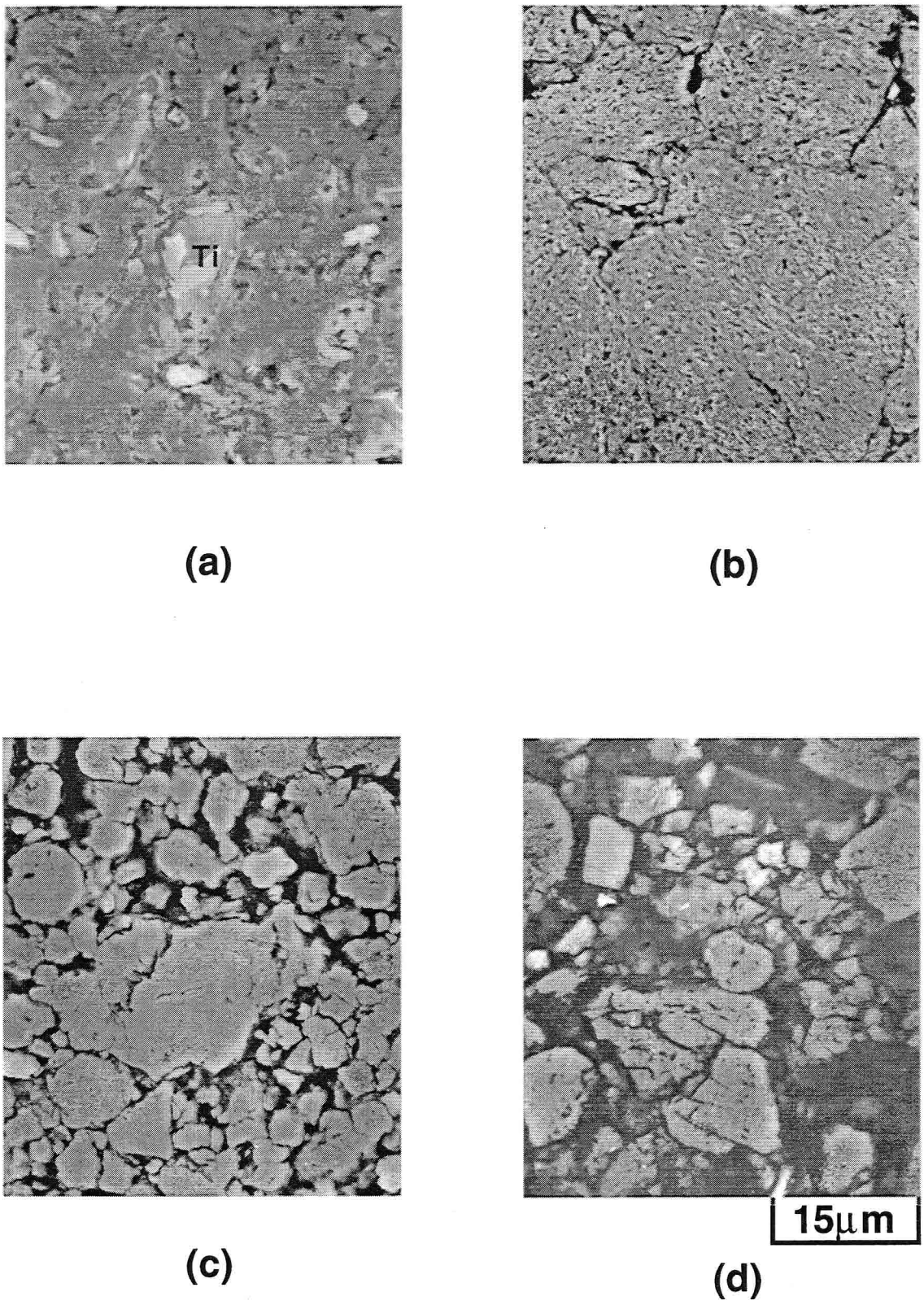

Fig. 3.5 *Microstructures of the powders mechanically alloyed for (a) 18ks, (b)36ks, (c) 72ks and (d) 144ks.*

temperature phase, Al_5Ti_2 was also formed in the powders mechanically alloyed for more than 72ks. Gerasimov *et al.* reported that the Al_5Ti_2 phase formed by the annealing of MA powders with a composition of Al-25at.%Ti at low temperature (870K) [13].

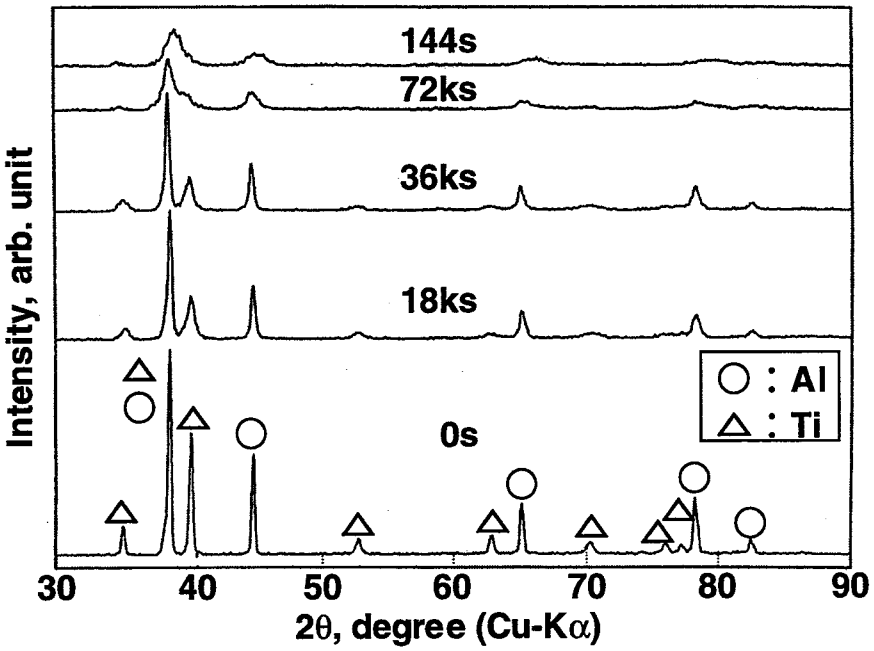

Fig. 3.6 X-ray diffraction patterns of the powders mechanically alloyed for various time.

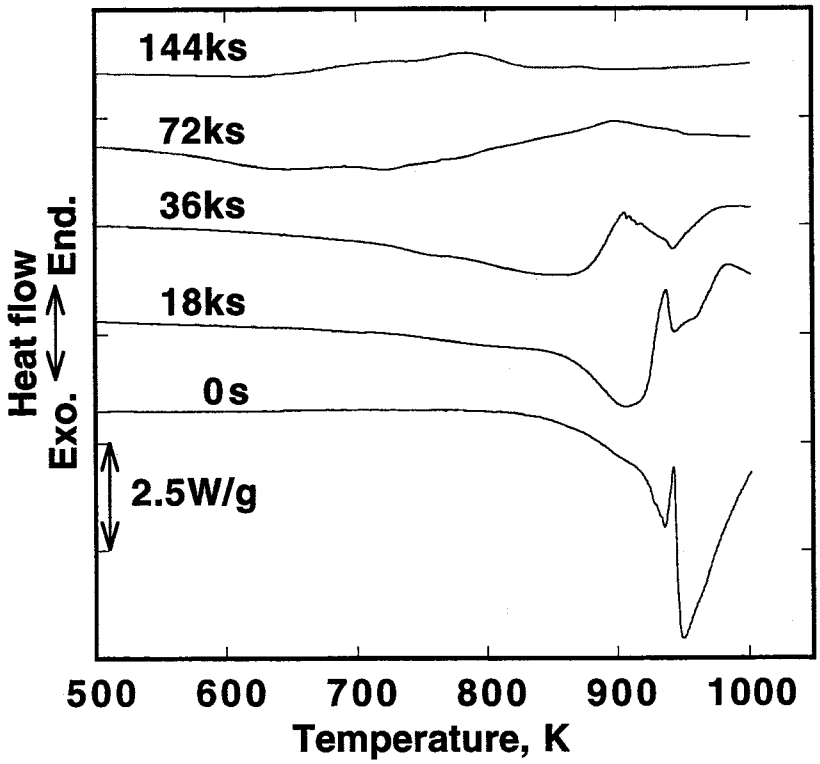

Fig. 3.7 DSC traces of the powders mechanically alloyed for various time.

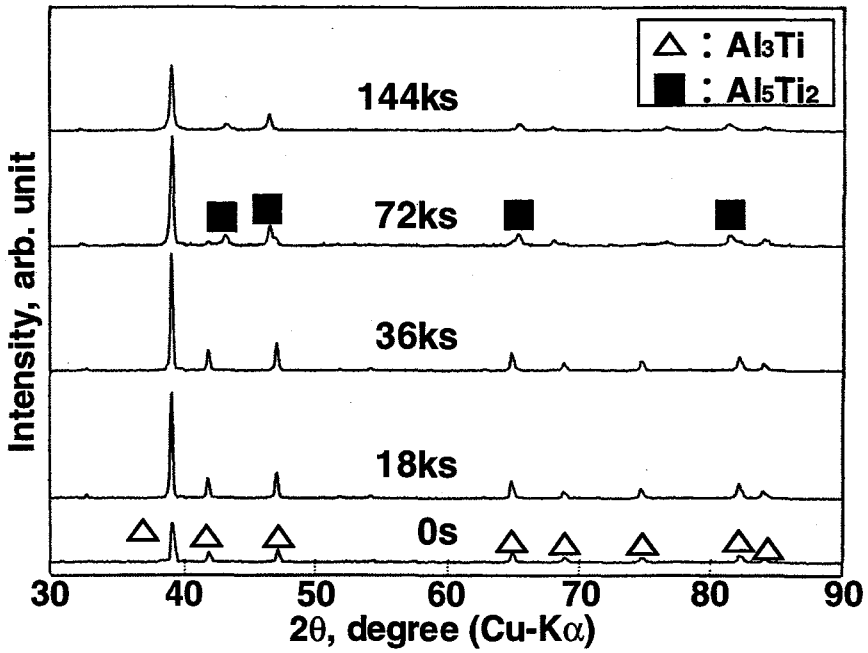

Fig. 3.8 X-ray diffraction patterns of the powders mechanically alloyed for various time and heated to 1003K in DSC measurement.

Since this surface modification process is also carried out at relatively low temperature, it can be considered that too long time of MA causes inhomogeneous microstructures. **Figure 3.9** shows the microstructures of the MA powders after continuous heating to 1003K in DSC measurement. It is found that unreacted residual Ti particles were included in the 18ks MA powders. However, the 36ks MA powders made the Al_3Ti almost homogeneous.

In conclusion, by using MA powder as a starting material, the Al_3Ti could be synthesized at lower temperature and its microstructure revealed the homogeneous Al_3Ti without unreacted elements.

3.3.3 Formation of homogeneous Al_3Ti coatings and their properties

Figure 3.10 shows the microstructures of the Al_3Ti coating on a Cu substrate formed at 973K for 180s under 20MPa. **Figure 3.11** shows the X-ray diffraction patterns of the reaction layers. The reaction layers formed at the bonding interface were the fcc Cu(Al) solid solution, $Ti(Al,Cu)_2$ and Al_5CuTi_2 from the Cu substrate as shown in **Fig. 3.10(c)**, and their widthes were 40, 20 and 70μm, respectively. Though the reaction layers were composed of same phases as when using the as-mixed powder, their width decreased. As the reaction between fine mixed Al and Ti in the MA powders started below the ignition temperature for the Al-Cu combustion synthesis, Al reacts with Ti earlier than with Cu. Therefore, the reaction between the coating and the Cu substrate changes mainly to the reaction between Al_3Ti and Cu, resulting in the decrease in the width of reaction layers.

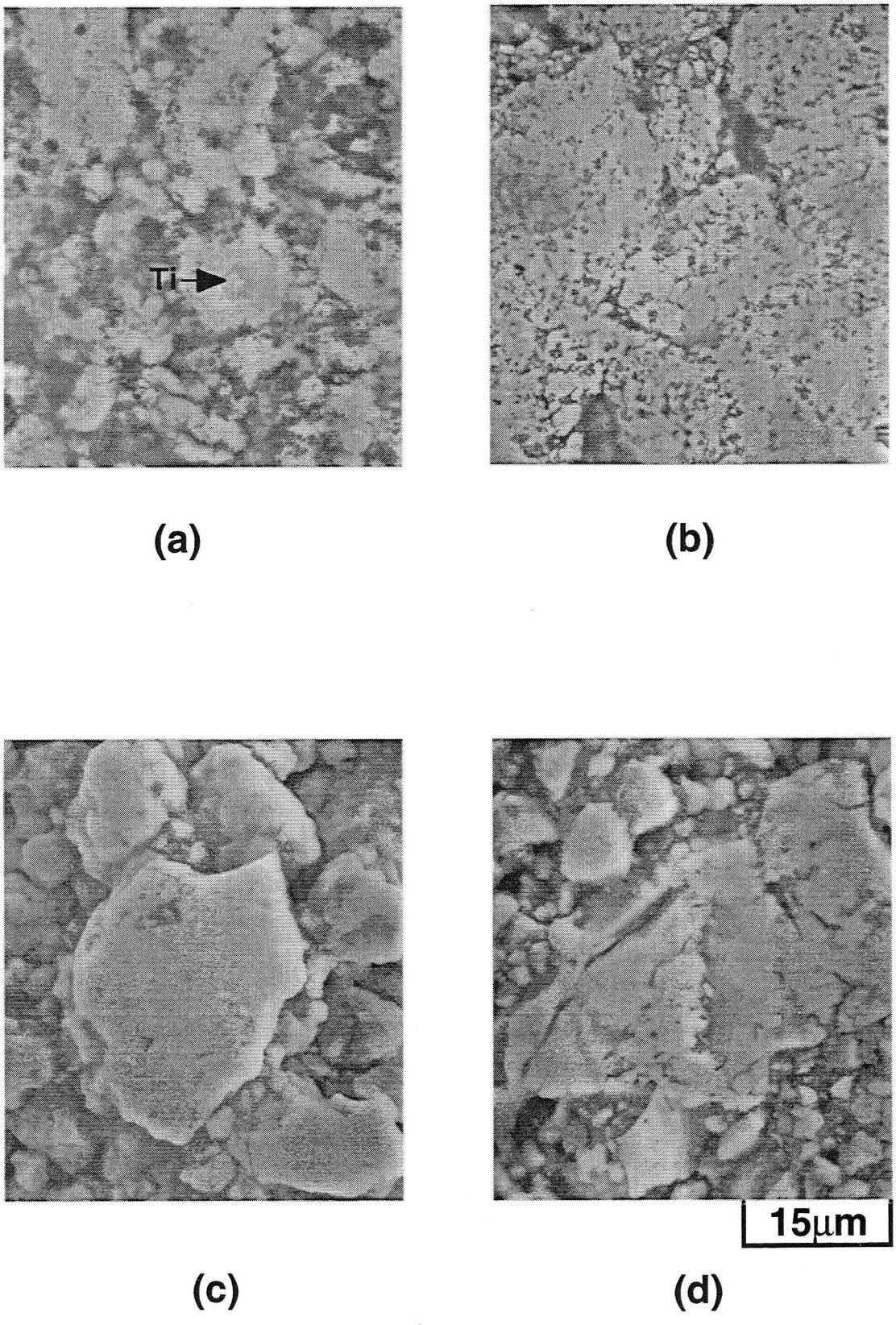

Fig. 3.9 *Microstructures of the powders mechanically alloyed for (a) 18ks, (b)36ks, (c) 72ks and (d) 144ks and heated to 1003K by DSC.*

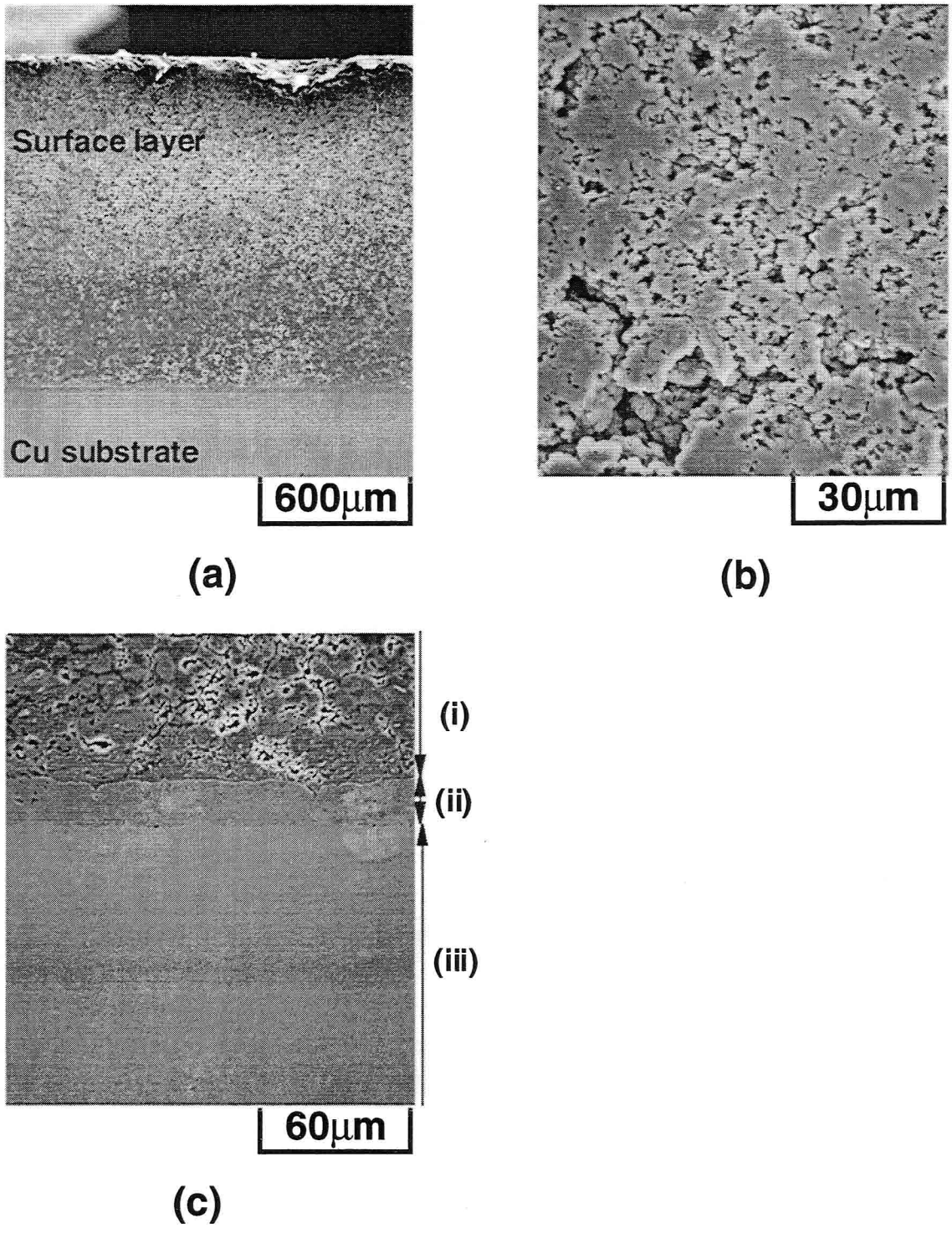

Fig. 3.10 *Al_3Ti coating formed on the Cu substrate using the 36ks MA powders at 973K for 300s under 20MPa. (a) General view, microstructures of (b) coating, and (c) bonding interface.*

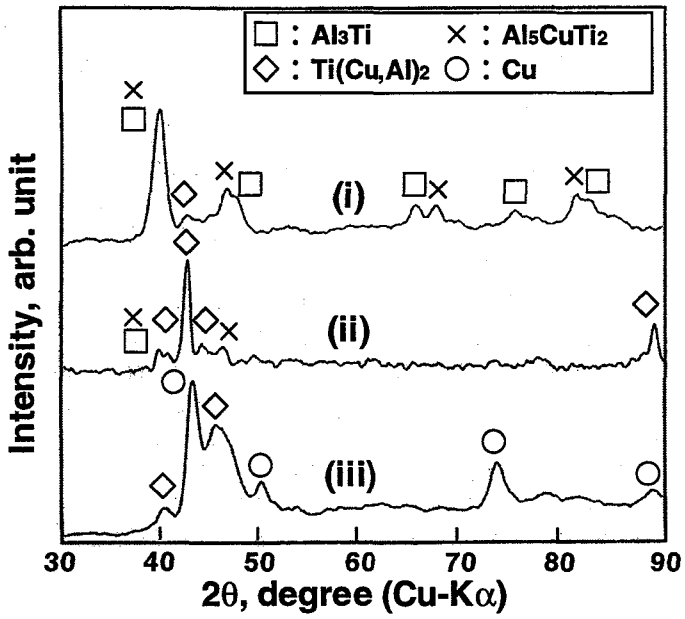

Fig. 3.11 X-ray diffraction patterns of the reaction layers formed at the bonding interface of the Al_3Ti coating on the Cu substrate.

In the coating, a homogeneous Al_3Ti phase was formed and no unreacted residual element was observed. As mentioned in Chapter 2, it is generally recognized that the combustion synthesized compounds easily introduce many voids which are distinguished into two different types of void (1) intrinsic and (2) extrinsic. Thus it would be required for the densification of the synthesized Al_3Ti to apply the external pressure, hold at high temperature and prepare the green compact with fewer voids.

However, the increase of the external pressure causes the deformation of Cu substrates as shown in **Fig. 3.12**. Therefore, the pressure was fixed to 20MPa in this research. **Figure 3.13** shows the changes in void ratio as a function of holding time. When the sample was held at 973K for 3.6ks, the voids in Al_3Ti layer decreased from 11.8% to 8.2%, but further densification was not achieved by holding longer time than 3.6ks at 973K. To decrease voids in the green compact, it was hot pressed at 773K, which was lower than the ignition temperature, under the pressure of 100MPa for 3.6ks. The application of this pre-sintered compact decreased the void ratio to 6.1%, but the value was still larger compared with the sintered products using no MA powders. It can be considered for this reason that powders were hardened by the reduction of grain size and the deformation hardening of powders during MA process. In conclusion, although application of fine mixing powders by MA process as a precursor was advantageous to form homogeneous Al_3Ti layer, it was difficult to eliminate voids and achieve high densification.

Figure 3.14 shows a Vickers hardness distribution of the Al_3Ti coating formed on the Cu substrate. The Vickers hardness increased gradually from the Cu substrate to the

Al_3Ti coating, and no brittle layer was formed on the bonding interface. The hardness of the Al_3Ti coating was HV600 and similar to the bulk material. **Figure 3.15** shows the specific wears of the Al_3Ti coating, Cu and Ti substrates. By application of pre-sintered compacts, the wear property of the Al_3Ti coating was almost the same as that of the cast bulk material.

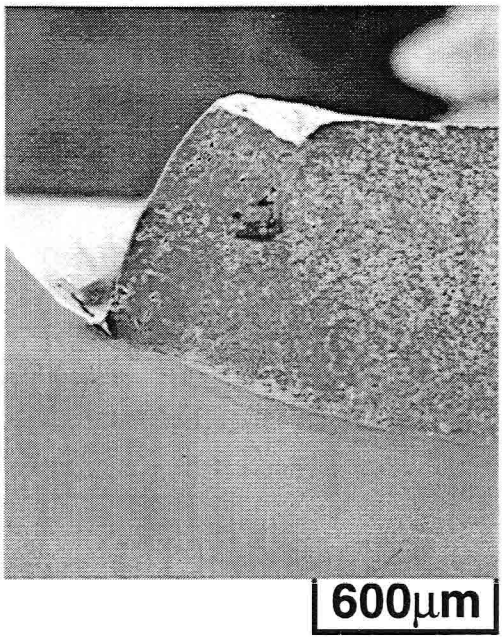

Fig. 3.12 General view of the Al_3Ti coating formed on the Cu substrate under 40MPa.

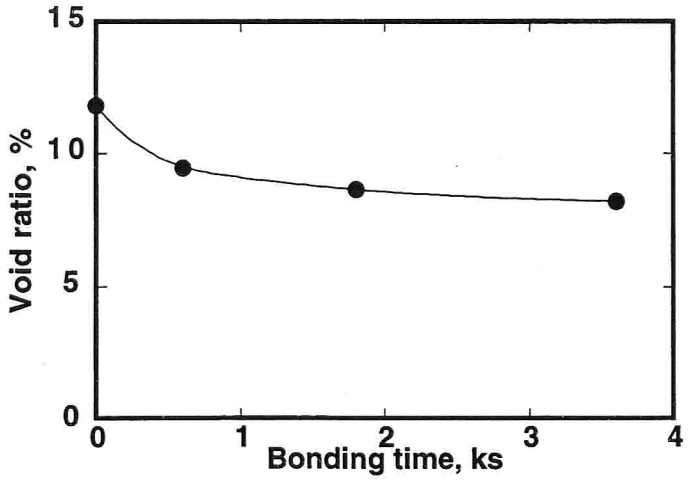

Fig. 3.13 Effect of holding time on the void ratio of the Al_3Ti coating.

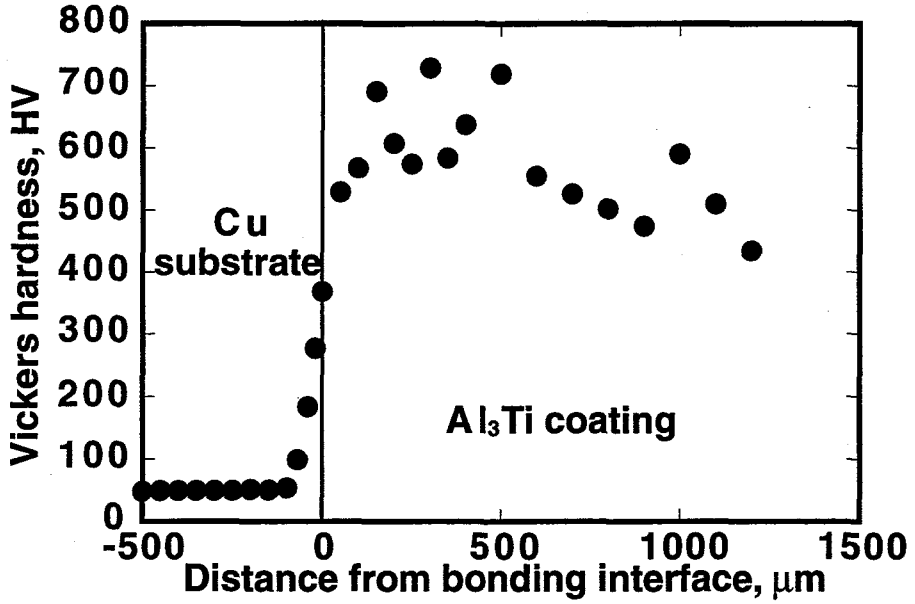

Fig. 3.14 Vickers hardness distribution of the Al_3Ti coating formed on the Cu substrate using the pre-sintered 36ks MA powders.

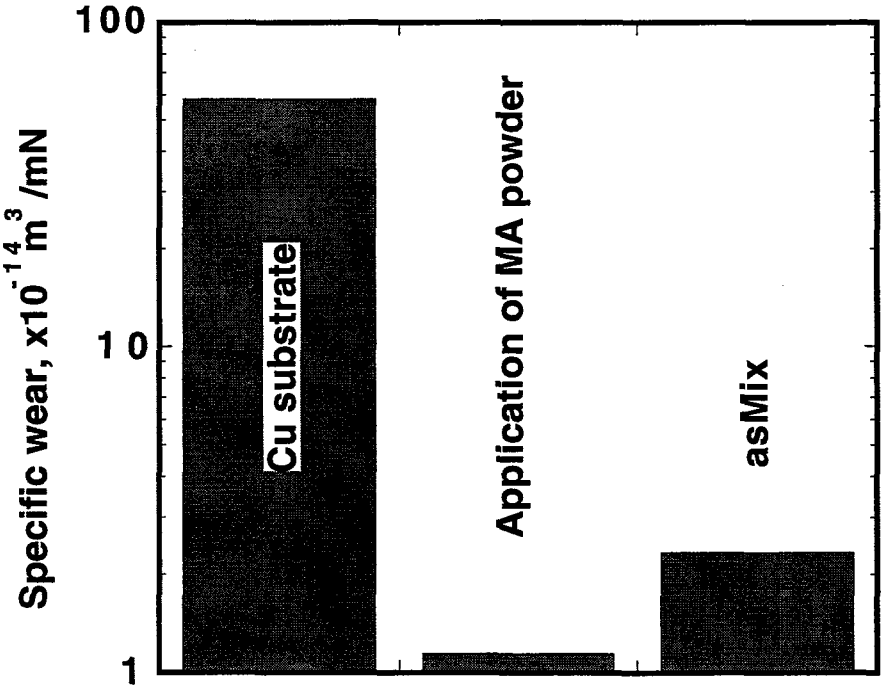

Fig. 3.15 Specific wears of the Cu substrate and Al_3Ti coatings

3.4 Conclusions

The Al_3Ti was formed by the combustion synthesis of the MA powders and simultaneously bonded with the Cu substrate. The main results obtained in this chapter can be summarized as follows.

(1) When larger (<44μm) Ti particles were used, the combustion synthesis reaction hardly occurred due to the decrease of the Al/Ti interface area.

(2) By a spherical shell model including the diffusion kinetics, the relation between Ti particle sizes and the heat treatment conditions to obtain a fully reacted Al_3Ti was estimated.

(3) By applying the fine mixed MA powders including Ti powders with a particle size less than 1μm, completely homogenized Al_3Ti coatings could be formed. However, it was difficult to obtain fully densified coatings due to hardening of powders.

(4) Preparation of dense green compacts were effective to minimize voids and densify the synthesized Al_3Ti coating.

(5) The obtained Al_3Ti coating showed almost the same wear resistance and hardness as a cast Al_3Ti.

References

[1] K.Ishihara, R.Maric, A.Kondo and H.Shingu, *J. Jpn. Soc. Powder Powder Metall.*, **41**(1994), 949.

[2] K.Kobayashi and K.Ozaki, *Mater. Trans., JIM*, **37**(1996), 738.

[3] A.Hibino and R.Watababe, *J. Jpn Inst. Metals*, **55**(1991), 1256.

[4] B.B.L.Seth and H.U.Ross, *Trans. Metall. Soc. AIME*, **233**(1965), 180.

[5] F.J.J. van Loo and G.D.Rieck, *Acta Metall.*, **21**(1973), 61.

[6] T.Enjo, K.Ikeuchi, M.Kanai and T.Maruyama, *J. Jpn. Welding Soc.*, **46**(1977), 32.

[7] K.Nonaka, H.Fujii and H.Nakajima, *J. Jpn. Inst. Metals*, **64**(2000), 85.

[8] J.Pouliquen, S.Offret and J.de.Fouquet, *C. R. Acad. Sci., Ser.C*, **274**(1972), 1760.

[9] G.Cocco, I.Soletta, L.Battezzati, M.Baricco and S.Enzo, *Phil. Mag. B*, **61**(1990), 473.

[10] T.Klassen, M.Oehring and R.Bormann, *J. Mater. Res.*, **9**(1994), 47.

[11] G.J.Fan, M.X.Quan and Z.Q.Hu, *Scripta Metall.*, **33**(1995), 377.

[12] F.Zhang, L.Lu and M.O.Lai, *J. Alloys Compounds*, **297**(2000), 211.

[13] K.B.Gerasimov and S.V.Pavlov, *J. Alloys Compounds*, **242**(1996), 136.

Chapter 4 Formation of homogeneous and dense coatings of Al_3Ti on Ti substrates by reactive-pulsed electric current sintering

4.1 Introduction

Ti and its alloys possess excellent resistance against severe corrosion and desirable specific strengths at ambient temperature. However, their poor resistance against adhesive wear or oxidation at elevated temperatures has prevented their utilization in such severe conditions. Surface modification is one of effective ways to improve these properties. Especially coatings of titanium aluminides is useful.

In the previous chapter, the combustion synthesis was successfully applied to the surface modification. For the formation of the Al_3Ti coating on the Ti substrate, the mixed powders of Al and Ti with a composition of Al_3Ti is heated to a temperature higher than the ignition temperature for the combustion synthesis. Application of the fine mixed MA powders as starting materials has been shown to be advantageous to form a homogeneous coating, as well as to enable the process at lower temperatures. On the contrary, since powders were hardened by the reduction of grain size and deformation hardening during MA, voids are more likely to be remained in the synthesized coatings and the densification became more difficult. This is a serious problem when the obtained coatings are subjected to an oxidizing atmosphere because excessive amounts of voids provide fast diffusion paths for oxygen [1].

In this chapter, the pulsed electric current sintering (PECS) was applied to synthesize and simultaneously densify the Al_3Ti coating. PECS has been reported to densify powders at lower temperatures, and for shorter time than other conventional sintering processes by charging a pulsed electric current directly through powders [2]. By using this process, the sintering condition was optimized to form homogeneous and dense Al_3Ti coatings as well as a defect free Al_3Ti / Ti interface in order to obtain the sound bonding strength.

4.2 Experimental

99.9% pure Al and 99% pure Ti with average particle sizes of 27 and 7μm respectively, were mixed in the composition of Al-25at.%Ti. MA was performed by using rotational ball milling for 144ks. The powder mixture of 50g was put into a cylindrical SUS304 vail ($1.7x10^{-3}m^3$) with SUS304 balls (ϕ11mm) in an Ar gas atmosphere. The weight ratio of balls to powders was fixed to 80:1. To avoid the adhesion of powders to balls and vail, ethanol of 0.5ml was added as a process control agent.

A commercially pure Ti bar (99.9%, ϕ10mmx3mm) was used as a substrate. Substrate surfaces were ground with 1.0μm alumina powders to obtain a flat and clean surface

prior to the formation of the Al_3Ti coating.

Figure 4.1 shows a schematic illustration of the mold part of the PECS equipment (SPS510L, Sumitomo Coal Mining Co.) used in this research. Hot pressing (HP) attached with high frequency induction heating was also performed by using the same mold to investigate the effect of PECS on the densification rate. MA powders and Ti substrate, contained inside a carbon die with an inner diameter of 10.5mm, were compressed in a vacuum of 5Pa under a uniaxial pressure of 20 or 40MPa, and then were heated up to various temperatures at a heating rate of 0.33 or 3.33K/s.

The microstructure of obtained samples was investigated by optical microscopy and scanning electron microscopy (SEM). Thin foil samples for transmission electron microscopy (TEM) were prepared by cutting in about 0.5mm thickness, then mechanically polished toward the total thickness of about 50μm. These specimens were further thinned to electron transparency by electropolishing. To identify the phases formed, X-ray diffraction analysis (Cu-Kα) and electron microprobe analysis (EPMA) were performed.

Vickers microhardness test with an applied load of 1.96N and Ogoshi abrasion test were performed as already described. A four-point bending test was performed at ambient temperature to estimate the bonding strength of the Al_3Ti / Ti joint. Oxidation resistance was evaluated by observing the oxidation layer which was formed in open air at 1273K for various times.

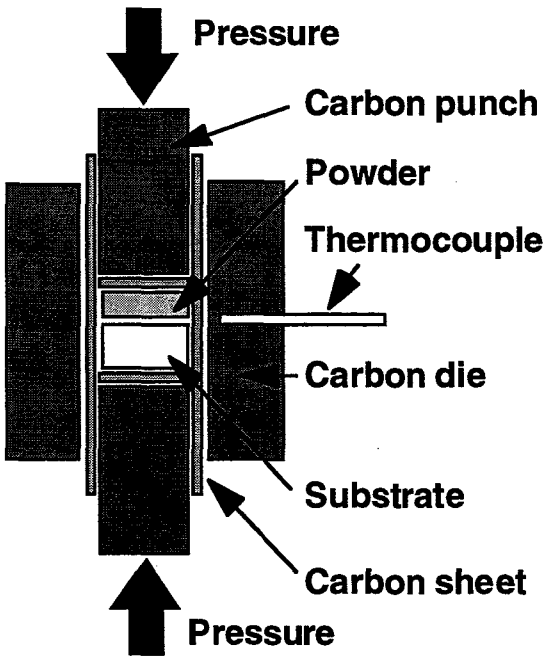

Fig. 4.1 Schematic illustration of the mold used for PECS and HP.

4.3 Results and discussion

4.3.1 Formation of Al_3Ti phase

Figure 4.2 shows the X-ray diffraction patterns of the MA powders heated to various temperatures by (a) DSC and (b) PECS. As shown in **Fig. 4.2(a)**, Al and Ti in MA powders reacted and formed the Al_3Ti phase when they were heated to 773K. As shown in **Fig. 4.2(b)**, however, the reaction occurred at a lower temperature for PECS than for DSC. The temperature of PECS is generally measured by using a thermocouple put into the carbon die. However, it has been suggested that there is a considerable temperature difference between the carbon die and powders [3]. Therefore, the measured temperature of the carbon die should not show the actual temperature of samples. **Figure 4.3** shows the measured temperature profiles of the carbon die and the sample powders during continuous heating by PECS. In the present research, the temperature of the powders was 40 ~ 80K higher than that of the carbon die. Therefore, the temperature of the powders was calibrated in accordance with **Fig. 4.3**. Though the exothermic reaction was detected during continuous heating by DSC, there was no significant increase of temperature showing the trace of the combustion synthesis. Farber *et al.* reported that the heat exchange with the environment affected the reaction paths in the combustion synthesis, for example self-sustaining mode or solid state reaction mode [4]. In PECS, a carbon mold used to charge an electric current has such a high heat conductivity, that most of the generated heat was transferred to the mold and the reaction mode changed to the solid state reaction.

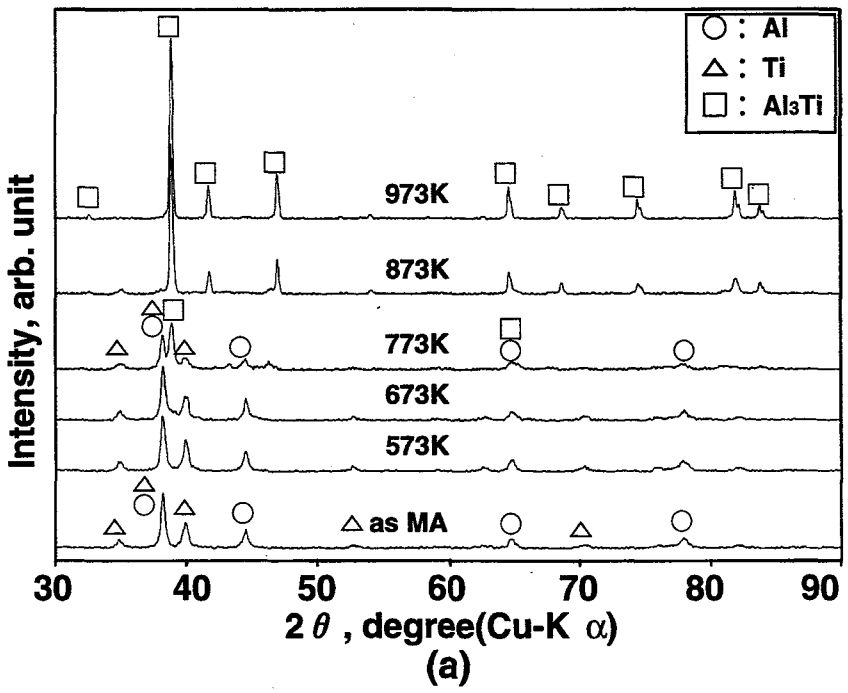

Fig. 4.2 X-ray diffraction patterns of the MA powders heated to various temperatures by (a) DSC and (b) PECS. The temperature of PECS was measured in a carbon die shown in ***Fig. 4.1.***

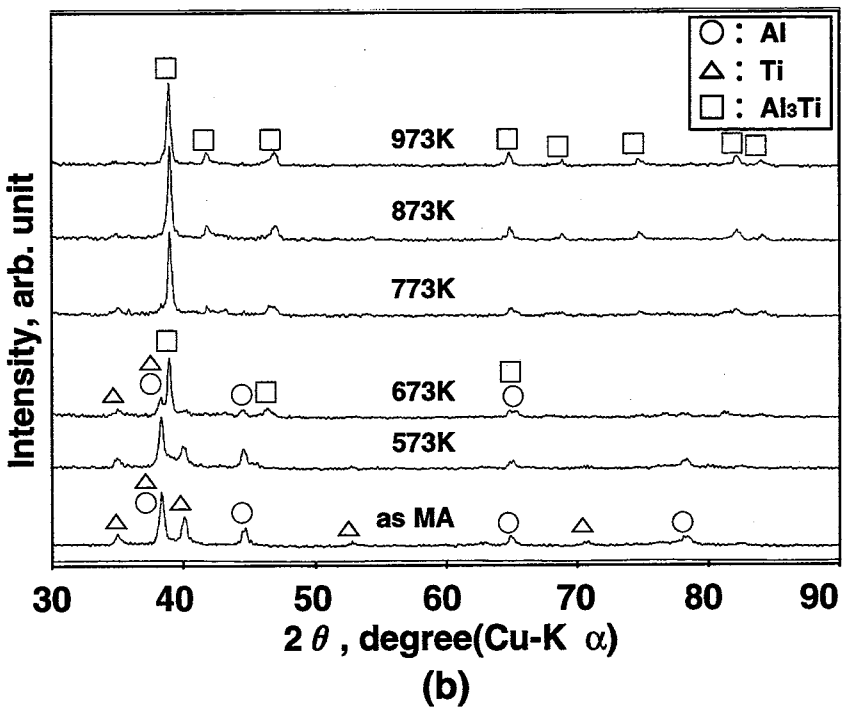

Fig. 4.2 Continued.

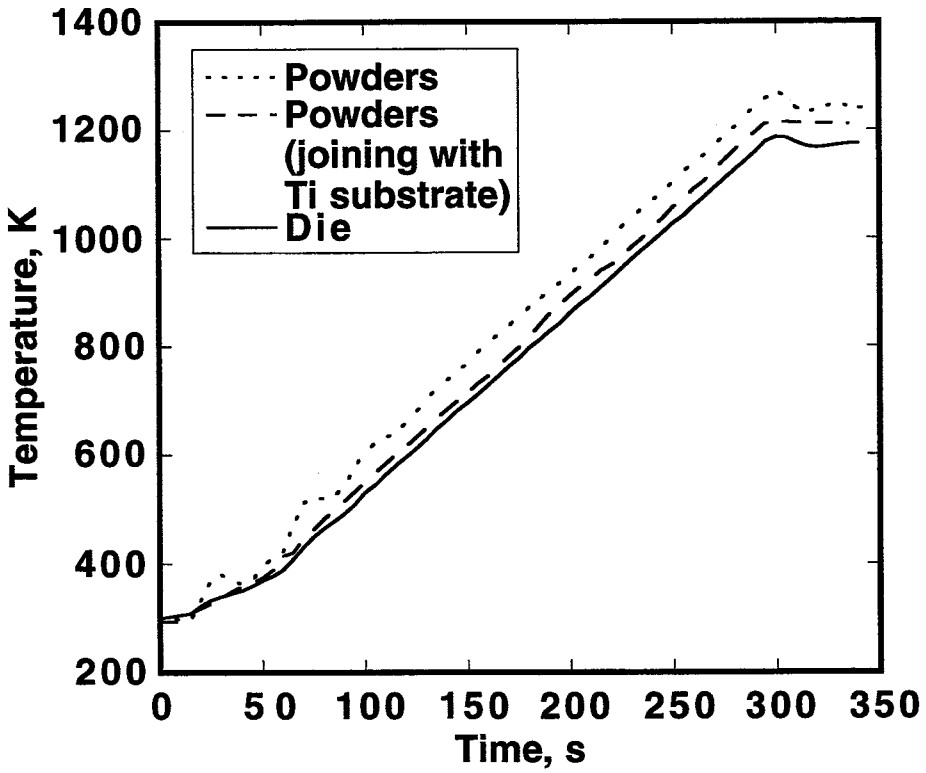

Fig. 4.3 Measured temperature profiles of the powders and a carbon die during continuous heating by PECS.

Since the PECS is a process to heat powders by directly charging a pulsed electric current, it is worth investigating whether or not there are any local areas to be super-heated by Joule heating or by spark plasma at contacting points between powders or at interfaces between the substrate and powders. **Figure 4.4** shows the microstructures of the MA powders heated to 650K, 750K and 850K by PECS. MA powders heated to a lower temperature than the reaction temperature hardly changed their microstructure from that of the as-mechanically alloyed powders consisted of fine Al and Ti developed

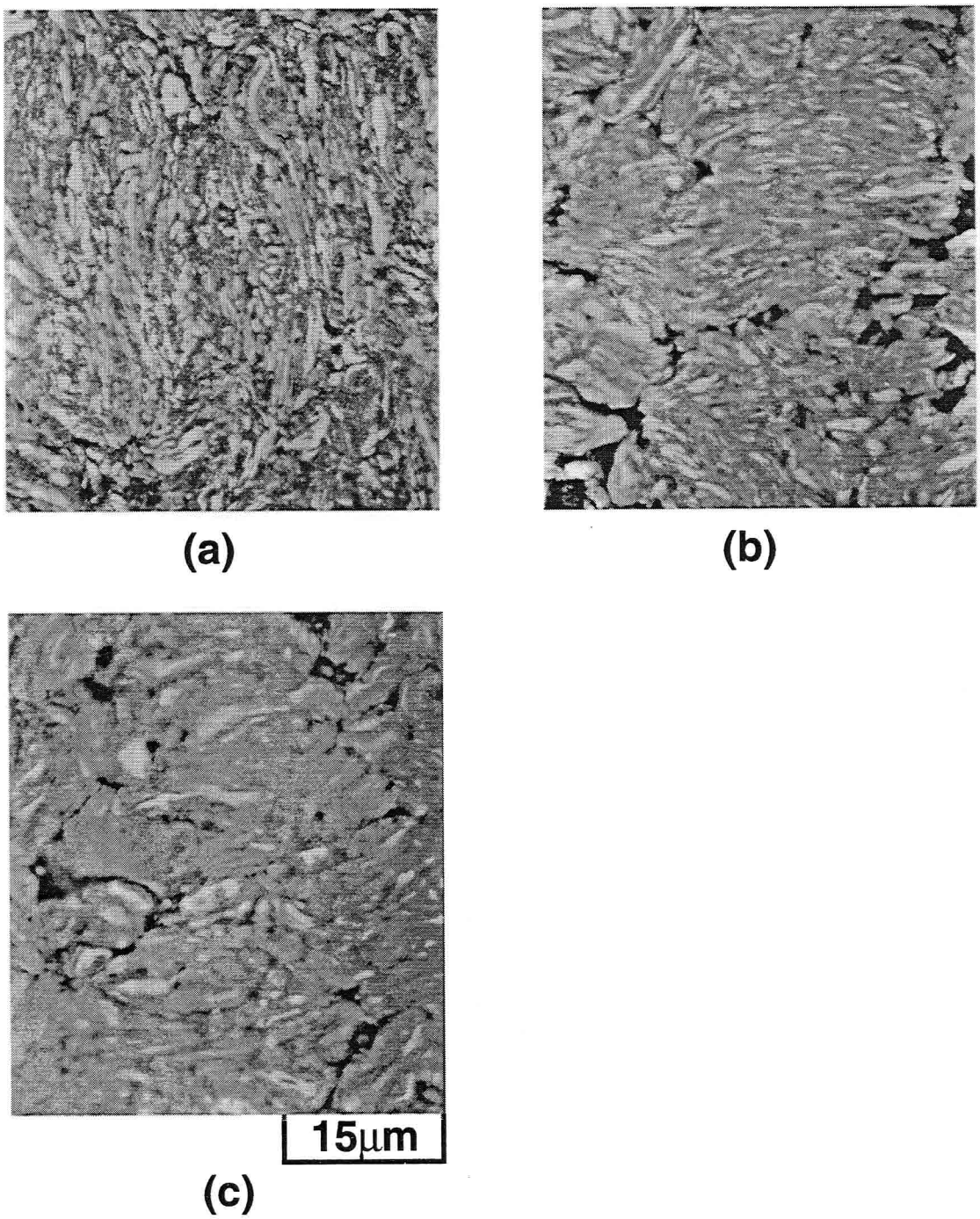

Fig. 4.4 Microstructures of the MA powders heated to (a) 650K, (b) 750K and (c) 850K under 40MPa by PECS. The temperatures were measured in the powders.

by repetitive fracturing and kneading during MA. By heating above the reaction temperature, these lamellar structures disappeared and the Al_3Ti phase was formed. If there are regions locally super-heated by PECS, the local reaction should occur prior to the homogeneously heated region. However, such locally reacted regions were not identified. So it may be concluded that these MA powders were heated homogeneously in the present conditions.

Figure 4.5 shows changes in the shrinkage ratio toward the applied pressure during continuous heating of the MA powders and pre-alloyed Al_3Ti powders. These powders started to shrink from about 400K and 700K, respectively. This temperature difference is caused by existence of soft, pure Al in the MA powders. Application of the MA powders is more advantageous for forming a dense Al_3Ti comparing with the pre-alloyed powders. Though the influence of pulsed electric current ratio (on:off=3:4, 12:2, 99:1) on the shrinkage ratio was investigated, no changes were observed, indicating that the pulse ratio hardly affected the densification behavior.

Figure 4.6 shows changes in the relative density of the Al_3Ti using the MA powders as a function of holding time during isothermal sintering at various temperatures under pressure of 20MPa. By increasing the sintering temperature and time, the densification was developed. If the densification is governed by plastic flow of materials at a sintering temperature (T), a Johnson-Mehl-Avrami type relation can be applied between relative density (D) and holding time (t) as shown in eq. (4.1) [5].

$$\ln(1-D) = -K_s(T)\cdot t \qquad (4.1)$$

where K_s is densification coefficient and also described by eq. (4.2).

$$K_s(T) = K_{so}\exp\left(-\frac{Q_s}{RT}\right) \qquad (4.2)$$

where K_{so} is constant, and Q_s is the apparent activation energy required for densification. R is gas constant.

Since K_s is constant at the same sintering temperature, ln(1-D) and holding time will have a linear relationship. **Figure 4.7** shows this relationship between ln(1-D) and t. These plots showed a good agreement with eq. (4.1). The K_s values can be estimated from the slope of regression lines using least-square analysis. The Q_s value can be also estimated from an Arrhenius plot of the K_s value in eq. (4.2). This Q_s value was 61.72kJ/mol as shown in **Fig. 4.8** that can decide the densification process by PECS. Though a K_s value obtained for conventional hot-pressing was slightly smaller than that of PECS, it located near the regression line obtained by PECS. Hence, it can be concluded that the development of densification by PECS at isothermal sintering was governed mainly by the thermally-activated plastic flow of materials and hardly accelerated by the effect of pulsed electric current charge.

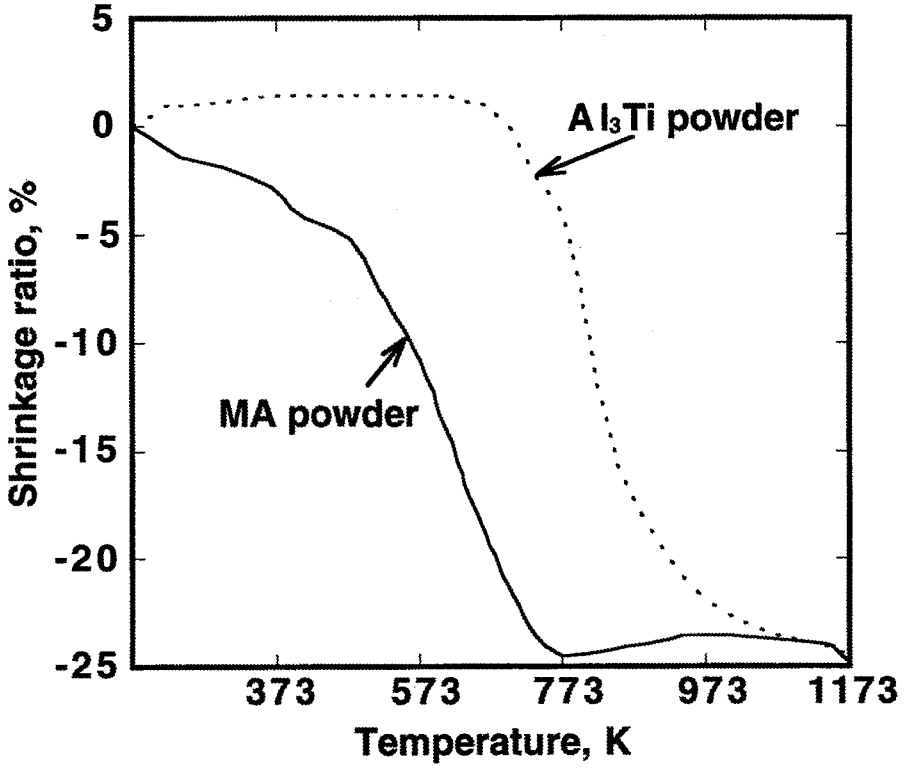

Fig. 4.5 Changes in the shrinkage ratio toward the applied pressure during continuous heating of the MA and pre-alloyed Al_3Ti powders.

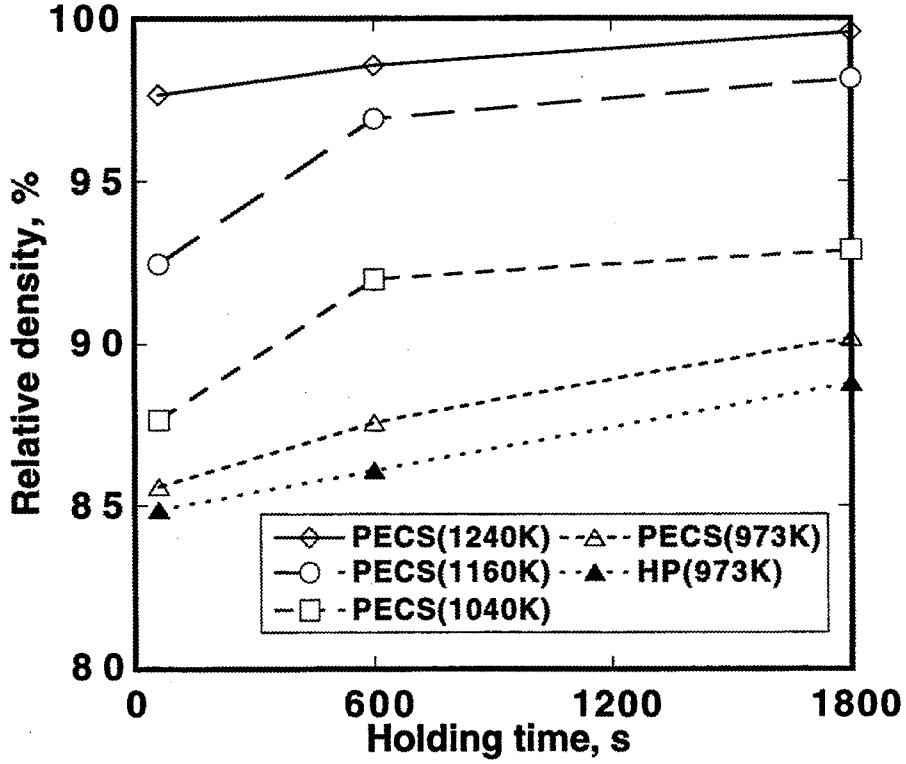

Fig. 4.6 Changes in the relative density of the Al_3Ti during isothermal holding under 20MPa.

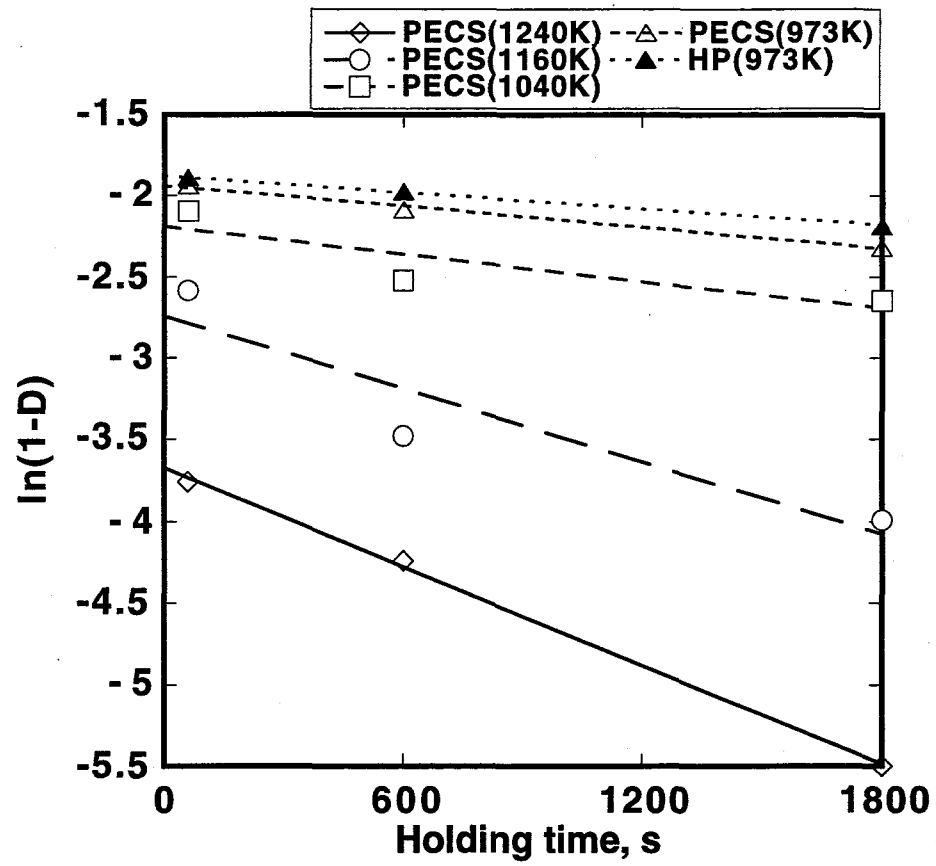

Fig. 4.7 Relationships between ln(1-D) and holding time at various temperatures.

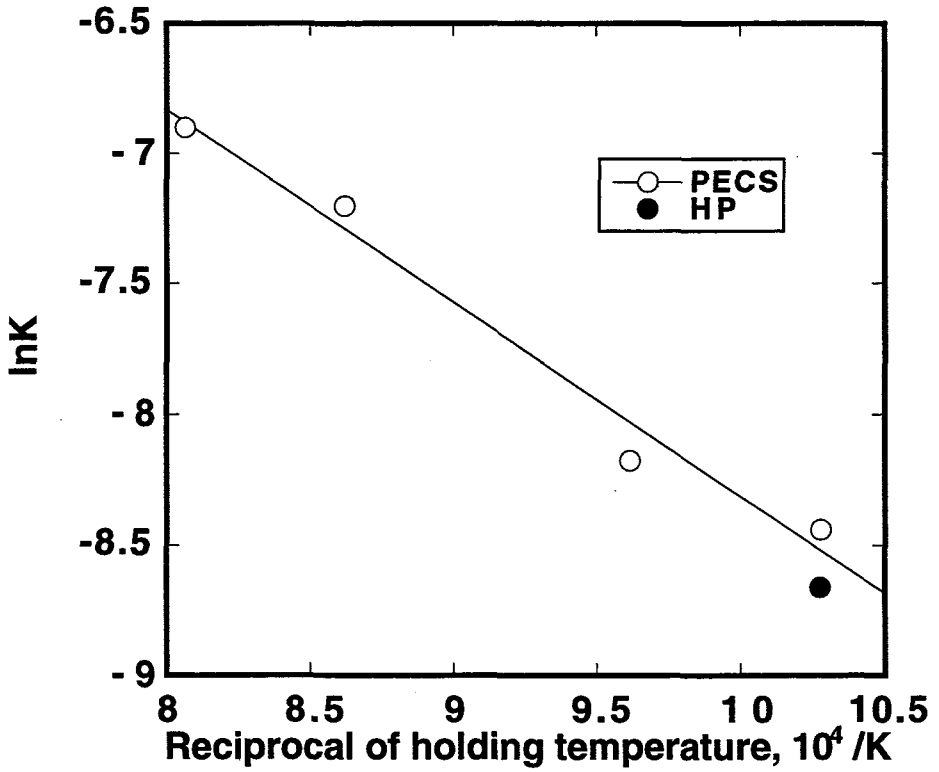

Fig. 4.8 Arrhenius plot of lnK against the reciprocal temperature.

4.3.2 Formation of Al_3Ti coatings

Figure 4.9 shows the Al_3Ti coating on the Ti substrate formed at 1210K for 180s under 40MPa by PECS. The Al_3Ti coating exhibited a smooth surface, of which thickness was about 1600μm. As shown in **Fig. 4.9(b)**, the Al and Ti completely reacted and formed the fully densified Al_3Ti coating. **Figure 4.10** shows a TEM image of the Al_3Ti coating, which retained nano structure with an average grain size of 150nm. **Figure 4.11** shows the effect of heating temperature and time on the void ratio in the coating and the bonding interface. Compared with the densification behavior in the Al_3Ti coating, the bonding interface required a higher temperature and longer holding time for densification. This is because the flat-surface of the Ti substrate has a much larger curvature than spherical the MA powders, so that it needs larger deformation to eliminate voids.

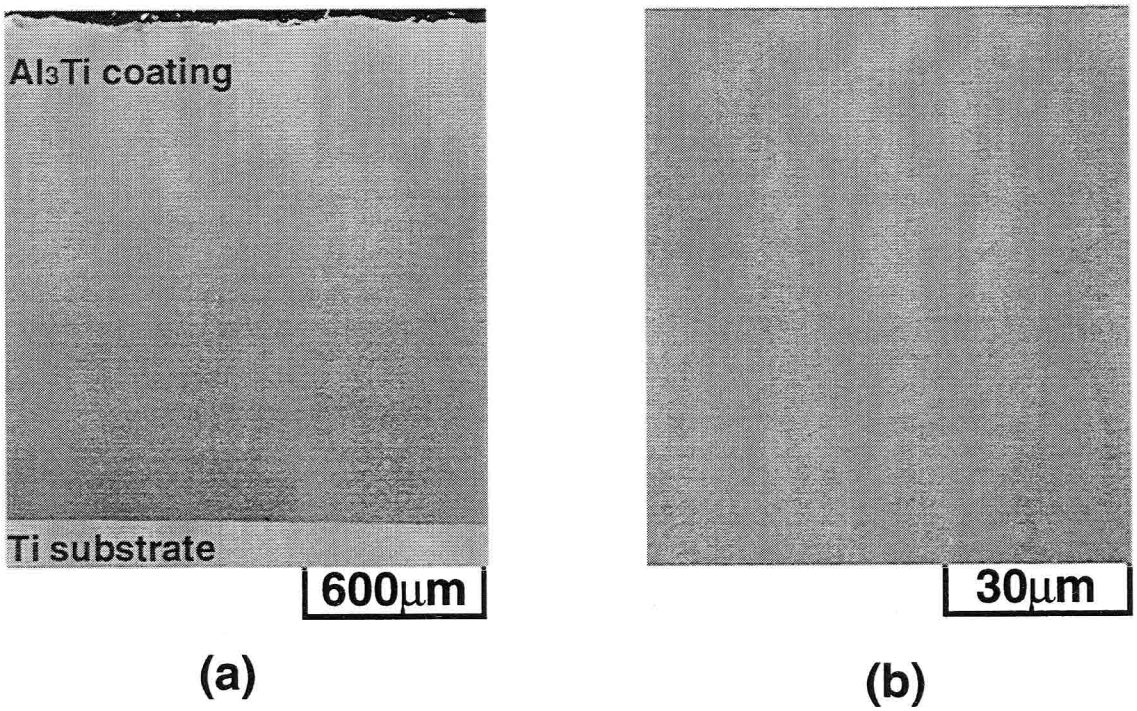

Fig. 4.9 (a) General view and (b) microstructure of the Al_3Ti coating on the Ti substrate formed at 1210K for 180s under 40MPa by PECS.

The reaction layers formed at the bonding interface were investigated to identify the initial interface by inserting a mica sheet as a marker on the periphery of the interface before the bonding. As the result, the reaction layers were confirmed to be formed mainly towards the direction of the Ti substrate as shown in **Fig. 4.12.**. By EPMA analysis shown in **Fig. 4.13** and **Table 4.1**, these layers were identified α-Ti, α_2 (Ti_3Al), γ (TiAl), Al_2Ti and Al_3Ti, respectively, from the Ti substrate to the Al_3Ti coating. Among these intermetallic layers the Al_3Ti layer exhibited a higher growth rate with holding time. If the growth of the reaction layer is governed by diffusion of atoms, the thickness (x) is described as a function of the square root of time (t) [6].

Fig. 4.10 *TEM image of the Al_3Ti coating formed at 1100K for 180s by PECS.*

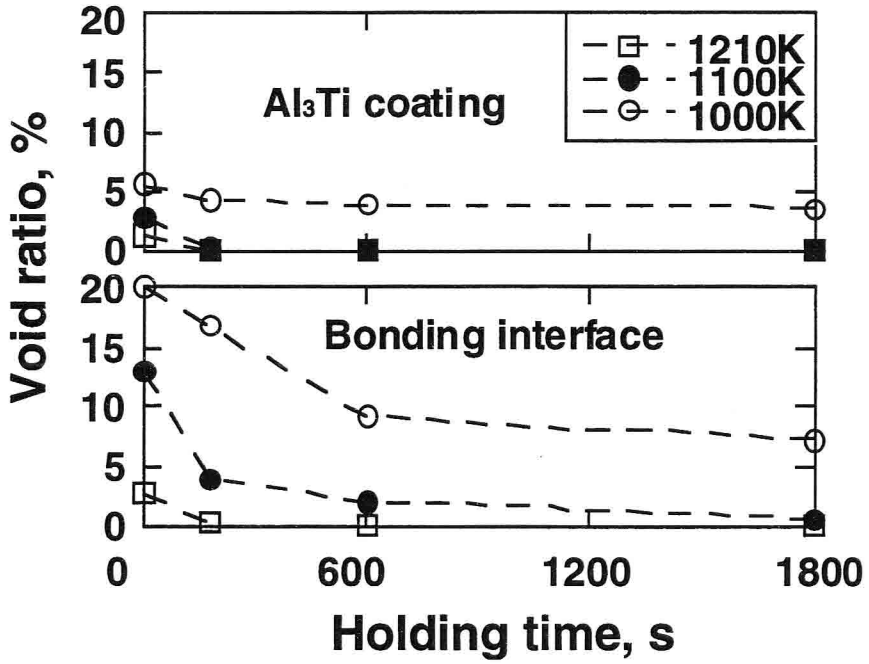

Fig. 4.11 *Changes of void ratio in the Al_3Ti coating and at the bonding interface as a function of holding time.*

$$x = k\sqrt{D \cdot t} = K_g\sqrt{t} \qquad (4.3)$$

where k is constant. D and K_g are diffusion coefficient and growth coefficient, respectively, which are also described like eq. (4.2). From eq. (4.3), the apparent activation energy required for growth corresponds to half the value of that for diffusion.

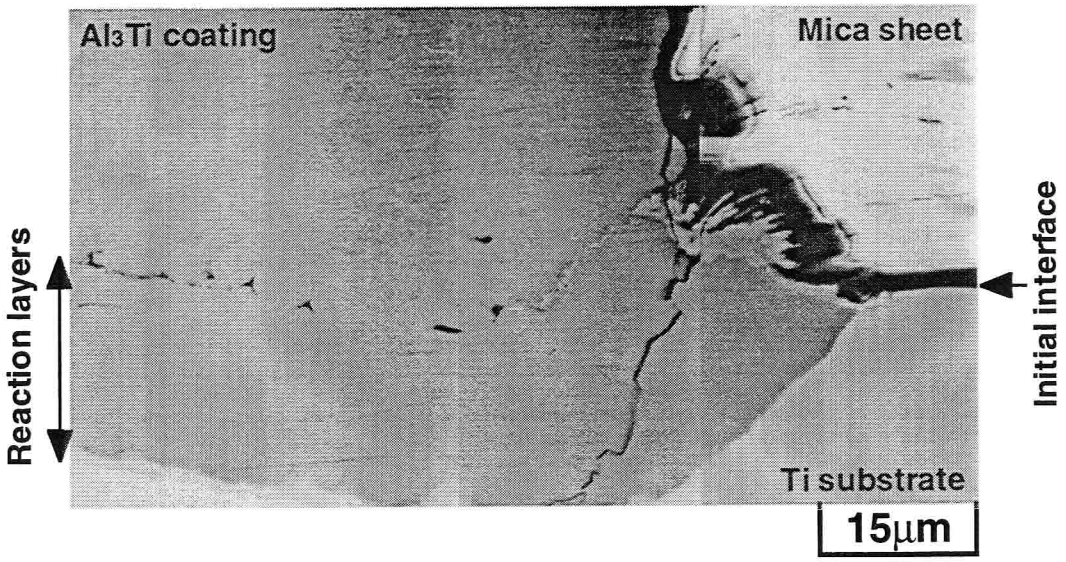

Fig. 4.12 Microstructure of the bonding interface formed at 1100K for 1800s by PECS. The position of a mica sheet indicates the initial interface.

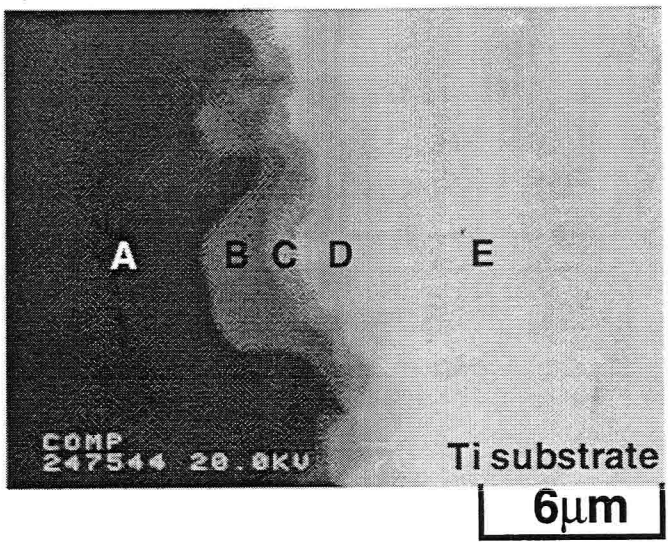

Fig. 4.13 BE image of the reaction layers formed at 1100K for 1800s by PECS.

Table 4.1 *Results of quantitative analyses at each local areas shown in* ***Fig. 4.13.***

Analysis point	Composition, at.%		Predicted phase
	Al	Ti	
A	76.98	23.02	Al_3Ti
B	71.02	28.98	Al_2Ti
C	59.04	40.96	γ(TiAl)
D	36.38	63.62	$\alpha_2(Ti_3Al)$
E	4.99	95.01	(Ti)

Figure 4.14 shows the relationship between the thickness of the Al_3Ti reaction layer and square root of holding time. The growth of the Al_3Ti reaction layer showed a parabolic relation against holding time. The activation energy obtained from the Arrhenius plot of K_g was 153.1kJ/mol for the temperature regioin below the α/β transformation temperature of the Ti substrate, which is compatible with a half value of activation energy for Al diffusion in the intermetallic compound Al_3Ti (291.1kJ/mol) [7]. It can be concluded that the growth of the Al_3Ti reaction layer was governed by Al diffusion in Al_3Ti. This result indicates that the Al diffusion was hardly accelerated by pulsed electric current like the densification behavior. A bonding which is free from voids on the bonding interface exhibited the fracture strength 150MPa by a four-point bending test. The fracture originated in the Al_3Ti coating, not on the bonding interface.

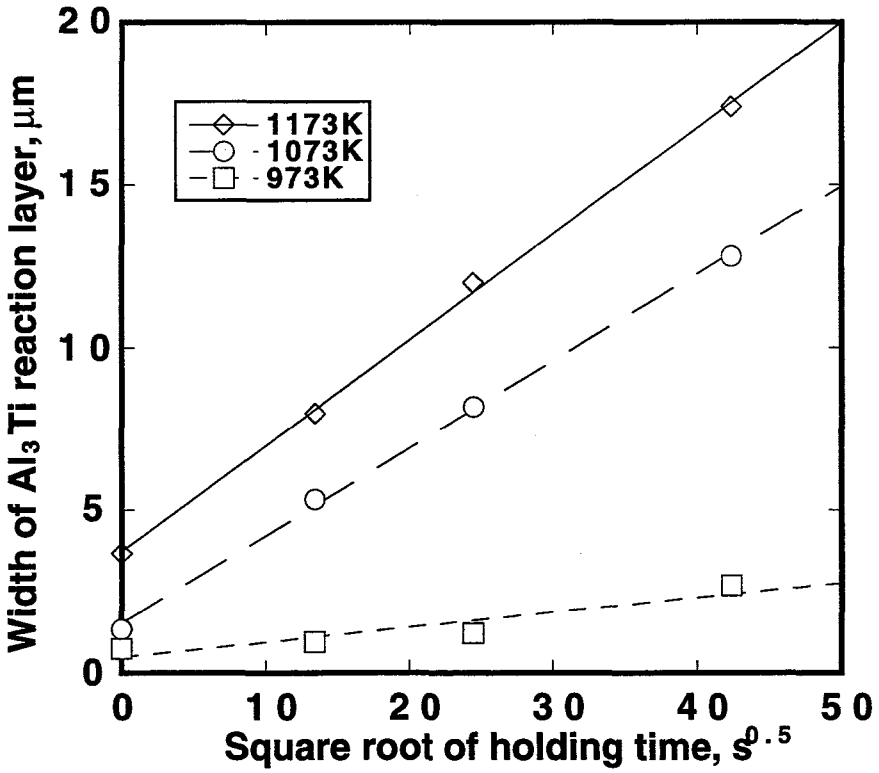

Fig. 4.14 Relationships between thickness of the Al_3Ti reaction layer and square root of holding time.

4.3.3 Properties of Al3Ti coatings

Figure 4.15 shows the Vickers hardness distribution of the Al_3Ti coating on the Ti substrate formed at 1210K for 180s under 40MPa by PECS. Since the coating was dense and homogeneous, the Al_3Ti coating had a nearly constant hardness of about HV600, which was almost the same as that of the cast Al_3Ti.

Figure 4.16 shows the specific wear of the Al_3Ti coating and Ti substrate. The Al_3Ti coating obtained by this research showed more excellent wear property than that obtained by laser cladding process [8], probably because the grain size of the combustion-synthesized Al_3Ti is much smaller and the microstructure is more

homogeneous than that of the laser-clad Al_3Ti.

Figure 4.17 shows microstructures of the oxide layer on the Ti substrate and on the Al_3Ti layer formed by oxidizing the samples at 1273K in open air. The TiO_2 layer formed on the Ti substrate for 14.4ks was broken away, and the substrate was attacked by oxygen solution, while the Al_3Ti coating was hardly damaged by oxidation over 230.6ks. The growth of oxidation on the Al_3Ti coating was much slower, because the Al_2O_3 scale formed on the Al_3Ti coating and acted as a protective layer against oxidation.

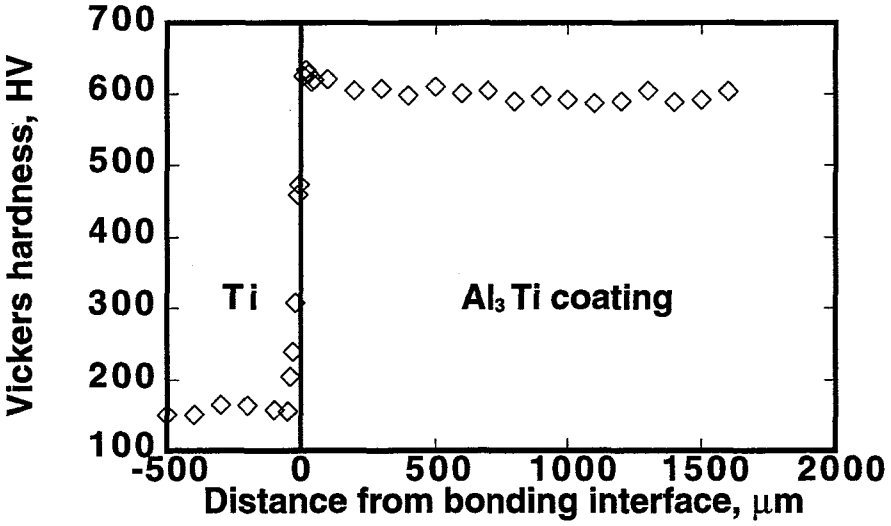

Fig. 4.15 Vickers hardness distribution of the Al_3Ti coating on the Cu substrate formed at 1210K for 180s under 40MPa by PECS.

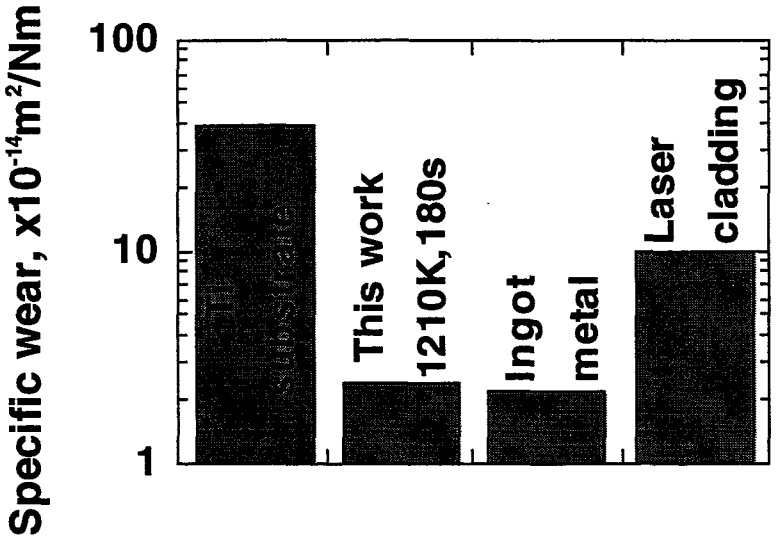

Fig. 4.16 Specific wears of the Ti substrate and the Al_3Ti formed by various methods.

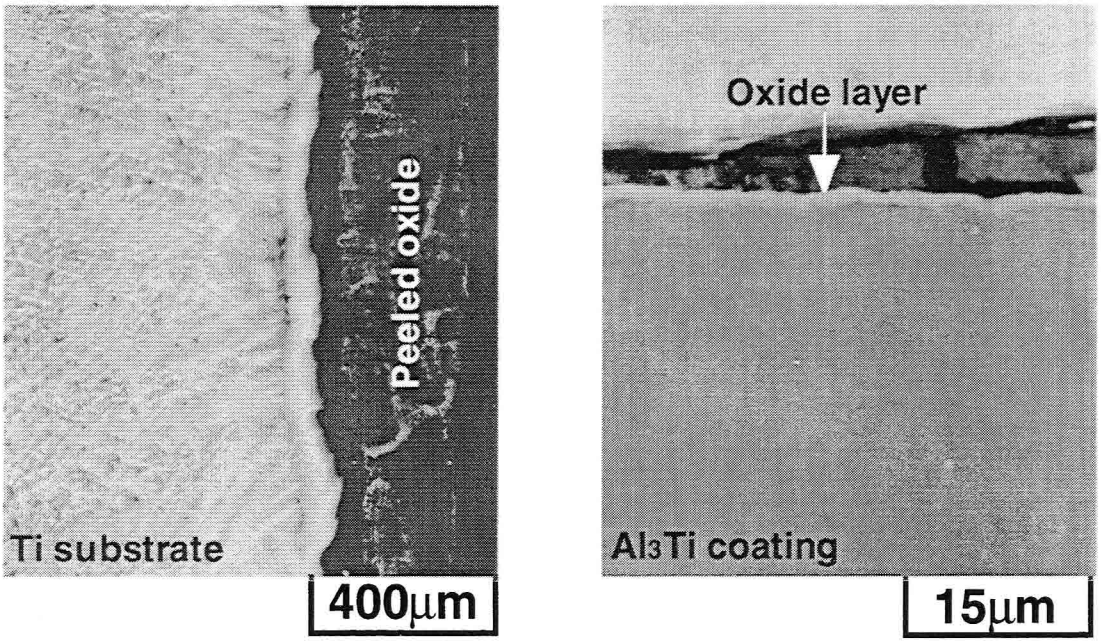

Fig. 4.17 Microstructures of the oxide layer on (a) the Ti substrate and (b) the Al_3Ti coating after oxdizing at 1273K for 14.4ks and 230.6ks in an open air.

4.4 Conclusions

The Al_3Ti was formed by reactive-PECS from the MA powders and simultaneously bonded with a pure Ti substrate. The main results obtained in this chapter can be summarized as follows,

(1) In PECS, the temperature of the sample was higher than that of the carbon die.

(2) The Al_3Ti phase was formed from the MA powders at 773K by a solid state reaction.

(3) The densification behavior by PECS was governed by the plastic flow of Al_3Ti, which is almost the same as by conventional hot pressing method. Moreover, it was hardly accelerated by the effect of the pulsed electric current.

(4) The Al_3Ti coating formed on the Ti substrate was fully densified and homogenized at 1100K for 180s by PECS. The Al in the MA powders diffused toward the substrate and reacted forming the Al_3Ti reaction layer, resulting in bonding of Al_3Ti with Ti.

(5) The microhardness, wear and oxidation properties of the Al_3Ti coating exhibited almost the same values as those of the cast Al_3Ti.

References

[1] W.W.Lee, D.B.Lee, M.H.Kim and S.C.Ur, *Intermetallics*, **7**(1999), 1361.

[2] O.Yanagisawa, T.Hatayama and K.Matsugi, *Materia Jpn.*, **33**(1994), 1489.

[3] H.Tomino, H.Watanabe and Y.Kondo, *J. Jpn. Soc. Powder Powder Metall.*, **44**(1997), 974.

[4] L.Farber, L.Klinger and I.Gotman, *Mater. Sci. Eng. A*, **254**(1998), 155.

[5] J.K.Mackenzie, R.Shuttleworth, *Proc. Phys. Soc. B*, **62**(1949), 833.

[6] G.V.Kidson, *J. Nucl. Mater.*, **3**(1961), 21.

[7] J.Pouliquen, S.Offret and J.de.Fouquet, *C. R. Acad. Sci., Ser.C*, **274**(1972), 1760.

[8] K.Uenishi, A.Sugimoto and K.F.Kobayashi, *Z. Metallkd.*, **83**(1992), 241.

Chapter 5 Formation of thick coatings of ceramic particles dispersed Al_3Ti on Ti substrates by reactive-pulsed electric current sintering

5.1 Introduction

In the previous chapter, a novel powder metallurgical technique combining the combustion synthesis, MA and PECS was successfully applied to the surface modification of metal substrates. By applying this process, a dense and homogeneous Al_3Ti coating could be formed and exhibited almost the same hardness, wear and oxidation resistance as the cast Al_3Ti. The advantages of this process are the capability for obtaining the coating with high bonding strength at lower temperatures for shorter time, and for controlling the thickness or microstructure of coatings only by changing the thickness or composition of starting powders.

It has been shown that incorporation of various reinforcements within the intermetallic compound called intermetallic matrix composites (IMC) can improve mechanical properties of the monolithic one [1, 2]. The reinforcements should be selected in terms of the stiffness, strength, or chemical compatibility from candidates including morphology such as continuous fibers or particles. Since particle reinforced composites are easy to fabricate, they have been commonly used and processed by powder techniques to date.

In this chapter, ceramic particles dispersed Al_3Ti coatings to further enhance the wear properties are formed on a Ti substrate by PECS. By taking chemical compatibility with the Al_3Ti matrix into consideration [3, 4], TiB_2 and Al_2O_3 particles were selected as reinforcing phases. They have been considered neither to form any reaction layer with matrix, nor to degrade the composites. TiB_2 and Al_2O_3 exhibit high hardness, superior wear resistance and a high melting point [5, 6]. The combustion synthesis reaction and densification of the MA powders started from the mixture of Al-Ti-TiB_2, Al-Ti-B and Al-Ti-Al_2O_3 were investigated to form sound IMC coatings. Effects of particles dispersion on the wear and oxidation properties of the IMC coatings were also examined as well as on the bonding behavior to the Ti substrate.

5.2 Experimental

Al (99.9%, 27μm), Ti (99%, 7μm), B (95.7%, 1μm), TiB_2 (99%, 44μm) and Al_2O_3 (99.9%, 2μm) powders were used for MA. These powders were blended to the Al-Ti-TiB_2, -B or -Al_2O_3 mixed powder in the composition of Al_3Ti/10vol.%TiB_2 or Al_2O_3. MA was performed with a rotational ball mill for 144ks as described in chapter 4.

PECS, microstructural observation and evaluation of the obtained coatings were performed as described.

5.3 Results and discussion

5.3.1 MA and subsequent heat treatment

Figure 5.1 shows the microstructures of the MA powders. For the Al-Ti MA powders, a lamellar structure of fine Al and Ti was developed by repetitive fracturing and kneading during ball milling. For the Al-Ti-TiB_2, -B and -Al_2O_3 MA powders, the contrasting white TiB_2 and Al_2O_3 particles or black elemental B particles are confirmed

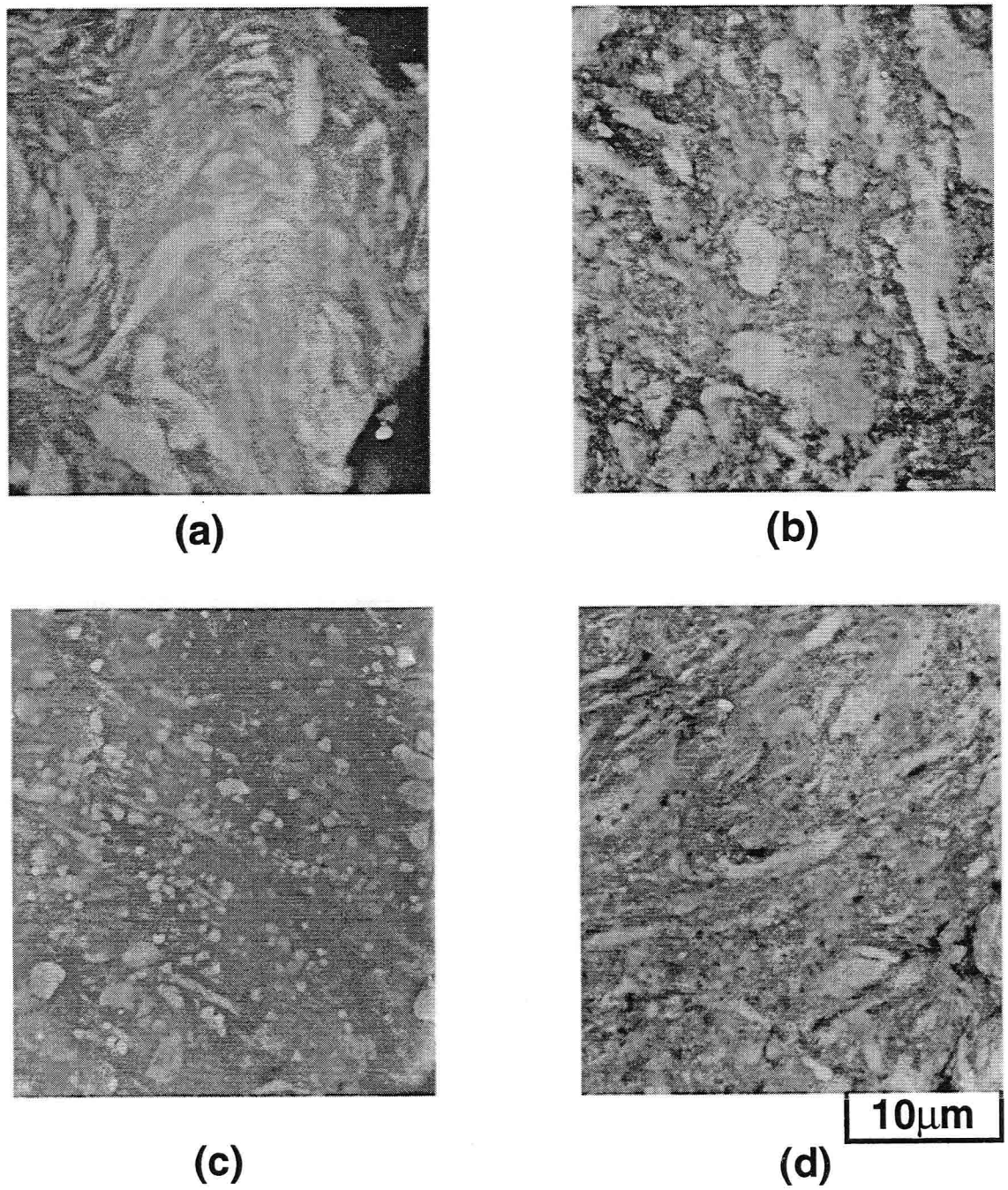

Fig. 5.1 Microstructures of the MA powders started from various mixed powders of (a) Al-Ti, (b) Al-Ti-Al_2O_3, (c) Al-Ti-TiB_2 and (d) Al-Ti-B

to be distributed homogeneously in the matrix, and Al/Ti lamellar structures were further refined than that in the Al-Ti MA powders. Addition of these ceramic particles enhanced the kneading efficiency.

Figure 5.2 shows the DSC traces of the MA powders. For the all MA powders, exothermic reactions occurred from 600K. Since the Al melting point is 933K, this reaction was interpreted to be a solid state reaction. Compared with the combustion synthesis of elemental mixed Al-Ti powders ignited at the Al melting point, the exothermal peak was broadened and shifted to a lower temperature. **Figure 5.3** shows the X-ray diffraction patterns of the MA powders continuously heated to 1003K. The Al_3Ti phase was found to be formed for the all powders. A high temperature phase (Al_5Ti_2) described in Chapter 3, was formed in the Al_2O_3, TiB_2 and B added powders as well. The AlB_2 and residual Ti phases were also detected for the elemental B added powders. Brinkman *et al.* studied the reaction mechanism and phase formation sequence in the reactive sintering of Al-TiB_2 composites from elemental Al-Ti-B powders using DSC. They found that TiB_2 was not formed until the AlB_2 intermediate reaction product decomposed, and the heat treatment above 1273K was needed to form the Al_3Ti/TiB_2 composite from the mixed Al-Ti-B powders [7].

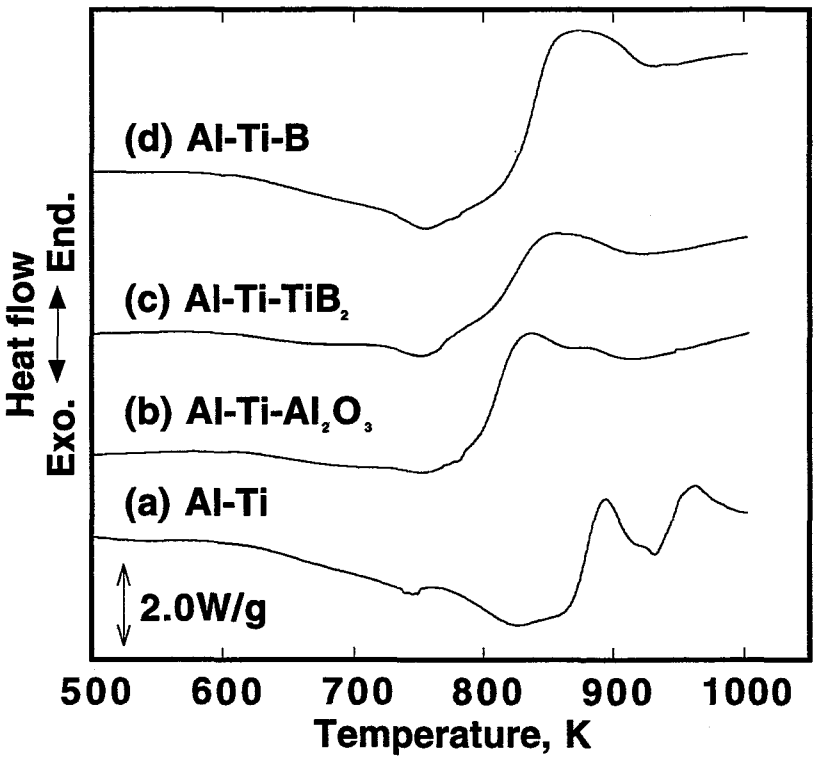

Fig. 5.2 DSC traces of the MA powders started from various mixed powders.

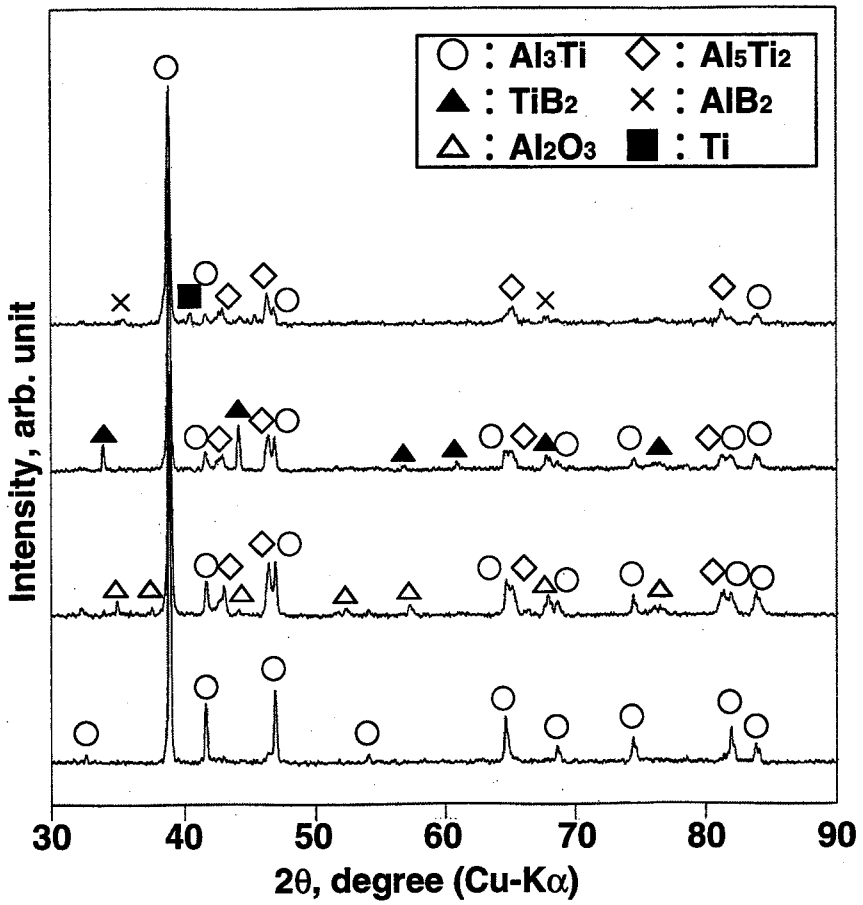

Fig. 5.3 X-ray diffraction patterns of the MA powders continuously heated to 1003K started from various mixed powders of (a) Al-Ti, (b) Al-Ti-Al_2O_3, (c) Al-Ti-TiB_2 and (d) Al-Ti-B.

5.3.2 Densification and phase formation of IMC coatings

Figure 5.4 shows the changes in the shrinkage ratio of the MA powders to monitor the sintering behavior by PECS under 40MPa during continuous heating. Densification was decelerated by adding TiB_2 and Al_2O_3, but not affected by B addition. TiB_2 and Al_2O_3 with high elastic constants are considered to have prevented the densification.

Figure 5.5 shows the changes in the relative density of the synthesized IMC coatings from the MA powders as a function of holding time at various sintering temperatures.

Figure 5.6 shows the relationship between ln(1-*D*) and the holding time. In the same way of densification for the monolithic Al_3Ti, these plots showed almost linear relationships except for the plots obtained from the Al-Ti-TiB_2 at 1173K. The plastic flow model does not seem to apply in the last stage of densification for the Al-Ti-TiB_2 system. The apparent activation energy for densification, Q_s value estimated from the Arrhenius plot of the K_s value, shown in **Table 5.1** decides the densification mechanism. The full densification of the IMC coatings was difficult, *i.e.* required higher temperature and longer holding time comparing with the densification of the monolithic Al_3Ti.

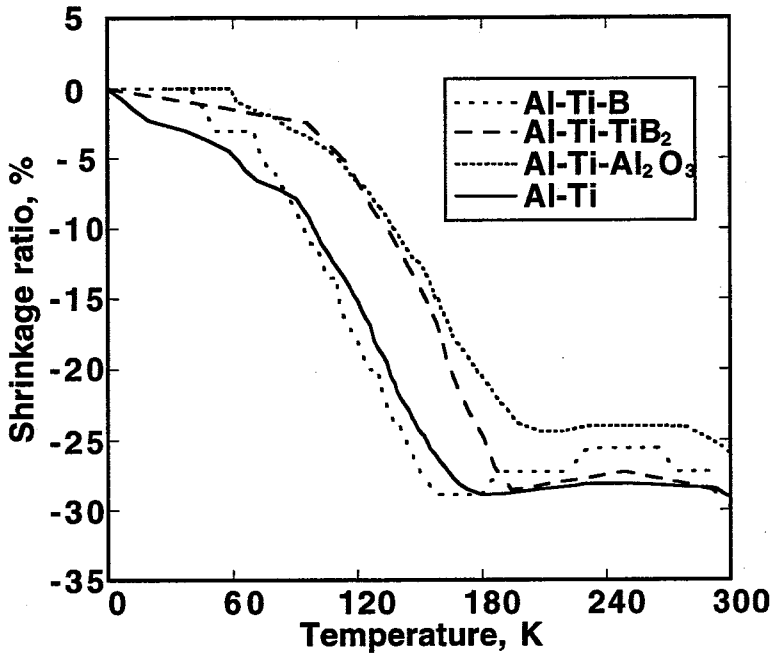

Fig. 5.4 *Changes in the shrinkage ratio of the MA powders under 40MPa during continuous heating by PECS.*

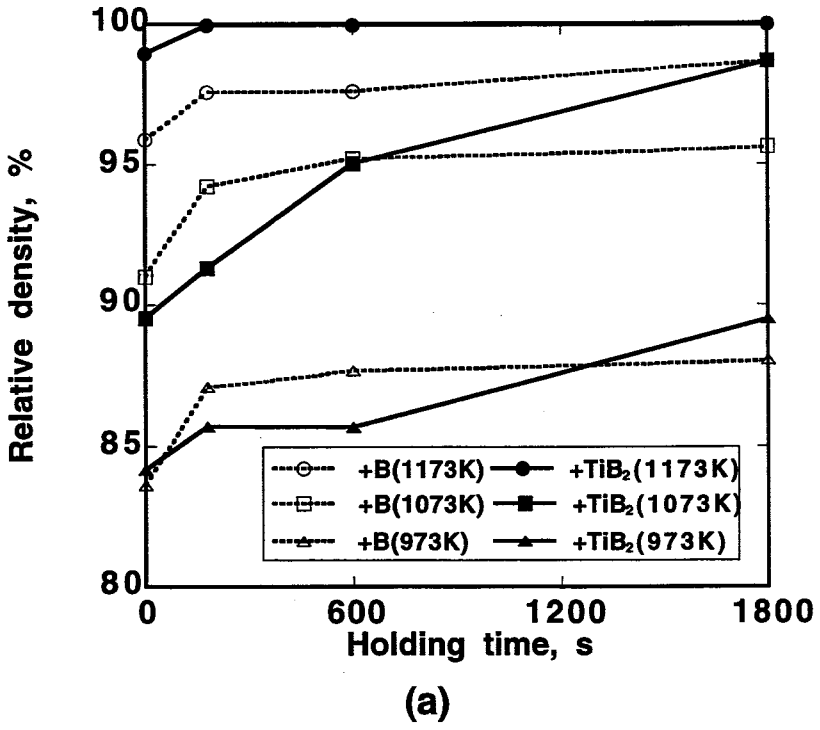

Fig. 5.5 *Changes in the relative density of the IMC coatings formed from the MA powders of (a) Al-Ti-B and Al-Ti-TiB_2, and (b) Al-Ti-Al_2O_3 during isothermal holding at various temperatures under 40MPa by PECS.*

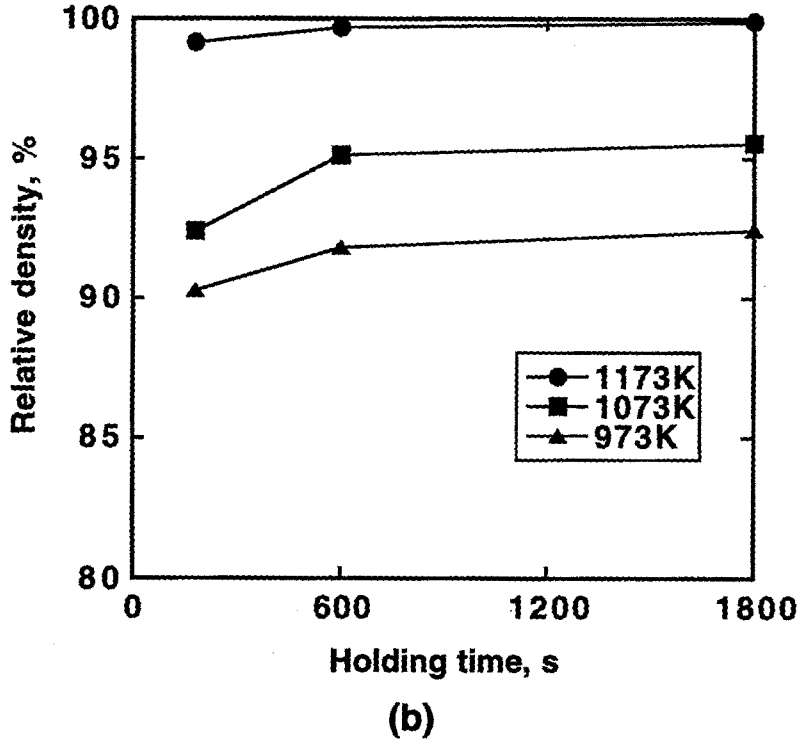

Fig. 5.5 Continued.

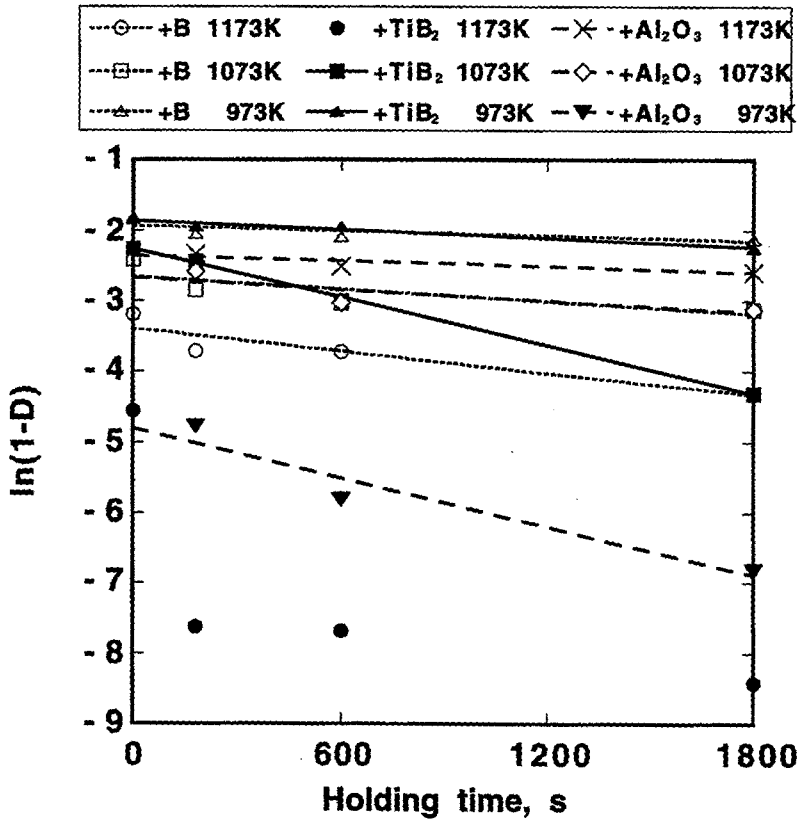

Fig. 5.6 Relationship between ln(1-D) and the holding time.

Table 5.1 Apparent activation energies for the densification.

Powder	Q_s, kJ/mol
Al-Ti	61.0
Al-Ti-Al_2O_3	110.3
Al-Ti-TiB_2	107.6
Al-Ti-B	77.9

Although the IMC coating synthesized from the Al-Ti-TiB_2 was densified at 1173K, the coating synthesized from the Al-Ti-B required a higher temperature. As seen in **Fig. 5.3**, the layer formed from the Al-Ti-B at 1003K consisted of AlB_2 and Ti in the Al_3Ti matrix. **Figure 5.7** shows the change in free energy (ΔG) for boride formation as a function of temperature [9]. As is evident from this figure, the affinity of B with Ti is much stronger than that with Al. Thus, the following reaction (eq. (5.1)) is considered to occur.

$$AlB_2 + \frac{4}{3}Ti \rightarrow \frac{1}{3}Al_3Ti + TiB_2 \qquad (5.1)$$

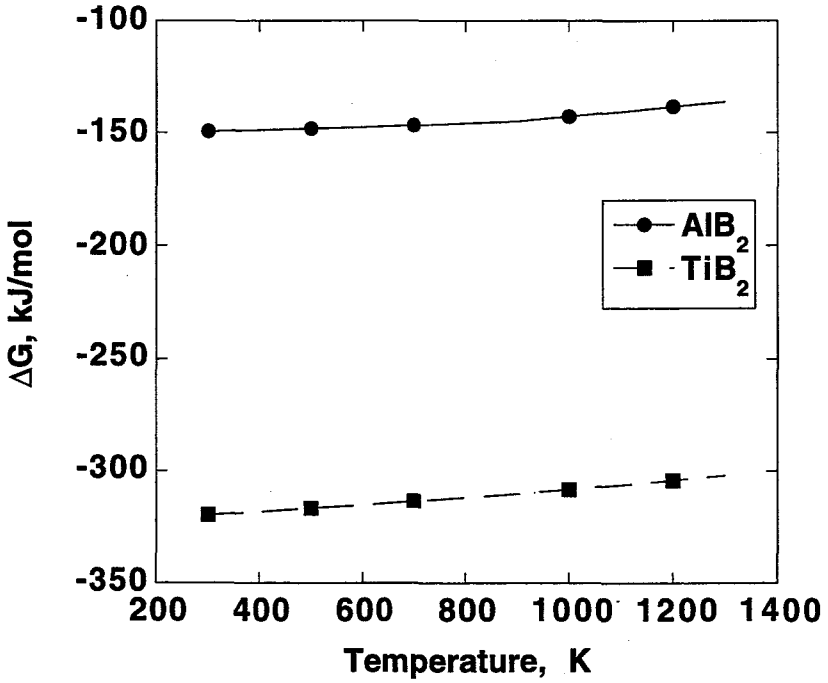

Fig. 5.7 Changes in free energy for boride fomations.

During this reaction to form Al_3Ti and TiB_2 phases from AlB_2 and Ti, the molar volume change estimated from their crystal structures was 4.2%. Since this reaction accompanying the volume change continues until the homogeneous microstructure is formed, the full densification at 1173K required a longer holding time. **Figure 5.8** shows a TEM image of the Al_3Ti/TiB_2 coating formed from the Al-Ti-B at 1173K for 180s under 40MPa. Though the sintering temperature is below the decomposition temperature of AlB_2, a plate like TiB_2 with 300nm in size was observed to be homogeneously dispersed in the Al_3Ti matrix. The TiB_2 formed in-situ from the Al-Ti-B powders was much smaller than that formed from the Al-Ti-TiB_2.

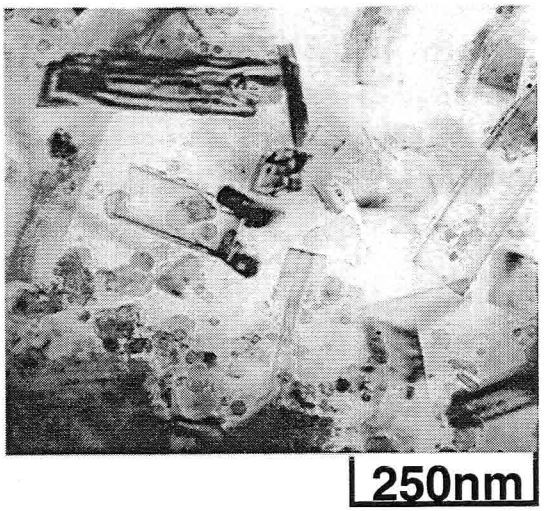

Fig. 5.8 *TEM image of the Al_3Ti/TiB_2 coating formed from the Al-Ti-B MA powders at 1173K for 180s under 40MPa by PECS.*

5.3.3 Reactions with Ti substrate

Figure 5.9 shows the microstructures of the bonding interface formed at 973K for 180s under 40MPa. Though there were some voids at the bonding interface for the (a) monolithic Al_3Ti coating, voids were hardly observed for the Al_2O_3, TiB_2 and B added coatings. Addition of these particles seems to effective to reduce voids at the bonding interface. Ashby *et al.* reported that the local plastic flow was generated at the interface between the particle and the metal during the compaction of metal containing particles with different elastic constants [10]. In this research, almost no deformation of Ti substrate was confirmed at the bonding interface with the monolithic Al_3Ti coating, but the irregular rugged face was observed at the bonding interface with the IMC coatings. This suggests that the substrate deformation was enhanced to fill up voids on the bonding interface when particles with high elastic constants are added in the coating.

To investigate the reaction layers formed at the bonding face, the initial interface was identified by inserting a mica sheet as a marker on the periphery of the interface before

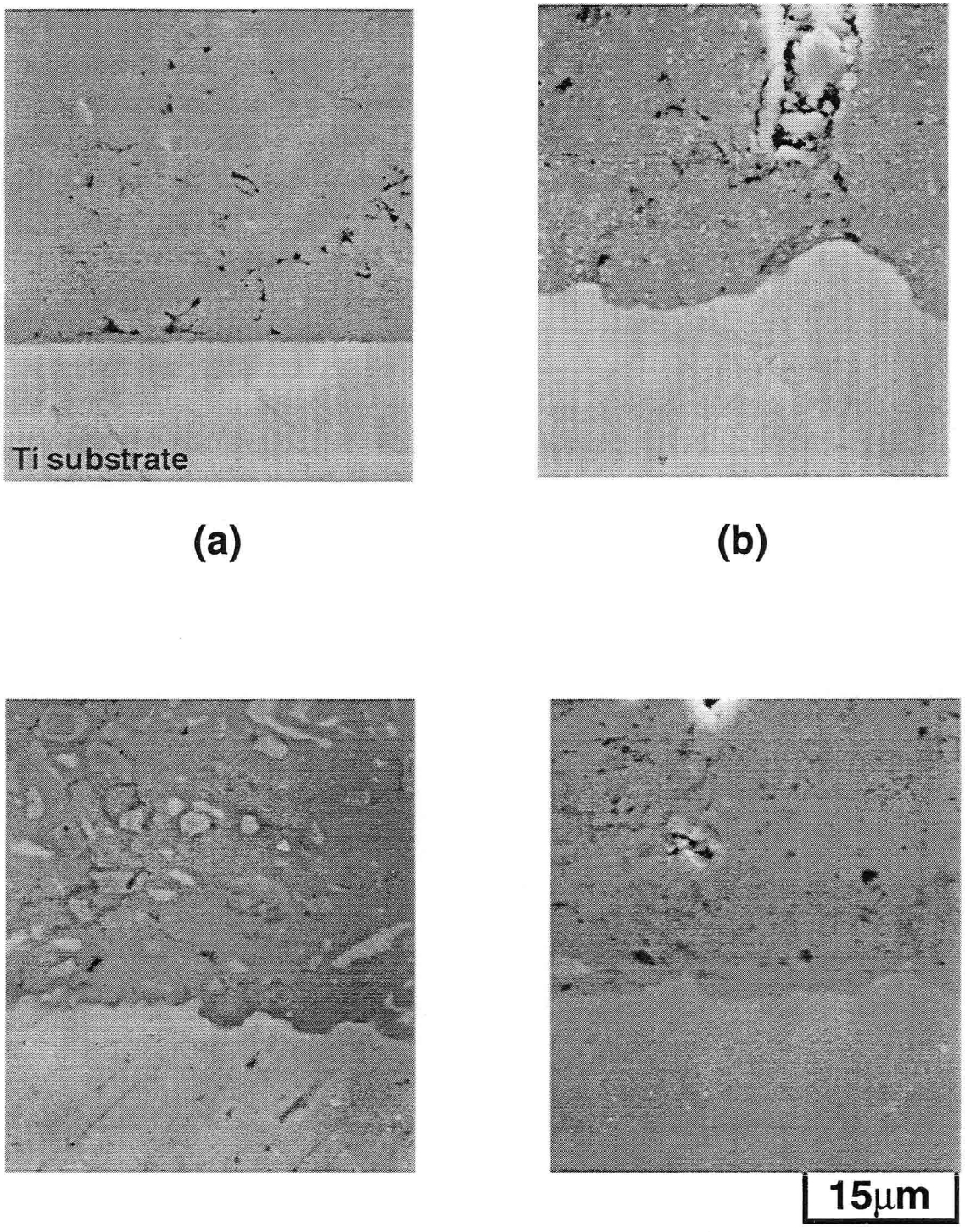

Fig. 5.9 *Microstructures of the bonding interface formed at 973K for 180s under 40MPa. The coatings were formed from the MA powders of (a) Al-Ti, (b) Al-Ti-Al_2O_3, (c) Al-Ti-TiB_2 and (d) Al-Ti-B.*

the bonding. **Figure 5.10** shows the microstructure adjacent to the bonding interface formed from the Al-Ti-TiB_2 at 1173K for 1800s under 40MPa, and the mica sheet indicates the initial interface. From this figure, the reaction layers were found to form mainly in the direction of the Ti substrate. These layers were identified as α_2 (Ti_3Al), γ (TiAl) and Al_2Ti from the Ti substrate to the IMC coating. The obtained results were consistent with those reported by Loo *et al.* who investigated the interdiffusion phenomena of a Ti-Al_3Ti couple [11].

Figure 5.11 shows the relationship between the total thickness of the reaction layers ($\alpha_2 + \gamma + Ti_2Al$) formed from the Al-Ti-$TiB_2$ and the square root of the holding time. The growth of the reaction layers exhibited a parabolic relation with the holding time [12]. The activation energy obtained from the Arrhenius plot of K_g was 82.8kJ/mol. **Table 5.2** shows the activation energy for the growth of the reaction layers. The value obtained by the same calculation from the research of Loo *et al.* is also shown. The values obtained from this research couples were a little larger than those obtained by them. The reaction between the Al_3Ti coating and the Ti substrate might be suppressed by the dispersion of Al_2O_3 and TiB_2 particles. Although the voids on the bonding interface were easily eliminated, the bonding between the coating and the substrate included some voids in the coating and exhibited low fracture strength (about 50MPa). The bondings with a high fracture strength (about 150MPa) were obtained when voids in the coating were eliminated or the reaction layer with a thickness over 1μm was formed.

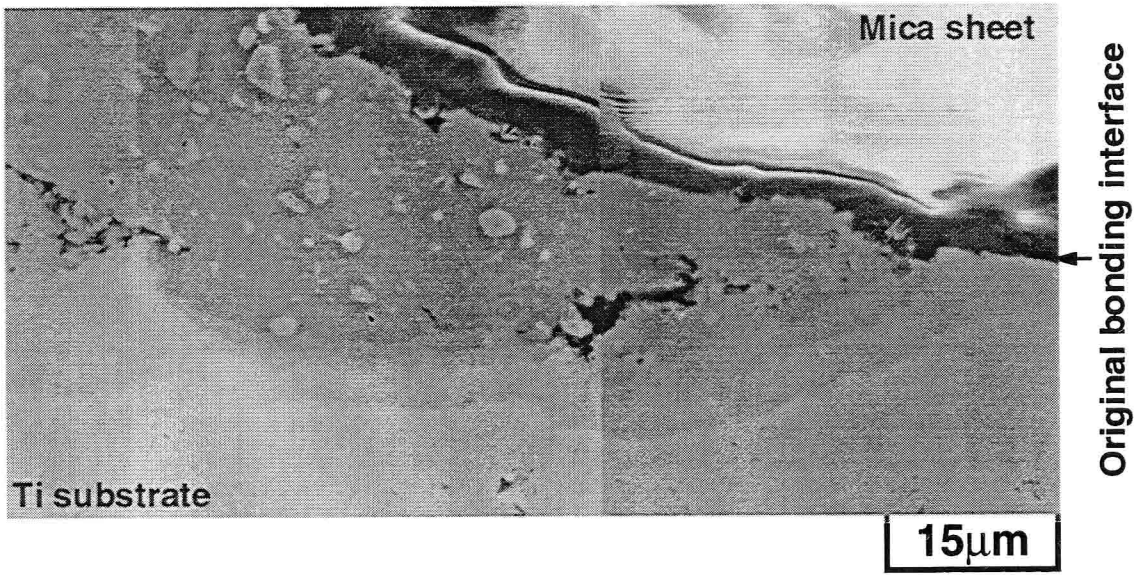

Fig. 5.10 *Microstructures of the bonding interface formed from the Al-Ti-TiB_2 MA powders on the Ti substrate at 1173K for 180s under 40MPa, and the mica sheet indicates the original interface.*

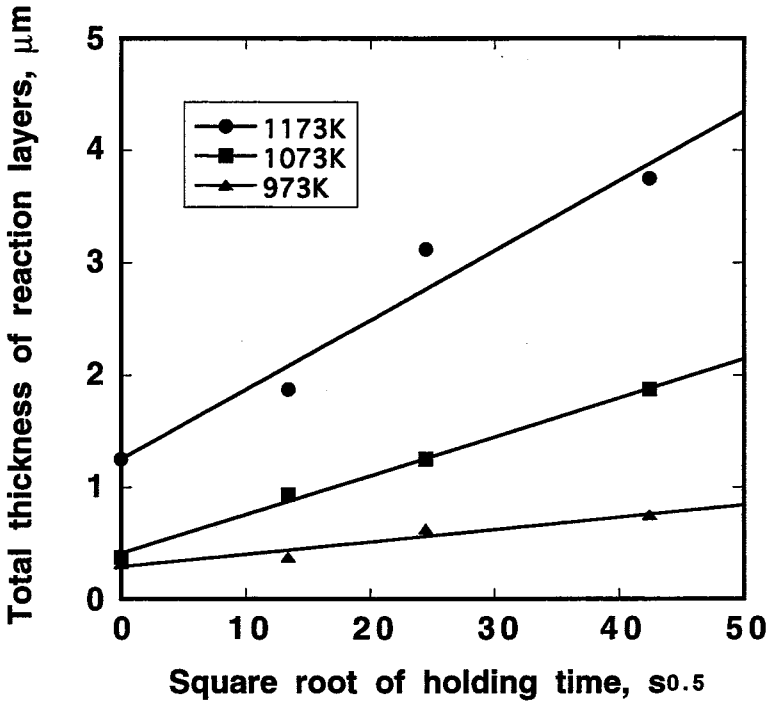

Fig. 5.11 Relationship between the total thickness of the reaction layers ($\alpha_2 + \gamma + Ti_2Al$) formed from the Al-Ti-$TiB_2$ MA powders on the Ti substrate and the square root of the holding time.

Table 5.2 *Apparent activation energies for the growth of the reaction layers.*

Powder	Q_g, kJ/mol
Al-Ti	70.3
Al-Ti-Al_2O_3	77.5
Al-Ti-TiB_2	82.8
Al-Ti-B	79.8
Al_3Ti/Ti diffusion couple (Loo *et al.* [11])	76.2

5.3.4 Properties of IMC coatings

Figure 5.12 shows the microstructure of the dense and homogeneous IMC coatings which were obtained at 1173K for 600s from the MA powders of the Al-Ti-Al_2O_3 and -TiB_2, at 1273K for 600s from the Al-Ti-B by PECS.

Figure 5.13 shows the Vickers hardness distribution of the IMC coatings as a function of distance from the bonding interface. The hardness of the IMC coatings is about Hv800 for the Al_3Ti/TiB_2 coatings, and HV750 for the Al_3Ti/Al_2O_3 coating which

are higher than that of a monolithic Al_3Ti layer (HV600). Besides, the IMC coatings obtained from the Al-Ti-B MA powders exhibited a slightly greater hardness, probably because the dispersed in-situ formed TiB_2 is much fine comparing with that obtained from the Al-Ti-TiB_2.

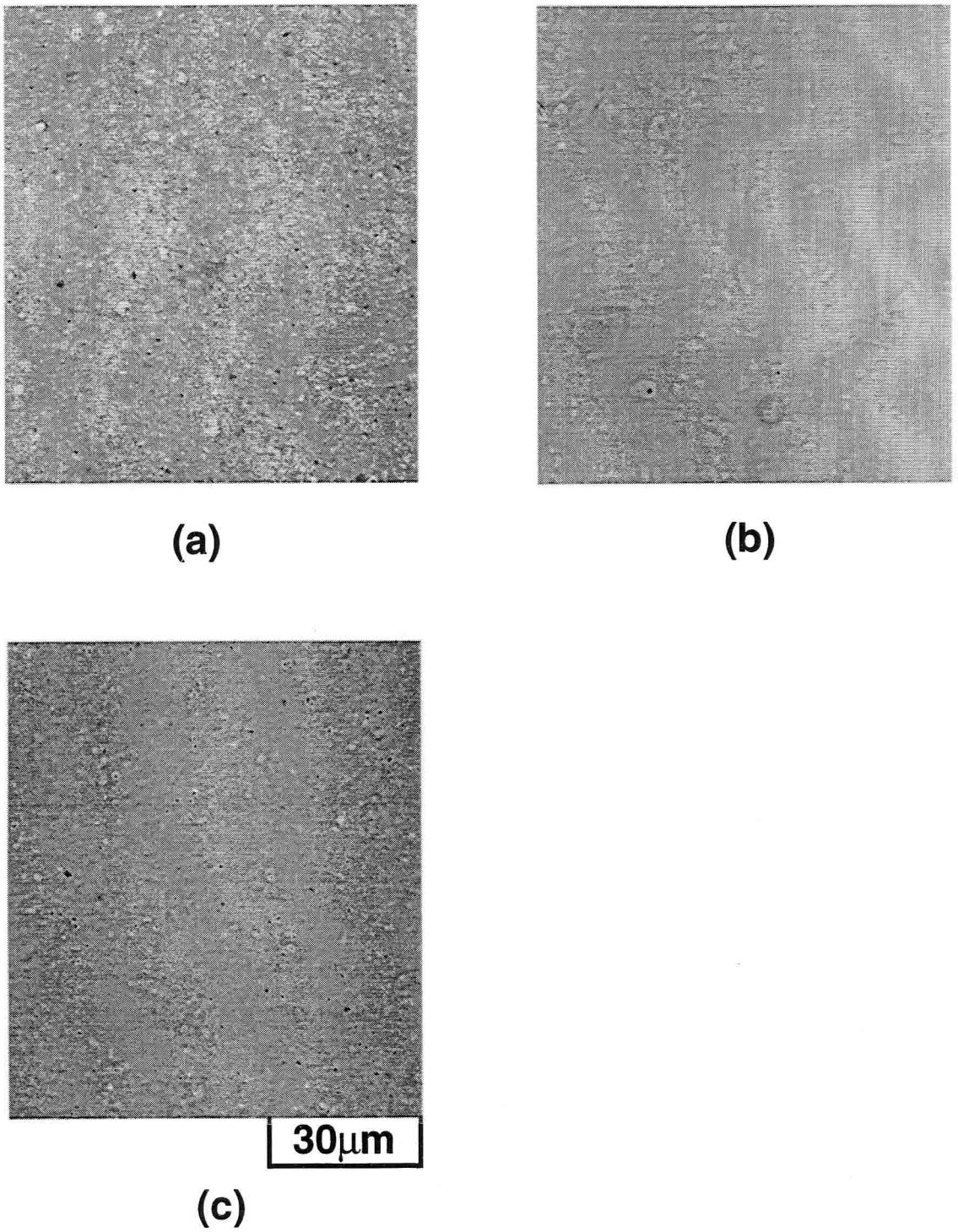

Fig. 5.12 *Microstructures of the IMC coatings formed from the MA powders of (a) Al-Ti-Al_2O_3, (b) Al-Ti-TiB_2 and (c) Al-Ti-B by PECS.*

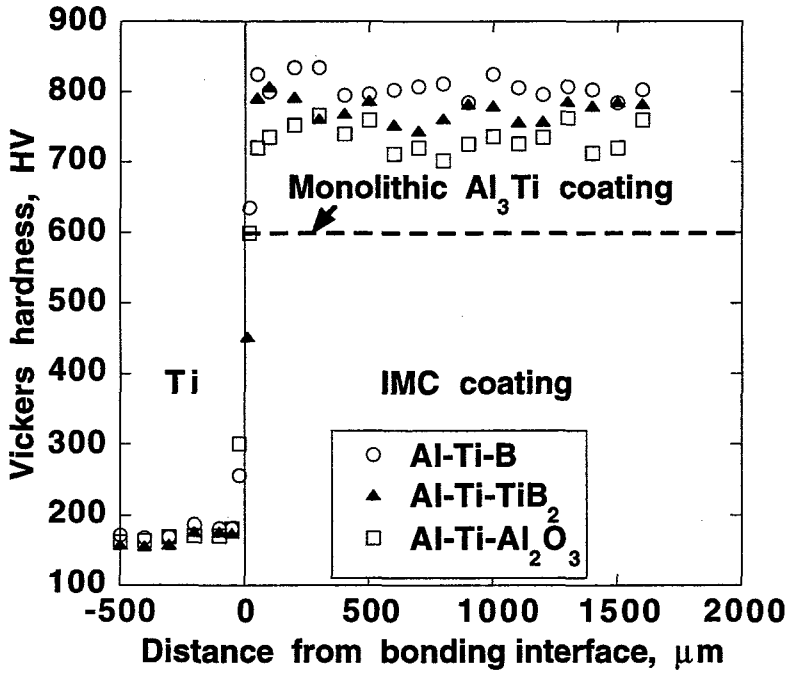

Fig. 5.13 Vickers hardness distributioin of the IMC coatings.

Figure 5.14 shows the specific wear of the IMC coatings and the Ti substrate. The Al_3Ti coatings reinforced with the TiB_2 and Al_2O_3 particles with greater hardness exhibited better excellent wear properties than the monolithic Al_3Ti coating.

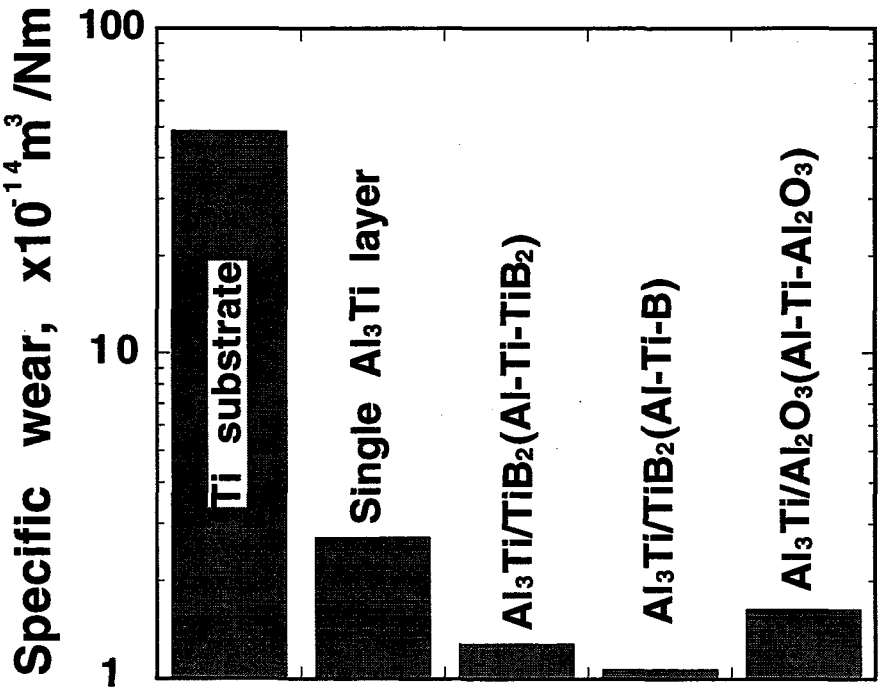

Fig. 5.14 Specific wears of the Ti substrate and the IMC coatings.

Figure 5.15 shows the microstructures of the Al_3Ti/TiB_2 coatings after oxidizing at 1273K for 28.8ks in an open air. Though the monolithic Al_3Ti coating exhibited excellent oxidation properties and it was hardly damaged by the formation of protective Al_2O_3 scale, many cracks were observed in the IMC layer and TiO_2 scale was formed on the surface. Pregger *et al.* showed that the oxide scale formed on the $NiAl/TiB_2$ composite by the isothermal oxidation and TiB_2 dissociated within the void regions leading to the outward diffusion of titanium through the oxide scale and to the formation of TiO_2 at the outer surface [13]. In this research, similarly, it seems that TiB_2 decomposes to diffuse Ti toward the surface, resulting in formation of TiO_2 on the surface. In conclusion, TiB_2 is not a proper reinforcement particle for relating the excellent oxidation resistance of Al_3Ti.

Figure 5.16 shows the microstructures of the Al_3Ti/Al_2O_3 coating after oxidizing at 1273K for 230.4ks. Although the oxidation time was longer than the case shown in **Fig. 5.15**, the coating was hardly damaged by oxidation due to the formation of protective Al_2O_3 scale. **Table 5.3** shows the weight gain of the monolithic Al_3Ti and the obtained Al_3Ti/Al_2O_3 composite after oxidizing at 1273K for 230.4ks. As Umakoshi *et al.* reported that the weight gain of the bulk Al_3Ti oxidized in oxygen at 1273K for 180ks was about $3.0g/m^2$ [14], the Al_3Ti/Ti coating formed by PECS exhibited slightly excellent oxidation properties than the bulk Al_3Ti.

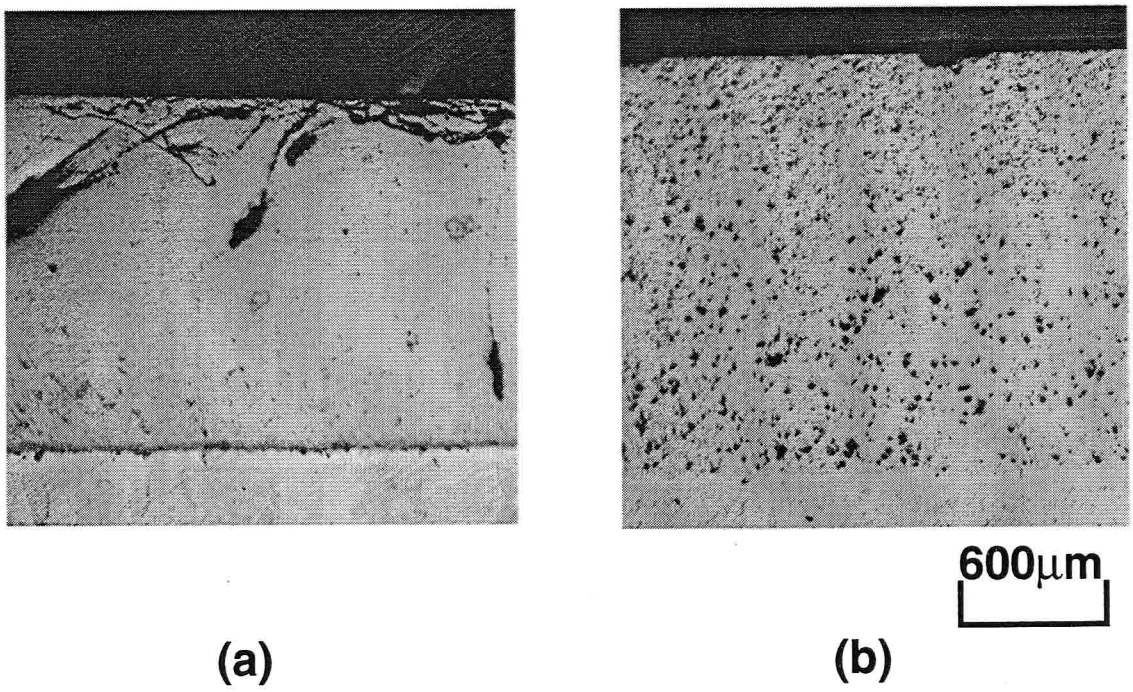

Fig. 5.15 General views of the Al_3Ti/TiB_2 coatings formed from the MA powders of (a) Al-Ti-TiB_2, (b) Al-Ti-B and (c) microstructure of the oxide layer, and (d) EDX analysis at the arrow in (c) after oxidizing in an open air at 1273K for 28.8ks.

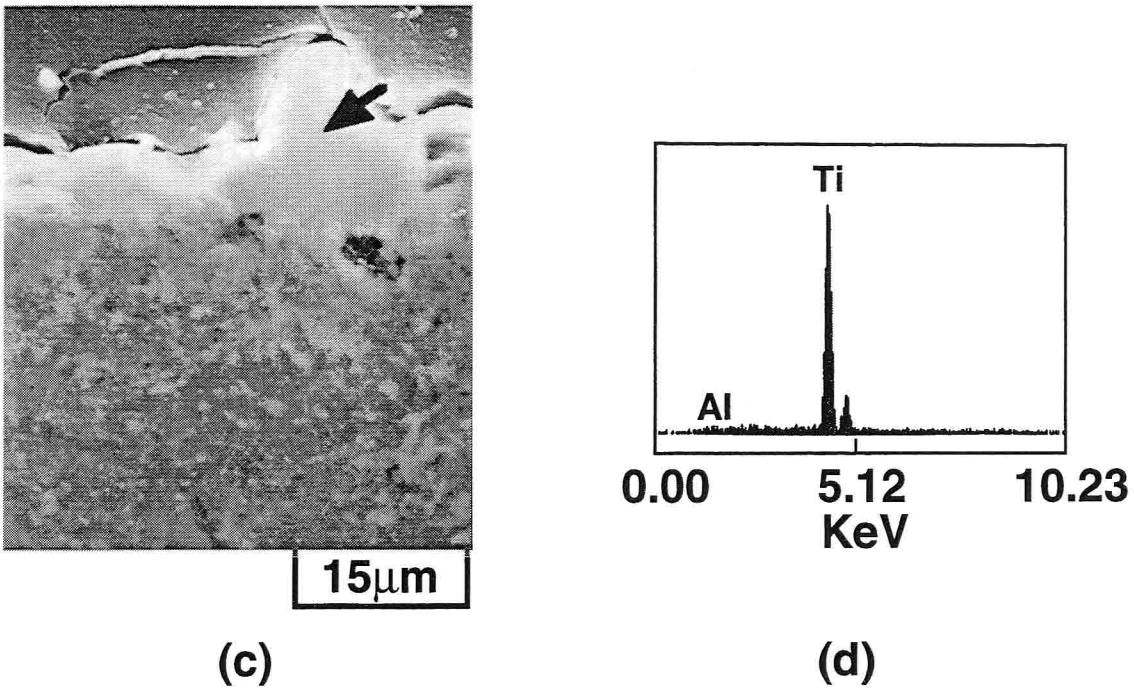

Fig. 5.15 Continued.

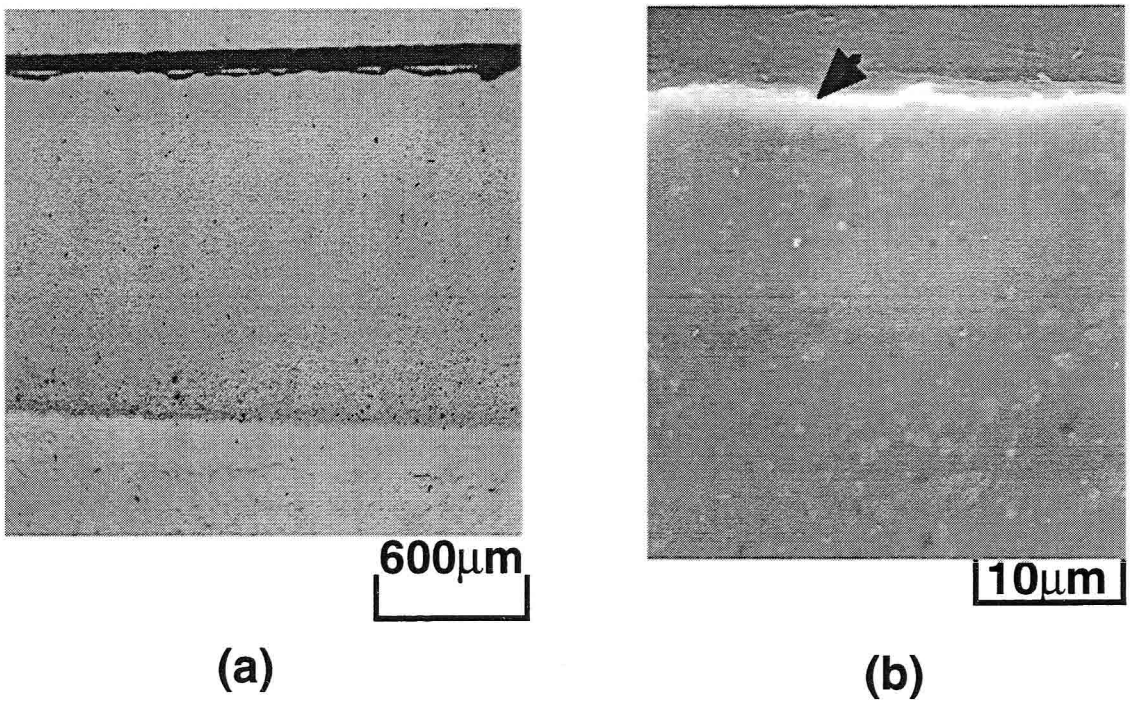

Fig. 5.16 *General views of the Al_3Ti/Al_2O_3 coatings formed from the MA powders of Al-Ti-Al_2O_3, (b) microstructure of the oxide layer, and (c) EDX analysis at the arrow in (b) after oxidizing in an open air at 1273K for 230.4ks.*

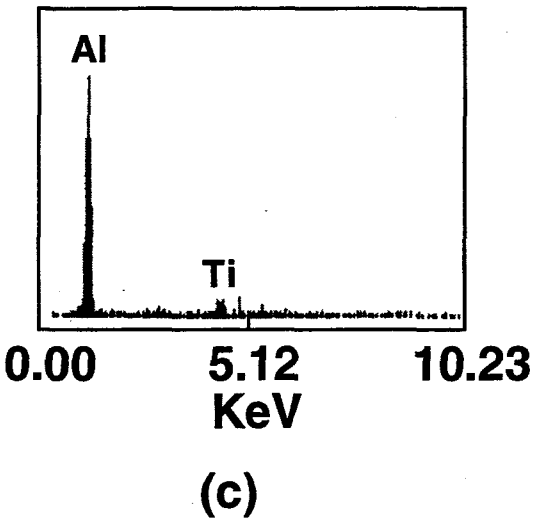

Fig. 5.16 Continued.

Table 5.3 Weight gain of the Al_3Ti and Al_3Ti/Al_2O_3 composite after oxidizing in an open air at 1273K for 230.4ks.

Sample	Weight gain, g/m^2
Al_3Ti	5.9
Al_3Ti/10vol.%Al_2O_3	3.6
ingot Al_3Ti (Umakoshi *et al.* [14])	3.0 (in an oxygen at 1273K for 180ks)

5.4 Conclusions

Ceramic particles reinforced Al_3Ti coatings were formed by reactive-pulsed electric current sintering from the MA powders of Al-Ti-Al_2O_3 and -TiB_2 or -B and simultaneously bonded with the Ti substrate. The main results obtained in this chapter can be summarized as follows.

(1) Fully dense IMC coatings were formed from the MA powders of Al-Ti-Al_2O_3 and -TiB_2 at 1173K for 600s under 40MPa by PECS. Using the Al-Ti-B MA powders needed higher temperature of 1273K for full densification compared with the TiB_2 addition although the grain size of in-situ formed TiB_2 became smaller down to 300nm.

(2) The existence of TiB_2 and Al_2O_3 particles in the coating enhanced the elimination of voids on the bonding interface. The interface became rough although it suppressed the growth of the reaction layers at the bonding interface due to the decreased effective diffusion path between the coating and the substrate.

(3) The hardness and wear properties of the Al_3Ti coating could be improved by the reinforcement of TiB_2 and Al_2O_3 particles.

(4) The oxidation resistance of the Al_3Ti/TiB_2 composite coatings was degraded due to the decomposition of TiB_2 to elemental Ti and B.

(5) Incorporation of Al_2O_3 particles within the Al_3Ti matrix gives slightly excellent oxidation properties than the bulk Al_3Ti.

Refereces

[1] C.H.Ward and A.S.Culbertson, *MRS Symp. Proc.*, **350**(1994), 3.

[2] C.M.Ward-Close, R.Minor and P.J.Doorbar, *Intermetallics*, **4**(1996), 217.

[3] I.Maxwell and A.Hellawell, *Metall. Trans.*, **3**(1972), 1487.

[4] M.X.Zhang, K.C.Hsieh, J.Dekock and Y.A.Chang, *Scripta Metall.*, **27**(1992), 1361.

[5] M.Kambara, K.Uenishi and K.F.Kobayashi, *J. Mater. Sci.*, **35**(2000), 2897

[6] N.J.Melham, *Intermetallics*, **6**(1998), 363

[7] H.J.Brinkman, J.Duszczyk and L.Katgerman, *Scripta Mater.*, **37**(1997), 293.

[8] D.S.Wilkinson and M.F.Ashby, *Acta Metall.*, **23**(1975), 1277-1285.

[9] I.Brain, *Thermochemical Data of Pure Substrate*, VCH, (1989)

[10] M.F.Ashby, G.H.Gelles and L.E.Tanner, *Phil. Mag.*, **18**(1969), 757-771.

[11] F.J.J.van Loo and G.D.Rieck, *Acta Metall.*, **21**(1973), 73-84.

[12] G.V.Kidson, *J. Nucl. Mater.*, **3**(1961), 21-29.

[13] B.A.Pregger, T.Kircher and A.Khan, *Mater. Sci. Eng. A*, **153**(1992), 567-572.

[14] Y.Umakoshi, M.Yamaguchi, T.Sakagami and T.Yamane, *J. Mater. Sci.*, **24**(1989), 1599.

Chapter 6 Summary

Intermetallic compound Al_3Ti is a promising material for structural applications at elevated temperatures because of its high specific strength, high melting temperature and excellent oxidation resistance. Although the Al_3Ti is difficult to use as a bulk material due to the poor ductility, it is expected to exhibit excellent wear and oxidation properties as a surface modified coating.

In this thesis, coatings of Al_3Ti and its composites were formed on metal substrates by applying the powder metallurgical techniques and their properties were evaluated. The main results confirmed can be summarized as follows.

1. The Al_3Ti was formed by the combustion synthesis from the elemental mixed powders of Al and Ti and simultaneously bonded with the TiAl and Cu substrates. The Al_3Ti phase was formed at the melting temperature of Al. At the same temperature, Al reacted with the TiAl substrate and formed an Al_3Ti reaction layer resulting in the bonding of the TiAl substrate and the Al_3Ti coating. When the coating was formed on the Cu substrate, Al and Cu reacted and formed the eutectic liquid phase below the melting temperature of Al, which ignited the combustion synthesis adjacent to the bonding interface. Exothermic reaction of the combustion synthesis to the direction of the coating. Bonding between Al_3Ti and Cu was achieved by the formation of three reaction layers which were identified to be $Ti(Cu,Al)_2$, Al_5Ti_2Cu and fcc Cu(Al) solid solution. Excess reaction of Al in the mixed powders with the Cu substrate changed the composition of coating richer in Ti than Al_3Ti, which caused the existence of unreacted Ti in the coating. By changing the composition of the mixed powders to Al-20at%Ti, the homogeneous Al_3Ti surface layer was synthesized. The obtained Al_3Ti coating densified by hot pressing exhibited almost the same wear properties as the cast Al_3Ti.
2. To obtain homogeneous compound layer which is free from unreacted elements, the relation between initial Ti particle sizes in the precursor and the heat treatment conditions was estimated by a spherical model including diffusion kinetics. Based on the calculated relations, the homogeneous Al_3Ti coating was formed by the application of finely mechanically alloyed powders with the Ti particle size less than 1.0μm in the Al matrix, and showed almost the same wear property and hardness as that of the cast Al_3Ti.
3. Reactive-pulsed electric current sintering (PECS) was applied to synthesize and simultaneously densify the Al_3Ti coating formed from the MA powders which were set on the Ti substrate. During heating by PECS, Al and Ti in the MA powders reacted and formed an Al_3Ti phase and simultaneously bonded with the Ti substrate. The densification of the coating was controlled by the plastic flow of powders and a fully dense and homogeneous Al_3Ti coating with

a thickness of about 1600μm was obtained by holding at 1100K for 180s under 40MPa. While, a higher temperature (1210K) or longer holding time (over 1800s) was required to eliminate voids on the Al_3Ti/Ti interface and bonding between the coating and the substrate was achieved by the formation of reaction layers. The obtained Al_3Ti layer exhibited almost the same hardness, wear, and oxidation resistance as the cast Al_3Ti.

4. To enhance wear properties, TiB_2 or Al_2O_3 particles reinforced Al_3Ti, *i.e.* the IMC coatings were fabricated by RPECS of the MA powders of Al-Ti-TiB_2, -B and -Al_2O_3. Although the dense and homogeneous Al_3Ti/TiB_2 coating was formed both from the Al-Ti-TiB_2 and Al-Ti-B powders, higher temperature was necessary for full densification when the Al-Ti-B powders were used. On the contrary, the grain size of in-situ formed TiB_2 became much smaller down to 300nm compared with the TiB_2 formed from the Al-Ti-TiB_2. The existence of ceramic particles in the coating enhanced the elimination of voids around the bonding interface by deforming the surface of substrate although it suppressed the growth of reaction layers formed at the bonding interface due to the decreased effective diffusion path between the coating and the substrate. The bonding strength between the coating and the substrate became higher than that of the coating not when void on the bonding interface annihilated completely but when the thickness of reaction layer exceeds 1μm. The dispersions of TiB_2 and Al_2O_3 particles were effective to enhance the wear properties of the monolithic Al_3Ti. Though the oxidation resistance of Al_3Ti/TiB_2 composite coatings was degraded due to the decomposition of TiB_2, the incorporation of Al_2O_3 particles within the Al_3Ti matrix slightly improved the oxidation resistance.

List of related publications

<Papers>

[1] T.Matsubara, S.Morino, K.Uenishi and K.F.Kobayashi, "Fabrication of Al_3Ti layer on Cu substrate by SHS reaction of mechanically alloyed powder", *J. Soc. Mater. Sci. Jpn.*, **47**(1998), 1106. (in Japanese)

[2] K.Uenishi, T.Matsubara and K.F.Kobayashi, "Combustion synthesis of intermetallic compound Al_3Ti and its simultaneous joining with TiAl", *Z. Metallkd.*, **90**(1999), 163.

[3] T.Matsubara, K.Uenishi and K.F.Kobayashi, "Fabrication of thick intermetallic compound Al_3Ti layer on metal substrate by combustion synthesis of ball-milled powder", *Mater. Trans., JIM*, **41**(2000), 631.

[4] T.Matsubara, T.Shibutani, K.Uenishi and K.F.Kobayashi, "Fabrication of a thick surface layer of Al_3Ti on Ti substrate by reactive-pulsed electric current sintering", *Intermetallics*, **8**(2000), 815.

[5] K.Uenishi, T.Matsubara, S.Morino and K.F.Kobayashi, "Formation of thick intermetallic compound Al_3Ti layer on Cu substrate by combustion synthesis", submitted to J. Mater. Sci. Tech.

[6] T.Matsubara, T.Shibutani, K.Uenishi and K.F.Kobayashi, "Fabrication of TiB_2 reinforced Al_3Ti composite layer on Ti substrate by reactive-pulsed electric current sintering", *Mater. Sci. Eng. A.*, (in press)

[7] K.Uenishi, T.Matsubara, M.Kambara and K.F.Kobayashi, "Nanostructured titanium-aluminides and their composites formed by combustion synthesis of mechanically alloyed powders", *Scripta Mater.*, (in press)

<International Conference>

[1] T.Matsubara, T.Shibutani, K.Uenishi and K.F.Kobayashi, "Fabrication of TiB_2 reinforced Al_3Ti composite layer on Ti substrate by reactive-pulsed electric current sintering", *5th Int. Conf. on Structural & Functional Intermetallics*, Vancouver, Canada, July 16-20, (2000)

[2] K.Uenishi, T.Matsubara, M.Kambara and K.F.Kobayashi, "Nanostructured titanium-aluminides and their composites formed by combustion synthesis of mechanically alloyed powders", *5th Int. Conf. on Nanostructured Materials (NANO2000)*, Sendai, Japan, Augst 20-25, (2000)